The Journal of Gemmology

Volume 28 No. 2
April 2002

Notes from the Laboratory

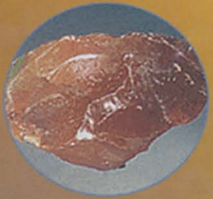

Chocolate-brown Opal

Inclusions in Gemstones

Natural Amethyst

The Gemmological Association and Gem Testing Laboratory of Great Britain

Gemmological Association
and Gem Testing Laboratory
of Great Britain
27 Greville Street, London EC1N 8TN
Tel: 020 7404 3334 Fax: 020 7404 8843
e-mail: gagtl@btinternet.com Website: www.gagtl.ac.uk

President:
Professor A.T. Collins

Vice-Presidents:
N. W. Deeks, A.E. Farn, R.A. Howie, D.G. Kent, R.K. Mitchell

Honorary Fellows:
Chen Zhonghui, R.A. Howie, R.T. Liddicoat Jnr, K. Nassau

Honorary Life Members:
H. Bank, D.J. Callaghan, E.A. Jobbins, H. Tillander

Council of Management:
T.J. Davidson, R.R. Harding, I. Mercer, J. Monnickendam,
M.J. O'Donoghue, E. Stern, I. Thomson, V.P. Watson

Members' Council:
A.J. Allnutt, S. Burgoyne, P. Dwyer-Hickey, S.A. Everitt, J. Greatwood,
B. Jackson, L. Music, J.B. Nelson, P.G. Read, P.J. Wates, C.H. Winter

Branch Chairmen:
Midlands – G.M. Green, North West – D. M. Brady, Scottish – B. Jackson,
South West – R.M. Slater

Examiners:
A.J. Allnutt, M.Sc., Ph.D., FGA, L. Bartlett, B.Sc., M.Phil., FGA, DGA,
S. Coelho, B.Sc., FGA, DGA, Prof. A.T. Collins, B.Sc., Ph.D, A.G. Good, FGA, DGA,
J. Greatwood, FGA, G.M. Howe, FGA, DGA, S. Hue Williams MA, FGA, DGA,
B. Jackson, FGA, DGA, G.H. Jones, B.Sc., Ph.D., FGA, Li Li Ping, FGA, DGA,
M. Newton, B.Sc., D.Phil., C.J.E. Oldershaw, B.Sc. (Hons), FGA, DGA,
H.L. Plumb, B.Sc., FGA, DGA, R.D. Ross, B.Sc., FGA, DGA, P.A. Sadler, B.Sc., FGA, DGA,
E. Stern, FGA, DGA, S.M. Stocklmayer, B.Sc. (Hons), FGA, Prof. I. Sunagawa, D.Sc.,
M. Tilley, GG, FGA, C.M. Woodward, B.Sc., FGA, DGA

The Journal of Gemmology
Editor: Dr R.R. Harding
Assistant Editors: M.J. O'Donoghue, P.G. Read
Associate Editors: Dr C.E.S. Arps (Leiden),
G. Bosshart (Zurich), Prof. A.T. Collins (London), Dr J.W. Harris (Glasgow),
Prof. R.A. Howie (Derbyshire), Dr J.M. Ogden (Hildesheim),
Prof. A.H. Rankin (Kingston upon Thames), Dr J.E. Shigley (Carlsbad),
Prof. D.C. Smith (Paris), E. Stern (London), Prof. I. Sunagawa (Tokyo),
Dr M. Superchi (Milan), C.M. Woodward (London)
Production Editor: M.A. Burland

Vol 28, No. 2, April 2002 ISSN: 1355-4565

Natural and heat-treated corundum from Chimwadzulu Hill, Malawi: genetic significance of zircon clusters and diaspore-bearing inclusions

Professor A. H. Rankin

School of Earth Sciences and Geography
Kingston University, Surrey, KT1 2EE

ABSTRACT: Laser Raman Microspectrometry (LRM) has been used to identify the solid, liquid and gaseous components of inclusions in colourless to pale yellow/green corundum and gem-quality rubies from the eluvial deposits of Chimwadzulu Hill, Malawi. Zircons and multiphase-diaspore-CO_2 inclusions are the dominant types present, but tiny rutile needles (less than a few microns) and a single inclusion of amphibole have also been identified. The zircons typically occur in clusters of elongate crystals up to a few hundred microns in size, with length to breadth 'aspect' ratios usually between 1.8 and 4.2. Multiphase diaspore-CO_2-bearing inclusions, with or without calcite, occur in planar groupings. These are interpreted as the heterogeneous products of once homogeneous fluids trapped at some elevated temperature and pressure. The overall inclusion characteristics suggest a 'metamorphic' rather than an alkali basaltic 'magmatic' source for the corundums. Whilst the overall inclusion assemblage may help to distinguish Chimwadzulu corundums from those from other areas, individually, the different inclusion types are not unique to this locality.

In heat-treated samples the diaspore-bearing inclusions are destroyed. Diaspore converts to corundum, and water and CO_2 are driven out from the inclusions via microfractures. Similar, thermally-induced microfractures are also developed as 'feathers' around zircons. In the wider context, it is suggested that the presence of radiating planes surrounding zircons, in untreated corundum samples, provides a useful criterion for recognizing alkali basalts as the primary host rocks for a particular specimen.

Introduction

Gem-quality corundum has been recovered intermittently from the eluvial soils of Chimwadzulu Hill, southern Malawi, since the 1960s. Previous, small-scale mining produced pale-coloured blue, green and yellow sapphires which required enhancement through heat-treatment (Emmett, 2000). In the mid-1990s

ISSN: 1355–4565

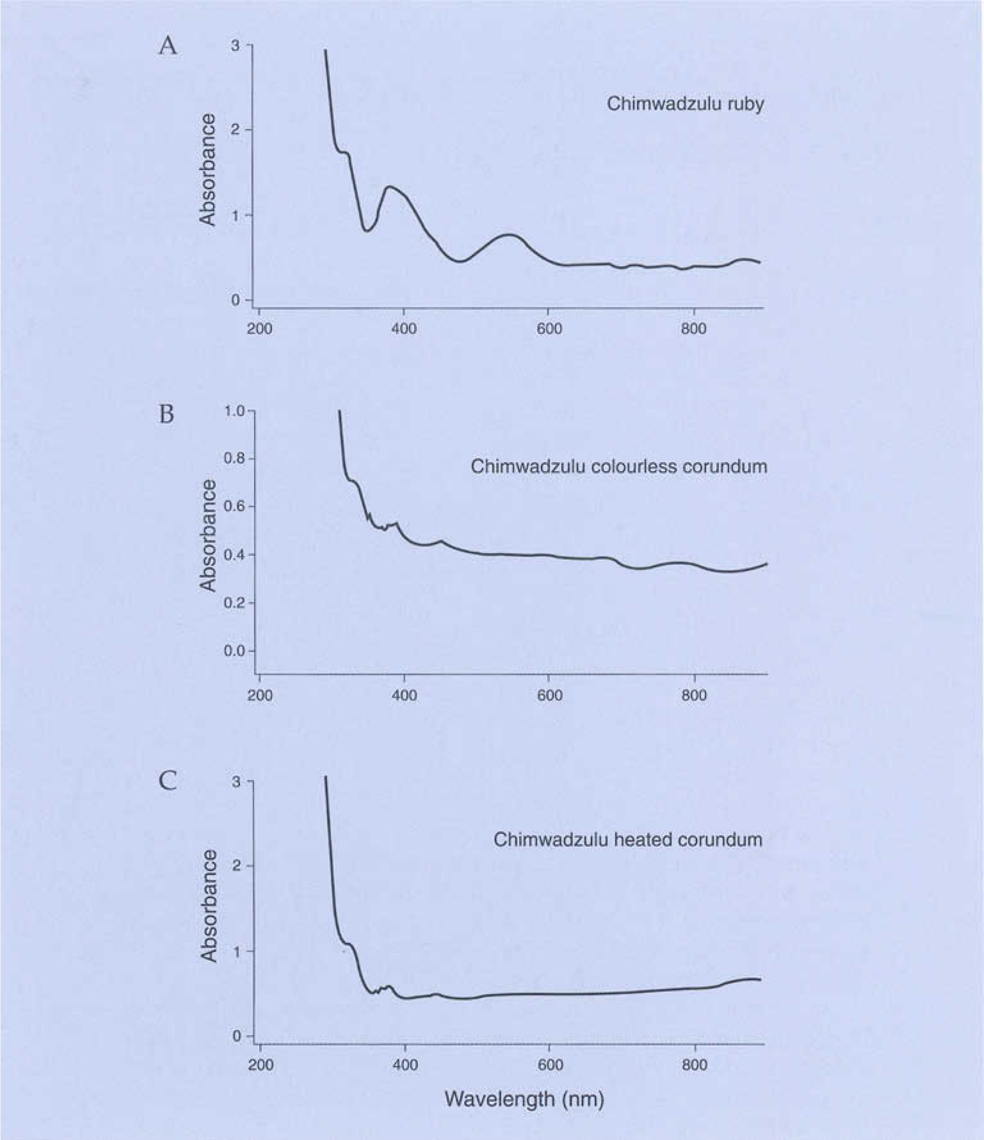

***Figure 1:** Absorption spectra (unpolarized) of Chimwadzulu corundums.*
- *(A) Gem-quality ruby showing strong absorbance bands at 550 nm and 380-400 nm attributable to Cr^{3+}.*
- *(B) Colourless corundum.*
- *(C) Heat-treated pale blue corundum.*

further exploration revealed sizeable deposits of gem-quality rubies that do not require heat treatment. These are currently being mined and extracted on a much larger scale by London-based, Agricola Resources plc with monthly shipments (July 2001) reported to be in excess of 10,000 carats.

As part of a more general investigation of the microscopic characteristics and geological significance of fluid inclusions in sapphires and rubies, the author has undertaken a preliminary study of inclusions in Chimwadzulu samples. This paper provides a first report on the identification and occurrence of distinctive zircon clusters and diaspore-bearing multiphase inclusions in natural ruby and heat-treated sapphire from this locality and discusses their gemmological and genetic significance.

Geological setting and gemmological properties

The gemmological and mineralogical features of the rubies, together with a geological overview have recently been summarised by Emmett (2000). Gem-quality rubies, and associated colourless and pale green/yellow corundum, occur as secondary deposits in eluvial soils associated with a weathered, serpentinized, ultramafic body intruded within a metasedimentary sequence of gneisses and schists; this ultramafic body is located at 15° 02'S, 34° 39' 30"E, about 80 km WNW of Zomba. Further details of the geology of Chimwadzulu Hill and notes on the occurrence of corundum in the deeply weathered soils at this locality are provided by Bloomfield (1958). However, the primary source(s) for these secondary corundum deposits has yet to be ascertained.

Uncut rubies typically form hexagonal or stubby euhedral crystals up to a few centimetres in size and range in colour from pale pink to blood red. One of the notable features of the gem rubies is that, unlike some current Burmese counterparts, they do not require heat treatment to enhance their colour. Consequently, Chimwadzulu rubies are able to attract a high price. A recent press release issued by David Williamson Associates Limited (July 2001), on behalf of Agricola Resources, reported on the sale of a fine 3.69 ct gem ruby at a price of $3600 per carat.

The colourless to pale yellow/green corundum crystals provided were less regularly-shaped crystals up to several centimetres in size. In heat-treated samples, pale blue and blue-green colours are developed, and the treatment imparts a glassy lustre to the surface of rough stones. Unfortunately, details of the heat treatment and temperatures involved are unavailable to the author.

The UV-visible spectra for heat-treatment and colourless corundum and also for deep red are shown in *Figure 1*. The only significant difference in the overall shape of the spectra between colourless and heated corundum is the disappearance of the minor absorbance peak at 350 nm in the heated sample. The UV-visible spectrum for ruby shows strong absorbance bands at c. 380–400 and 550 nm attributable to Cr^{3+}. This spectrum is very similar to those recently published for padparadscha samples from Sri Lanka and Madagascar (Milisenda *et al.*, 2001).

Samples studied and analytical methods

A total of 25 representative run-of-mine samples of uncut gem quality rubies, natural pale yellow / green to colourless corundum and pale blue sapphires formed from the pale yellow to green corundum by heat treatment were provided by Dr David

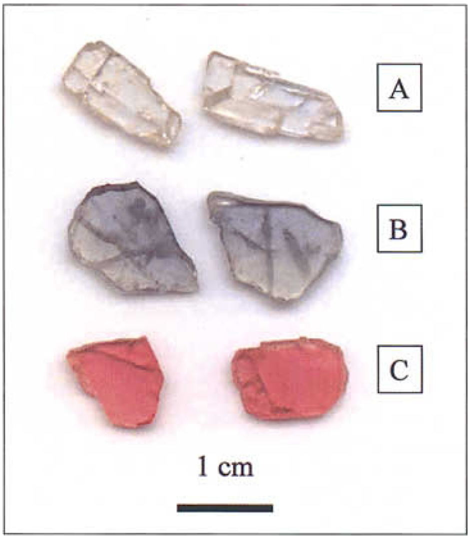

Figure 2: *Polished slices of Chimwadzulu corundum.*
(A) Colourless corundum.
(B) Pale blue, heat-treated corundum.
(C) Deep red, gem ruby.

Hargreaves, Managing Director of Agricola Resources plc. Individual crystals were between 0.5 and 1.5 cm in size and of variable clarity. In some of the rubies direct observation of inclusions was possible under the microscope through well-developed crystal faces, but in others this was only possible in cut and polished samples. A total of nine inclusion wafers, approximately 1 mm thick, were prepared using the procedures described by Shepherd *et al.* (1985). Parallel slices were cut using a diamond saw. These were then lapped and polished on both sides using progressively finer diamond grits down to 1 µm.

The inclusion wafers (*Figure* 2) were studied using a standard Olympus petrographic microscope attached to a Renishaw Laser Raman Microspectrometer (LRM). Inclusions were studied in plane polarized light and under crossed polars using both transmitted and reflected light. Magnifications up to x600 were used and Raman spectra were obtained, in confocal mode, using an Ar-ion laser (at 514.5 nm). Count times of 30 seconds were generally adequate to produce reasonable spectra. A pure silicon standard, with a single strong peak at 521 cm^{-1}, was used to calibrate the system at regular intervals. Raman shifts are reproducible to within ±1 cm^{-1}.

Some difficulties were experienced in obtaining reasonable Raman spectra from inclusions in the ruby samples. This was partly due to the strong laser-induced fluorescence above 1000 cm^{-1} but also because of a strong absorption of the laser light by the host ruby from inclusions deeper in the sample. The latter difficulty could sometimes be minimized by confining analysis to near surface inclusions.

Identification of the mineral and fluid components was based on their characteristic Raman peaks utilizing the fully-searchable Renishaw mineral database © and published reference spectra (Schubnel *et al.*,

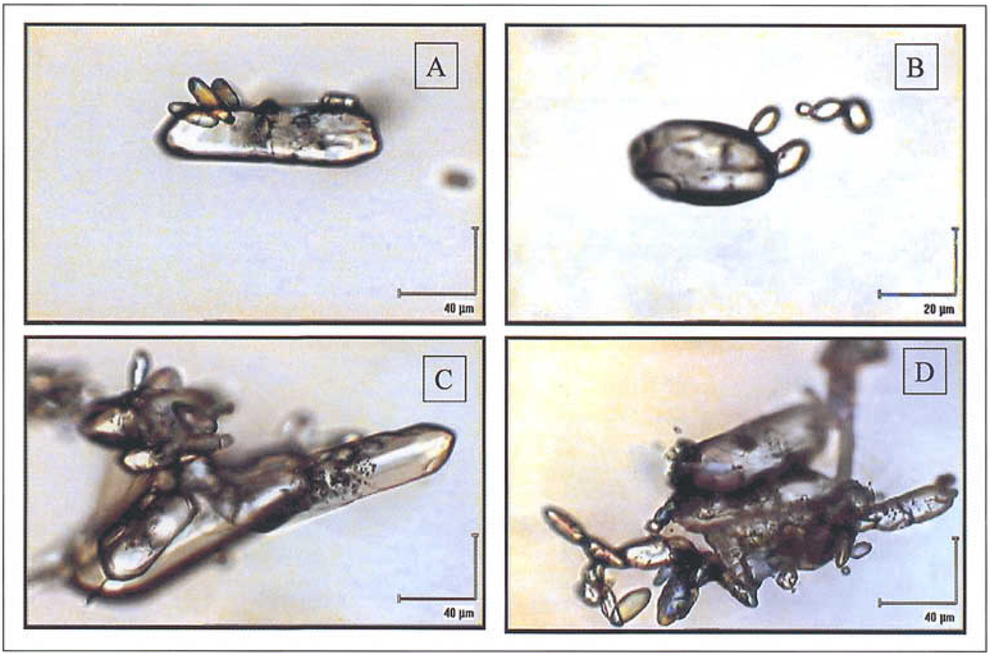

Figure 3: *Zircon clusters in colourless corundums (partially crossed polars). Scale bar represents 40 µm for A, C and D, and 20 µm for B.*

1992; Burke, 2001; California Institute of Technology, 2001).

Results

Zircon

Zircon ($ZrSiO_4$) is the most common solid inclusion in pale yellow / green to colourless corundum and in heat-treated sapphire. It has been tentatively identified in only two samples of ruby using optical methods because of strong absorption of light in these deeply coloured samples. The zircon inclusions are colourless and typically occur in clusters of between 5 and 10 crystals *(Figure 3)*. The clusters occur in planar arrays that appear to delineate crystal growth zones. Isolated crystals are rarely observed. Individual crystals in each cluster are randomly orientated. They range from a few microns up to 140 µm in size *(Figure 3)* and mostly fall in the size range 10 to 50 µm. The zircons typically occur as well-formed, elongate to stubby, sub-rounded crystals with variable length to breadth, or 'aspect', ratios of up to 5.8 *(Figure 4)*. In heat-treated samples the zircon clusters have a pronounced turbid appearance with clearly defined, radiating haloes of planes of secondary inclusions and darkened rims surrounding individual crystals *(Figure 5)*. Attempts to obtain Raman spectra from these haloes were unsuccessful due to the small size of individual inclusions therein. It is noteworthy that whilst these haloes are universally present in heated corundum, they have not been reported in untreated stones.

Diaspore-bearing multiphase inclusions

Diaspore, α-AlO(OH), was readily identified from its characteristic Raman peaks at 449 and 332 cm^{-1} as shown in *Figure 6* (California Institute of Technology, 2001) and platy crystalline form (Deer, Howie and Zussman, 1992). It is present in both yellow-green to colourless and in ruby

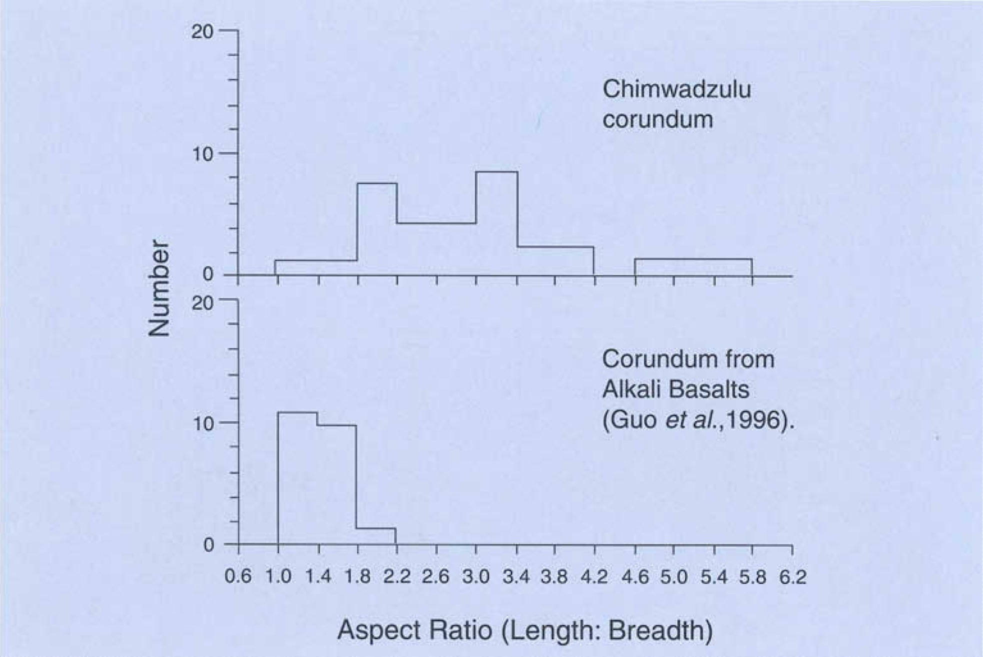

Figure 4: *Histogram of aspect ratios for zircon inclusions in Chimwadzulu corundums compared to published ratios for zircons in corundum from alkali basalts (Guo* et al.*, 1996).*

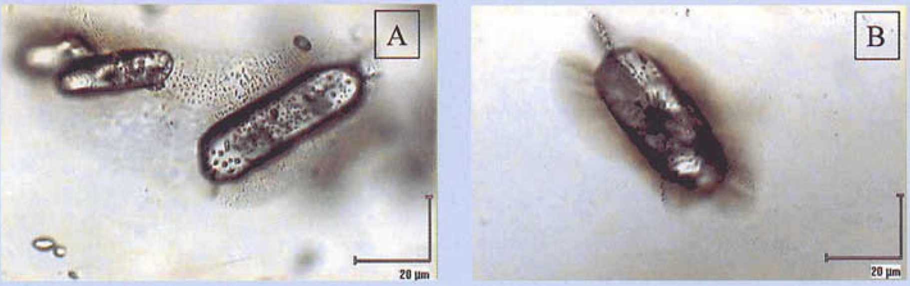

Figure 5: Zircon inclusions in heat-treated corundum with characteristic dark outlines, 'feathers' and trails of secondary inclusions in discontinuous fractures associated with each zircon. Scale bar represents 20 µm.

samples but has not been observed or detected in heat-treated Chimwadzulu sapphire samples. It characteristically occurs as the dominant crystalline component of multiphase inclusions in which a darkened area constitutes a consistent volumetric proportion of the inclusion between 30 and 40%. These inclusions typically occur as irregularly shaped cavities approximately 10 to 50 µm in size as planar groupings and arrays *(Figure 7)*. These have the characteristic appearance and distribution of pseudosecondary inclusions according to the criteria of Roedder (1984). The broad

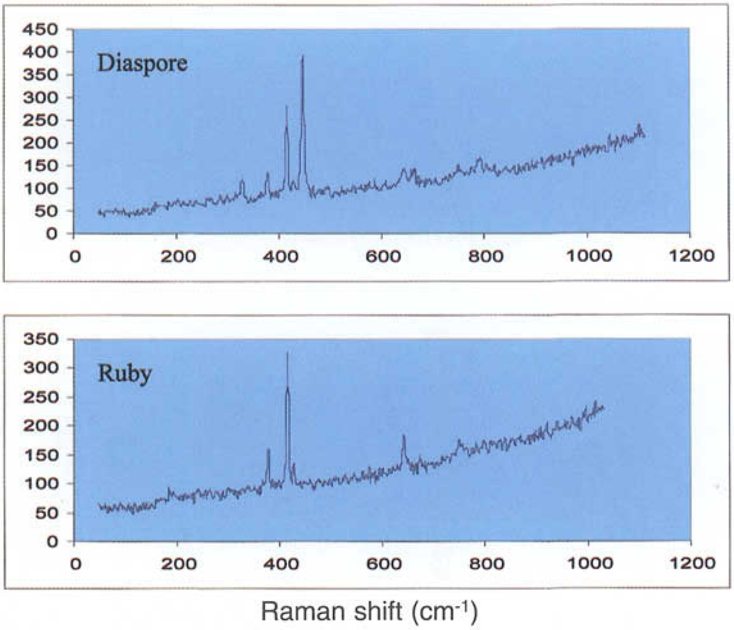

***Figure 6:** Raman spectrum of a single crystal of diaspore from unheated, colourless, Chimwadzulu corundum. Spectrum of ruby shown below for comparison.*

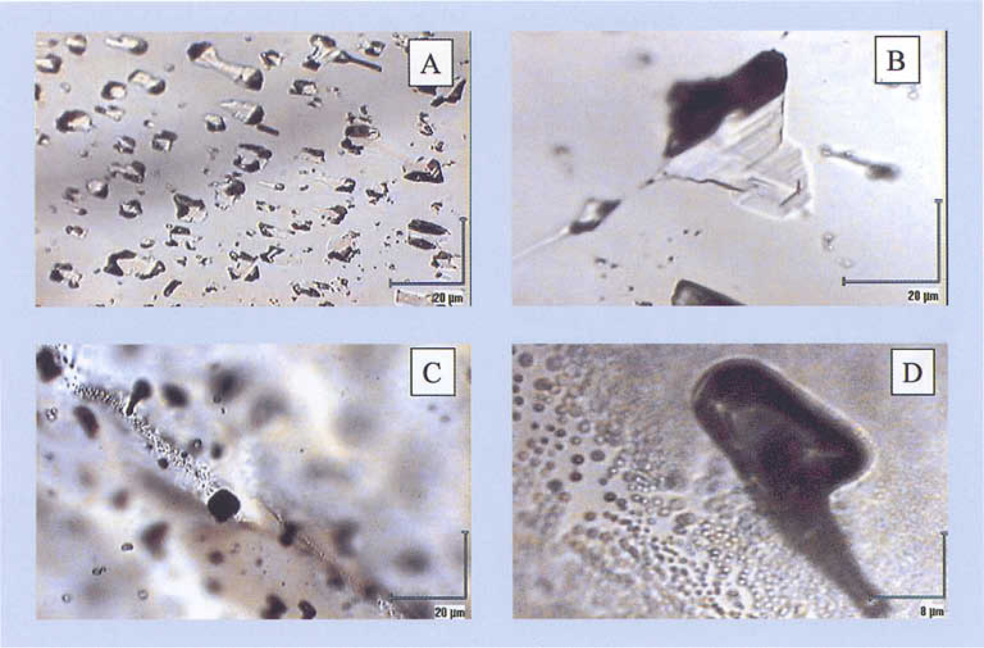

Figure 7: (A) Planar grouping of pseudosecondary, diaspore-CO_2 inclusions in colourless corundum. (B). Close-up of one of the inclusions in (A) showing a large diaspore crystal (lighter area) and a CO_2-rich phase (dark area). (C) and (D) Dark 'empty' inclusions in heat-treated corundum with associated trails of smaller, empty inclusions in microfractures. Scale bar for A, B, C: 20 µm. Scale bar for D: 8 µm.

consistency in the volumetric proportions of the light and dark components of the inclusions supports the view that they represent trapped portions of an originally homogeneous fluid at some elevated, but unknown, temperature. These components subsequently re-equilibrated on cooling to room temperature to form a heterogeneous mixture. Less commonly, isolated diaspore-bearing inclusions are found. Attempts to

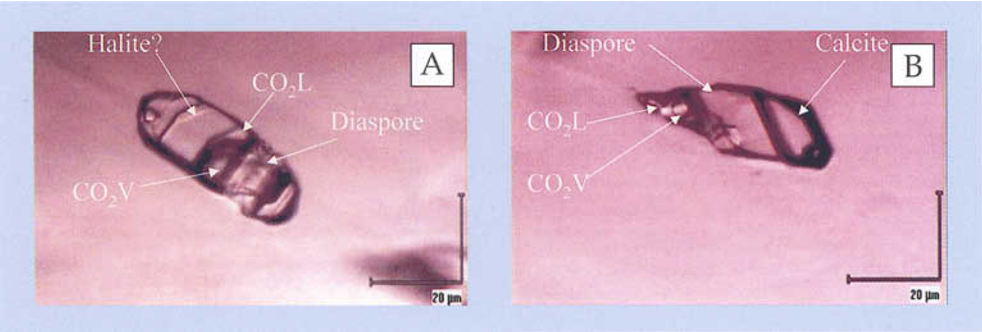

***Figure 8:** Multiphase CO_2-diaspore inclusions in gem ruby. Both CO_2 liquid and vapour are visible at room temperature (c. 20°C). (A) The inclusion also contains a cubic daughter phase believed to be halite. (B) The inclusion also contains calcite confirmed by LRM (see Figure 9).*

optically resolve and obtain Raman spectra from the dark components of these multiphase inclusions were difficult. In general, the only identifiable Raman peaks are those ascribed to CO_2. However, in one sample of ruby containing a well-developed group of diaspore-bearing inclusions (*Figure 8*), both CO_2 liquid and vapour, and a small crystal of calcite were observed at room temperature and identified by LRM (*Figure 9*). Halite, which is Raman-inactive, was also tentatively identified in these inclusions on the basis of its cubic crystal form and common occurrence as a daughter mineral in fluid inclusions (Roedder, 1984). Attempts to identify water in these multiphase inclusions based on the characteristic Raman band at around 3400 cm^{-1} proved impossible due to fluorescence from the host ruby at high wave numbers.

Inclusion trails in heated corundum

In the heat-treated corundum samples, CO_2-diaspore inclusions were not observed. Instead, inclusions showing a similar planar distribution and size range distribution were apparent. These lack the characteristic light and dark components observed in unheated samples, and the inclusions appear completely dark or 'empty'. The larger inclusions are typically surrounded by haloes of smaller inclusions (*Figure 7C, D*). Attempts to obtain Raman signals, other than those attributable to the host corundum, from any of these darkened and associated minion inclusions proved unsuccessful. The observed optical and textural features are characteristic of fluid inclusions that have suffered thermal decrepitation on heating (Shepherd *et al.*, 1985; Roedder, 1984). The mechanism by which this occurs involves a progressive increase in fluid pressure. As the inclusions are heated along an isochoric Pressure-Temperature (*P-T*) path, a point will be reached whereby the host crystal is unable to withstand the build-up of internal fluid pressure (mostly from CO_2) and decrepitation and/or partial leakage will occur. Expelled fluid would, in most crystals, migrate along thermally-induced, radiating fractures, and subsequent healing would form the characteristic planes of radiating micro-inclusions. The size, shape, distribution, darkened appearance and lack of any Raman-notable signals from these inclusions supports the view that they represent thermally decrepitated CO_2-diaspore inclusions whose contents have been expelled from the inclusions during excessive heating.

Other inclusions

A single large inclusion of amphibole, with well-developed crystal faces and characteristic green colour, and groups of crystallographically-orientated needles of rutile are the only other phases positively identified by Raman spectroscopy in the Chimwadzulu corundum samples.

Discussion

Zircon inclusions are common in corundum from a number of different gem localities (Guo *et al.*, 1966; Sutherland *et al.*, 1996). Most recently, Schwarz and Schmetzer (2001) reported on the occurrence of zircon clusters in rubies from Madagascar. Partly on the basis of these clusters and associated rutile needles, and partly on the basis of their chemical signatures, these authors suggest that it is possible to distinguish the Vatomandry rubies of Madagascar from their Asian counterparts from localities in Myanmar, Thailand and Cambodia. The present study shows that the combination of zircon clusters and rutile needles is by no means unique to Madagascar but can now be extended to include Malawi examples. Quantitative data on the major and trace element chemistry of Chimwadzulu corundum are currently unavailable. However, preliminary semi-quantitative point analyses of a single gem quality ruby from Chimwadzulu using the Laser ICP-MS technique (Williams and Greenwood, 2001, pers. comm.) shows Fe/Cr weight ratios of the order of 10 (±2 based on the mean of five analyses). These values are much closer to the ratios reported for rubies from

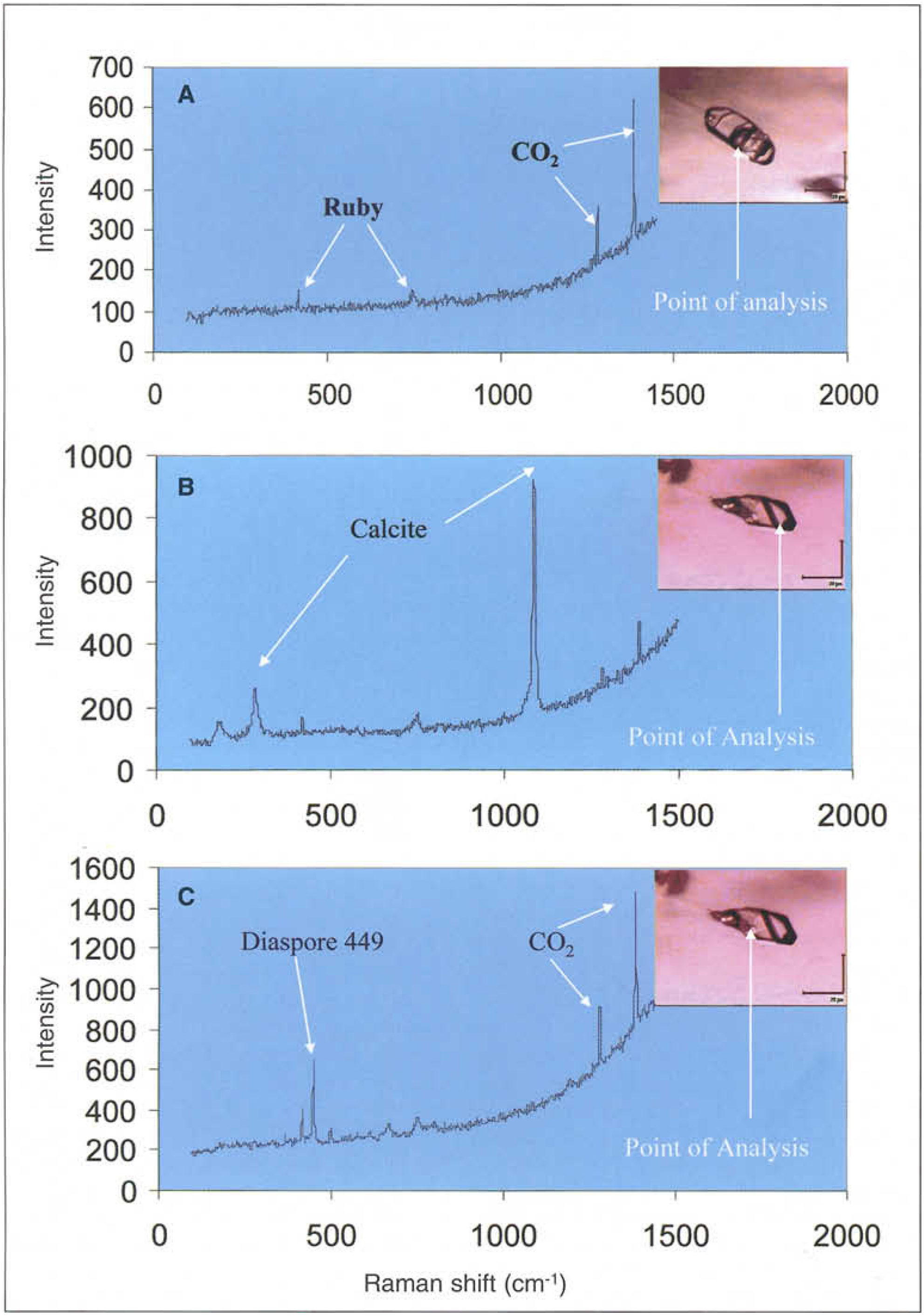

Figure 9: *Raman spectra of diaspore,* CO_2 *and calcite of inclusions shown in Figure 8 above. (A)* CO_2*-rich phase: note also peaks from the host ruby. (B) Calcite; note weaker 'interference' peaks from* CO_2 *and ruby. (C) Diaspore; note 'interference' peaks from* CO_2 *and ruby.*

Vatomandry and Thailand-Cambodia than those from Mong Hsu and Mogok (Schwarz and Schmetzer, op. cit.).

In a systematic study of zircon inclusions in blue, yellow and zoned blue corundum crystals from alkali basalts of Australia and China, Guo *et al.* (1996) showed that the aspect ratios for the majority of zircons are in the range 1.2 to 1.8. This contrasts with the aspect ratios of zircons from Chimwadzulu corundums, which are mostly between 1.8 and 4.2. Guo *et al.* (op.cit.) also noted that radiating cracks surrounding these zircons are a characteristic feature of corundum from these alkali basalt terrains. This feature also appears to be common in Thai sapphires associated with alkali basalts (Srithai and Rankin, 1999). Again this contrasts with the Chimwadzulu samples where heat-treated corundum typically shows fractures and feather-like planes of micro-inclusions emanating from the zircons. Such features are absent in unheated samples. Differential thermal expansion and contraction of zircon and host corundum on heating and cooling is one of several mechanisms proposed by Guo *et al.* (1996) to account for these features in natural corundum samples. Based on the current study this is undoubtedly the mechanism whereby heat-treated corundum from Chimwadzulu acquired these features. This adds weight to the argument that in natural corundums, derived from alkali basalts, overheating through incorporation of corundum megacrysts into a hot >1200°C ascendant alkali basalt magma, is the most probable cause of such features.

Sutherland *et al.* (1996) in their systematic study of inclusions in corundum from basalt fields, mostly from Asia and Australia, compiled a comprehensive list of primary solid inclusions that characterised the so-called BYG (Blue-yellow-green) 'magmatic' suite of corundum. Diaspore and amphibole, though present in Chimwadzulu samples, have not been reported from the BYG suite. Conversely, Fe- and Si-rich glassy inclusions, whilst common in the BYG corundums are absent from the Chimwadzulu specimens. In summary, the solid inclusion evidence strongly suggests that Chimwadzulu corundums do not belong to the 'magmatic' suite of Sutherland *et al.* (1996) and are unrelated to alkali basalts. This is consistent with the geological setting of Chimwadzulu Hill where such rocks are absent.

Multiphase diaspore-CO_2 inclusions in unheated Chimwadzulu corundum provide an additional clue for their primary origin. It is apparent from the consistency of phase proportions that these inclusions represent trapped portions of an originally homogenous fluid phase present during the primary growth and/or recrystallization of the host corundum. It is beyond the scope of this present study to provide a meaningful estimate of the *PT* trapping conditions for these inclusions in the absence of homogenisation temperature measurements. However, the trapped fluid has an Al-rich, CO_2-H_2O (±NaCl-$CaCl_2$) composition more compatible with a metamorphic or hydrothermal fluid than a silicate magma (see Roedder, 1984). Unfortunately, diaspore-CO_2 inclusions, though characteristic of Chimwadzulu corundums, do not appear to be unique to this locality. They are also reported to occur in Mong Hsu (Myanmar) rubies (Perretti and Mullis, 1997).

In heated Chimwadzulu samples it is suggested that the groups of darkened inclusions are the result of leakage and transformations within original CO_2-diaspore multiphase inclusions. The apparent 'emptiness' is due to the thermal decomposition of diaspore to corundum (Perkins *et al.*, 1979):

$$2AlO(OH) = Al_2O_3 + H_2O$$

The build up of internal fluid pressure on heating (from CO_2 and released water) would induce decrepitation and leakage of these volatiles out from the inclusions. The aluminium oxide produced would crystallize as corundum either inside the inclusions or within the heat-induced micro fractures as a sealant.

Conclusions

Clusters of zircon crystals and planes of multiphase diaspore-CO_2-bearing inclusions are the predominant inclusion types so far recognised in Chimwadzulu corundums. Rutile needles and a large amphibole crystal have also been identified. The observed inclusion assemblage, aspect ratios and lack of radial features surrounding individual zircon crystals, together with preliminary chemical data strongly suggest a primary metamorphic/hydrothermal rather than a magmatic alkali basalt source for the eluvial corundums and rubies of Chimwadzulu Hill.

The diaspore-CO_2-bearing inclusions are thought to represent trapped portions of Al-rich, CO_2-H_2O (±Ca-Na-Cl) metamorphic/hydrothermal fluids responsible for primary corundum deposition.

In heat-treated corundum, the diaspore-bearing inclusions have been destroyed. Thermal decomposition of diaspore to corundum takes place with the concomitant expulsion of CO_2 and H_2O from the inclusions. By analogy, the radiating features (so-called 'saturns') commonly reported around zircon inclusions in untreated corundums associated with alkali basalts from other localities have similar origin. They appear to be caused by differential expansion and contraction between zircon and corundum when cool corundum xenocrysts are incorporated into hot basaltic magma. In the wider context, therefore, it is suggested that their occurrence in untreated samples, may provide a simple criterion for distinguishing this environment from other primary geological/genetic environments (e.g. hydrothermal, metamorphic, pegmatitic).

Acknowledgements

David Hargreaves (Agricola Resources) kindly provided samples from Chimwadzulu and some background information on mine production. The author is grateful to Ian Gill, Vic Mansell and June Falla (Faculty of Science, Kingston University) for their help with sample preparation and UV-visible spectroscopic analysis, and to Dr J. Williams and Ms Joanne Greenwood (NERC ICP-MS facility, Kingston University) for providing preliminary Laser-ICP-MS analysis.

References

Burke, E.A.J., 2001. Raman microspectrometry of fluid inclusions. *Lithos*, **55**, 139-58

Bloomfield, K.L., 1958. The Chimwadzulu Hill ultrabasic body. *Trans. Geol. Soc. South Africa*, **61**

California Institute of Technology. Mineral Spectroscopy Server web pages (2001) http://www.minerals.gps.caltech.edu/files/raman/index/hmtl. Modified 7 April 2001

Deer, W.A., Howie, R.A., and Zussman, J., 1992. *An Introduction to the Rock-Forming Minerals*. 2nd edn. Longman, Harlow, UK. pp.696

Emmett, J.L., 2000. An update on ruby and sapphire from Chimwadzulu Hill, Malawi. *Gems and Gemology*, **36**(1), 71-3

Guo, J.F., O'Reilly, S.Y., and Griffin, W.L., 1996. Zircon inclusions in corundum megacrysts. 1. Trace element geochemistry and clues to the origin of corundum megacrysts in alkali basalts. *Geochim. Cosmochim.* Acta, **60**(13), 2347-63

Milisenda, C.C., Henn, U., and Henn, J., 2001. New gemstone occurrences in the south-west of Madagascar. *J. Gemmol.*, **27**(7), 385-94

Peretti, A., and Mullis, J., 1997. Distinction of natural and synthetic rubies by fluid inclusion analysis. Abstract, 14th Biennial meeting on European Current Research on Fluid Inclusions (ECROFI XIV), Nancy, France, July 1997, 264-265, Abstracts volume. Also available on http://www.gemresearch.ch/inclusions/inclanal.htm

Perkins, D., Essene, E.J., Westrum, E.F., and Wall, V.J., 1979. New thermodynamic data for diaspore and their application to the system Al_2O_3-SiO_2-H_2O. *Amer. Min.*, **64**, 1080-90

Roedder, E., 1984. Fluid Inclusions. *Amer. Min. Soc., Revs, in Mineral*, **12**, pp. 644

Schubnel, H.-J., Pinet, M., Smith, D.C., and Lasnier, B,. 1992. La microsonde Raman en Gemmologie. *Assoc. Franc. de Gemmol.*, Paris. pp. 61

Schwarz, D., and Schmetzer, K., 2001. Rubies from the Vatomandry area, eastern Madagascar. *J. Gemmol.*, **27**(7), 409-16

Shepherd, T.J., Rankin, A.H., and Alderton, D.H.M., 1985. *A practical guide to fluid inclusion studies*. Blackie, Glasgow. pp. 239

Srithai, B., and Rankin, A.H., 1999. Fluid inclusion characteristics of sapphires from Thailand. *In: Mineral Deposits: Processing to Processes, (Stanley, C.J., et al.,* Eds), Balkema Press, Rotterdam. Vol. 1, 107-10

Sutherland, F.L., Hoskin, P.W.O., Fanning, C.M., and Coenraads, R.R., 1996. Models of corundum origin from alkali basaltic terrains: a reappraisal. *Contrib. Min. Petrol.*, **133**(4), 356-72.

Williams, J., and Greenwood, J., 2001. Personal Communication. NERC ICP-MS Unit, Kingston University, Surrey, KT1 2EE

Notes from the Laboratory

Stephen Kennedy

The Gemmological Association and Gem Testing Laboratory of Great Britain
27 Greville Street, London EC1N 8TN

ABSTRACT: An unusually pungent amber imitation is encountered. YAG as an emerald imitation, a Gilson N-type synthetic emerald, a large synthetic amethyst and an annealed synthetic diamond are considered. An unusual situation of natural pearls being coated is presented.

Sweet smelling amber imitation

A bracelet of ten yellow beads (*Figure 1*), each including readily recognizable bees (*Figure 2*), was quickly identified as being plastic. In handling the bracelet you were also very quickly made aware of a pungent honey-like smell. It was difficult to ascertain if this was an intentional ploy or had occurred simply by accident. In some of the beads the included bee insects have been exposed at the surface and this could be the source of the sweet but somewhat unpleasant odour. The bracelet was quickly returned to the customer!

Figure 1: *A bracelet of 10 yellow plastic beads, each with an included bee insect.*

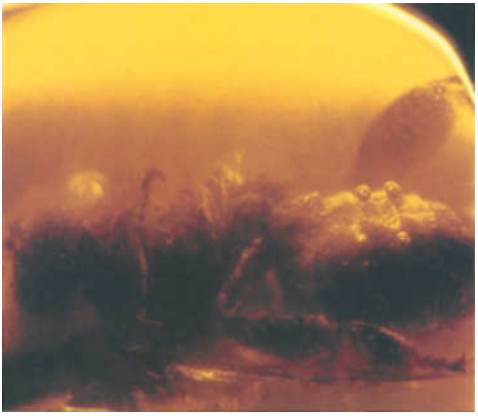

Figure 2: *A close-up view of a bee insect in a yellow plastic bead.*

An old favourite

A 10.29 ct green rectangular, cut-cornered, fancy-cut stone was submitted in the hope that it was an emerald. Some years ago a collection of rough green stones were similarly believed to be emeralds. All the stones were yttrium aluminium garnet (YAG) with rare-earth spectra. The faceted stone had an SG of 4.54 and a Brewster angle of 60.5 degrees. Green YAG does not duplicate the hues of emerald very well but it can still prove to be a problem.

Colourless YAG was the main diamond simulant used before the advent of cubic zirconia. It is rare to come across these in the trade today. The dispersion is lower than

ISSN: 1355–4565

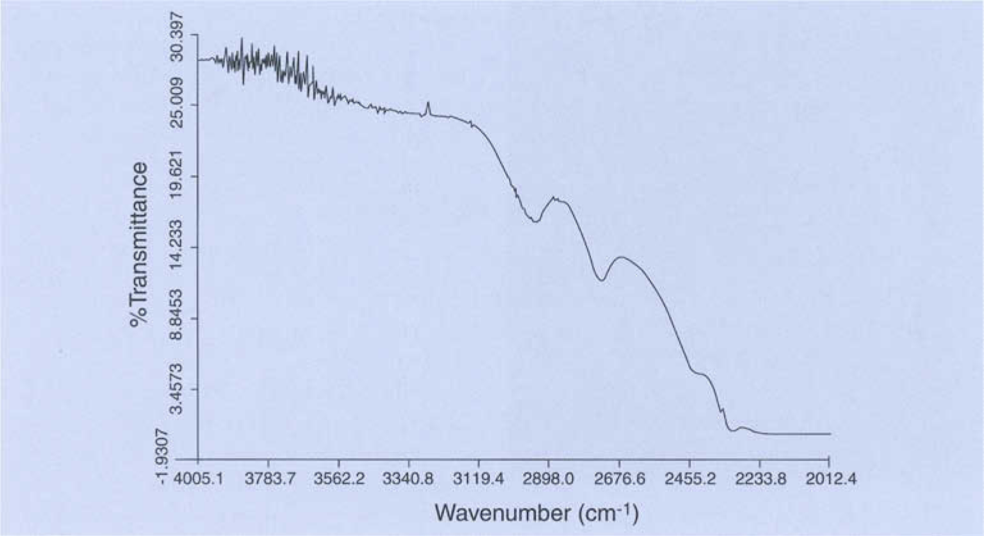

Figure 3: *FTIR spectrum of the Gilson N-type flux-melt synthetic emerald showing the lack of absorption between 3400 cm^{-1} and 4000 cm^{-1}.*

that of cubic zirconia, which makes YAG a less effective diamond simulant than CZ. Yellow YAG can more easily be confused with a fancy yellow diamond, since the perceived differences in dispersion are masked by the body colour. The confusion can be compounded if a fancy step-cut is utilized rather than a brilliant cut. The lack of brilliance may be mistakenly attributed to the way in which the stone has been cut, whereas in reality the stone is not diamond at all. Coloured YAG is becoming scarce.

Gilson N-type synthetic emerald

After a gap of fifteen years or more an uncommon synthetic flux-melt emerald was submitted mounted in a ring. The emerald-cut stone, weighing 2.05 ct, had refractive indices of 1.576 and 1.581. These refractive indices would normally be those expected for either a natural emerald or a hydrothermal synthetic emerald. The presence of vague twisted veils and straight zoning within the stone were more indicative of a flux-melt synthetic, and the FTIR spectrum (*Figure* 3) provided the evidence that the stone was synthesized in a non-aqueous environment – there is no absorption

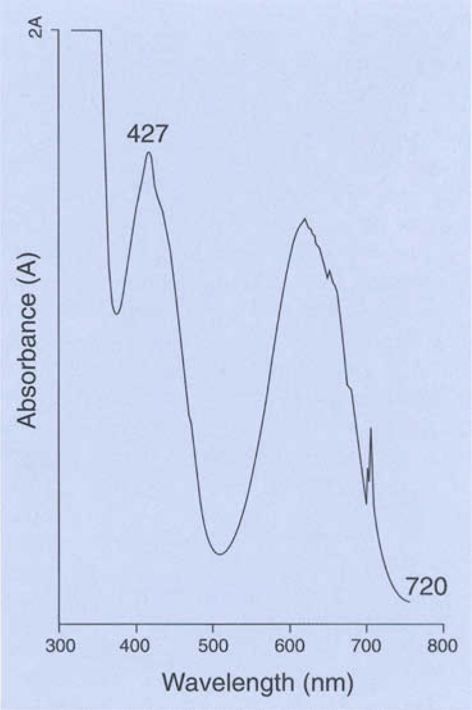

Figure 4: *The UV/Visible spectrum for a Gilson N-type flux-melt synthetic emerald displaying the 427 nm absorption band.*

Figure 5: *The cubic, octahedral and dodecahedral growth sectors of a 0.34 ct yellow synthetic diamond as seen on the DiamondView™.*

between 3400 cm^{-1} and 4000 cm^{-1} typical of natural emeralds and hydrothermal synthetic emeralds (Stockton, 1987). Gilson synthesized a limited quantity of his flux-melt emeralds with a small percentage of iron in the formula (Fryer,1969/70). These N-type synthetics have higher refractive indices and an absorption line in the violet at 427 nm. The absorption band in the violet can be observed with a hand spectroscope and is seen to be of similar strength to the absorption lines of aquamarine i.e. it is not strikingly apparent. The ultra-violet/visible spectrum (*Figure 4*) reveals that the 427 nm band is superimposed on the general absorption seen in emerald centred at 430 nm. A known sample from our collection showed a similar spectrum with refractive indices of 1.570 – 1.575.

Synthetic amethyst

The Laboratory was requested to determine whether a 63.96 ct amethyst was natural or synthetic. A colourless zone within the pavilion area was immediately noticeable. Immersed in water, this was seen to be a colourless band not quite parallel to the girdle and marked by two milky planes containing unrecognizable detritus but also including a few short needles. Furthermore all the zoning within the purple areas was parallel to the colourless zone. This had all the hallmarks of a seed crystal in a synthetic, and this interpretation was supported by the infrared spectrum, which revealed the 3542 cm^{-1} which is normally taken to be indicative of synthetic amethyst (Zecchini and Smaali, 1999).

Synthetic diamond

A round brilliant yellow diamond weighing 0.34 ct was submitted for an origin of colour determination. The stone was found to be a synthetic diamond, which had been subsequently annealed. The diamond fluoresced and phosphoresced a strong yellow under ultra-violet light, marginally stronger under long wave than short wave. However the presence of an inert narrow cross-shape observed on the pavilion side indicated that the diamond was synthetic. *Figure 5* shows the pattern to better effect as displayed on the DiamondView™. The inert cross-shape is related to the narrow sectors seen between the fluorescent blue areas (the fluorescing colours are different under the ultra-violet lamp), which are respectively the dodecahedral and octahedral growth sectors of the synthetic diamond crystal (Welbourn *et al.*, 1996) from which the stone was cut. The area above these sectors, seen as a relatively inert section of a rectangle, is the cubic sector of the cubo-octahedral crystal, which is a typical crystal habit for synthetic diamond. The phosphorescence on the DiamondView™ exceeded two minutes and was typical for a synthetic diamond.

The visible spectrum of the stone was recorded with a Pye Unicam PU8800 UV/VIS spectrophotometer with a liquid nitrogen cryogenic facility. The following peaks were noted: 468, 473, 478, 491, 494, 501, 503, 511, 516, 518, 527, 540, 547, 553 and 639 nm. These peaks have been attributed to nitrogen-containing synthetic diamonds grown in a nickel-containing flux and

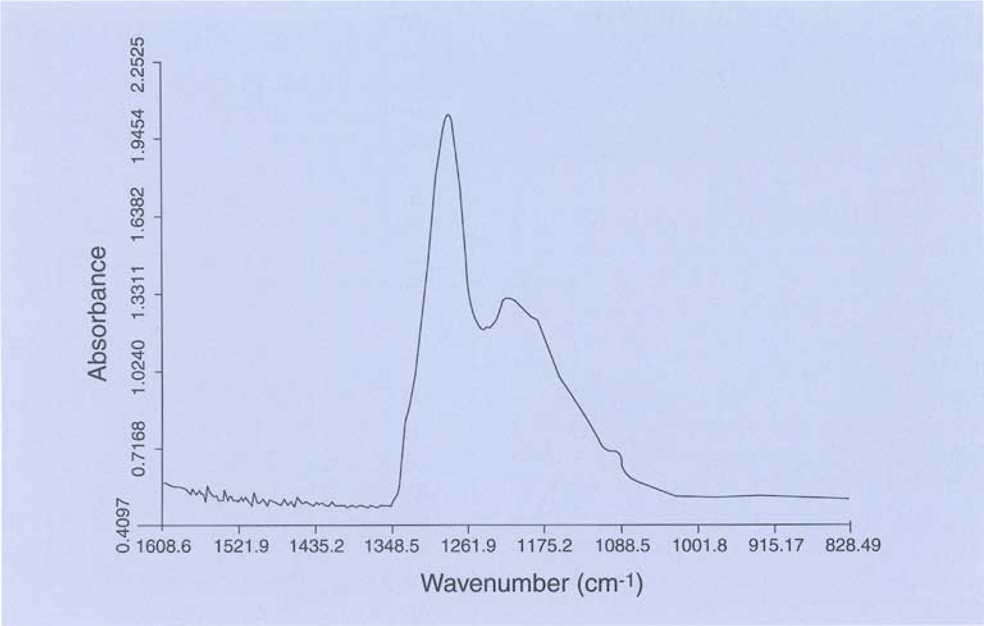

Figure 6: *The FTIR spectrum of the 0.34 ct yellow synthetic diamond. The main peak at 1282 cm*$^{-1}$ *categorizes the diamond as type IaA (pairs of nitrogen atoms). The shoulder on the left-hand side of the peak is in the general area of the 1344 cm*$^{-1}$ *peak, which indicates a small amount of type Ib (single nitrogen atoms).*

Figure 7: *Partly coated natural pearls. The grainy surface of the applied coating can be observed next to the platy nacreous surface.*

subsequently annealed to 1600° – 1900° Celsius (Shigley *et al.*, 1993). The conversion of dispersed nitrogen in the as-grown synthetic diamond to A aggregates (pairs of nitrogen atoms) after annealing is confirmed by the infrared spectrum (*Figure 6*), which categorizes the diamond as mainly type IaA with only a small amount of Ib (single nitrogen atoms) remaining.

It transpired that the Laboratory was being tested to see if it could differentiate between natural and synthetic diamonds. The diamond originated in Russia from an established industrial synthetic diamond supplier. The client had presented his stone to a British university, who had simply confirmed that it was a diamond. This situation has arisen before with other synthetic stones being submitted to academic institutions with similar results. Scientists in other fields may not necessarily be aware of the existence of the synthetic counterparts of natural minerals.

Coated pearls

Can you change an imitation pearl into a natural pearl? Yes, if what appears to be an imitation pearl is in fact a natural pearl to which an imitation-like coating has been applied!

Three bags of pearls were submitted for testing in advance of being strung as a three-row necklace. The X-ray radiograph isolated six nucleated cultured pearls and one non-nucleated cultured pearl. From the radiograph, samples of the remainder showed features typical of natural pearls. However, very early in the examination it had been noted that some of the pearls were partly or fully coated (*Figure 7*). In fact 78 out of the 233 pearls were partly or fully coated including one of the nucleated cultured pearls. For what reason would anyone want to do this? Especially as it was the larger pearls that had been coated (the 78 pearls are 56% of the weight of the 233 pearls). Admittedly the pearls were irregular in shape and many had been ground and buffed but still the nacreous surface was better than the coated appearance.

References

Fryer, C.W., 1969/70. Non-fluorescent high-property synthetic emeralds. *Gems & Gemology*, **13**(4), 106-11

Shigley, J.E., Fritsch, E., Koivula, J.I., Sobolev, N.V., Malinovsky, I.Y., and Pal'Yanov, Y.N., 1993. The Gemological properties of Russian gem-quality synthetic yellow diamonds. *Gems & Gemology*, **29**(4), 228-48

Stockton, C.M., 1987. The separation of natural from synthetic emeralds by infrared spectroscopy. *Gems & Gemology*, **23**(2), 96-9

Welbourn, C.M., Cooper, M., and Spear, P.M., 1996. De Beers natural versus synthetic diamond verification instruments. *Gems & Gemology*, **32**(3), 156-69

Zecchini, P., and Smaali, M., 1999. Identification de l'origine naturelle ou artificielle des quartz. *Revue de Gemmologie*, 138/139, 74-84

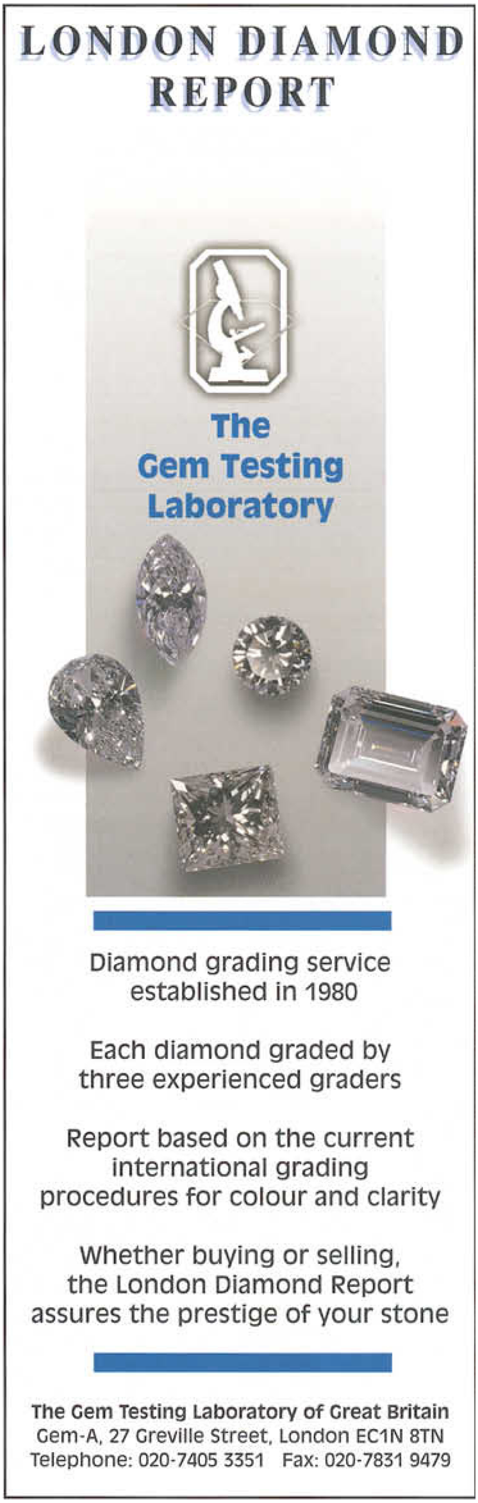

A note on chocolate-brown opal associated with volcanic rocks in Somaliland

Judith A. Kinnaird

Economic Geology Research Unit, University of Witwatersrand,
Private bag 3, 2050 Wits, South Africa

ABSTRACT: Precious opal from Somaliland comes from the Qabri Bahar area near Jodha close to the border with Ethiopia and Djibouti. The opal occurs as nodules associated with acid volcanic rocks of Miocene age and a range of colours are present; the best precious opal has a chocolate-brown body colour.

Introduction

Opal from Ethiopia has been reported in literature (Johnson *et al.*, 1996) and is now widely available in various markets. More recently, opal from Somaliland has also been shown to dealers and cutters on various continents and it was reported at the 1999 Tucson gem show (Weldon, 1999). However, the origin of the Somaliland opal has been questioned, with the implication that it too is of Ethiopian origin. It is the intention of this short paper to document the source of these Somaliland opals and to introduce them to a wider

Figure 1: *Uncut opal nodules 25 mm and 42 mm in diameter. The larger nodule shows the typical white crust, whilst the smaller nodule shows a little green fire (top left).*

ISSN: 1355–4565

community. Although the opal occurs in a variety of colours, the best gem material is unusual because of its brown body colour.

Opal characteristics

The opals occur as nodules with a thin white outer crust varying from 1-5 mm. The nodules are generally more or less spherical and range in size from 1 cm in diameter to more than 5 cm. The nodules are solid with no empty space at the centre, one onyx nodule with 'horizontal' brown and white colour bands has also been noted. There is a broad colour range in the opal nodules, and common opal varies from white to yellow, orange, red or chocolate-brown and may be transparent to translucent (*Figure 1*). Orange-coloured fire opal and other colours show a little play of colour, which is most easily visible in transmitted light. However, it is the chocolate-brown material that displays the most striking play of colours, with intense flashes of red and green and more rarely, royal blue. Colour patches are irregular, rounded or elongate, commonly reaching 5 mm or more in size. In some cabochons, there is a suggestion of banding with different colour flashes within each 'band' (*Figure 2*). Other patches of colour seem to derive from an amalgamation of smaller pin-fire colour spots. In some polished cabochons, irregular dark patches of a leopard-skin pattern characterise the stone, and are reminiscent of patterns described from artificial opal.

***Figure 2:** Chocolate-brown opal 21 x 19 mm in size weighing 8.10 ct showing faint banding and elongate red colour patches extending up to 5 mm or more in size. Green colour patches in this cabochon appear to be derived from an amalgamation of smaller pinfire colour spots. Cut by Mike Weston of Johannesburg, photographed by Paul Nex.*

Tens of kilos of opal nodules from Somaliland have been examined in the rough. Less than half of these are of gem quality and only a very small proportion, probably around 5% have a good play of colour. However, the abundance of the nodules on sale from artisanal miners and traders means that there is an abundance of good-quality gem material available. Because the nodules are spheroidal and solid with no central cavity, it is possible to cut any gem material with an intense play-of-colour into quite large thick pieces. A 65 ct opal measuring 30 x 27 mm across is shown in *Figure 3*. Brown opals, showing good colours, have been made into fine individual pieces of jewellery by Mike and John Weston of Johannesburg. These have attracted much attention both in local markets and in North America.

Stability of this brown gem material is good, with little or no crazing developing in the twelve months after cutting. Although sawn and cobbed paler stones have been known to develop crazing, the more precious material appears less likely to crack. A review of stability and durability of these opals is in progress. The water content of one precious brown opal was found to be 5%. Qualitative EDXRF on Somali samples showed the presence of calcium, iron, strontium, zirconium, potassium, niobium and sulphur as trace elements (Kinnaird and Jackson, 2000).

Origin of the opals

The Somaliland opals bear a remarkable similarity in terms of size, colour, nodular appearance and trace element chemistry to opals from the Shewa Province in Ethiopia, some 300km to the west (Johnson *et al.*, 1996). However, there are no descriptions of any brown opals with intense colour flashes from this source. The Shewa opals occur as nodules in acid volcanic rocks in a layer of welded tuff (approaching obsidian in character) about 3m thick, between sub-horizontal rhyolite layers (Johnson *et al.*, 1996). The volcanic pile is 300-400m thick and believed to be of Miocene age (8-27 Ma). Similar Miocene volcanic rocks occur in Somaliland west of Cabdulqaadir near the border with Ethiopia (Abbate *et al.*, 1993). The chocolate-brown opals from Ethiopia are said by traders to come from the Awash Valley area. On the Somaliland side of the border, opals are currently being exploited in the Qabri Bahar area close to a place called Jodha near the Ethiopian/Djibouti border. At present the nodules are simply collected from the surface and pits have not yet been developed.

Opals originating from rhyolites are known from elsewhere in the world especially Mexico, Honduras, Indonesia, the United States and Coromandel, New Zealand (O'Donoghue, 1988). Smith (1988) reported 'thunder eggs', in which geodes occur in glassy basal vitrophyric rhyolite at Opal Butte, Oregon, which has locally been altered to a pastel-coloured clay. Approximately 70% of the geodes contain botryoidal or stalactitic agate, banded agate, quartz, etc, with no opal, 20% of the geodes contain common opal and <10% contain some gem opal with only 1% having opal with a prominent play of colour. Spencer *et al.* (1992), suggested that orange-to-red fire opals from rhyolites at Querétaro, Mexico formed at temperatures <160°C from fluids with moderate salinity and a high proportion of silica in solution. In these localities, the opal is found as secondary fillings in gas cavities and voids within the lava.

Figure 3: *A 65 ct chocolate-brown opal measuring 30 x 27 mm across showing a good play of green and red colours. Cut by Mike Weston of Johannesburg, photographed by Paul Nex.*

Discussion

Opals in volcanic environments generally have a structure based on disordered interlayering of cristobalite and tridymite, with the play in spectral colours produced from a three-dimensional array of silica spheres and voids which have to be regularly stacked for diffraction to take place (O'Donoghue, 1988). Whilst the size of these spheres is commonly regarded as ranging from 150-400 nm, according to Fritsch *et al.* (2001) the spheres in Mexican and Ethiopian fire opals are 10-40 nm in size and the nanoparticles may be fully disordered. Opals with a play of colour from Mexico and Ethiopia show higher degrees of organisation in which the nanoparticles form pseudospheres or aggregates of appropriate size (about 200 nm) with diffraction due to contrast in index of refraction between spheres of different degrees of crystallinity (Fritsch *et al.*, 2001). Thus volcanic opals from Mexico and Ethiopia have much smaller spheres (10-40 nm) than the building blocks of typical Australian opals (140 to 250 nm). Fritsch *et al.* (2001) have also shown that the orange-to-brown colour in Mexican orange-to-brown fire opal is due to nanoinclusions of needles of an iron-containing mineral such as hematite 10-20 x 100-200 nm in size rather than to dispersed metal ions. Although it remains to be proved, it is envisaged that the Somaliland chocolate-brown colour may also be due to the occurrence of such nanoinclusions, possibly of iron, strontium, zirconium or niobium phases based on EDXRF analyses of the opals.

Conclusion

What makes the Somaliland/Ethiopian occurrence of gem opals of such interest is the size, unusual colour and availability of the gem material. The nodular form of the chocolate-brown gem opals means that when nodules with a good play of colour are found, large cabochons can be cut and the durability of the material so far produced is encouraging for the development of this gem material from Somaliland. In addition, there is the potential for a sustained and long-term supply.

Acknowledgements

The author would like to thank Kasbo International and particularly Mohammed Abubakar for organizing a trip around Somaliland. Thanks to all those people who helped to get me to various remote gem localities on my last visit. Mike Weston and Paul Nex are thanked for their help and infectious enthusiasm.

References

Abbate, E., Sagri, M., and Sassi, F.P., 1993. Geology and Mineral resources of Somalia and surrounding regions (with a geological map of Somalia 1:1,500,000). A: regional geology 416 pp; B: Mineral and Water resources 417-733. N113B. Relazioni e Moniografie Agrarie Subtropicali et Tropicali Nuova Serie. Istituto Agronomico per L'Oltremare, Firenze

Fritsch, E., Ostrooumov, M., Rondeau, B., Barreau, A, Albertini, D., Marie, A-M., Lasnier, B., and Wery, J., 2001. Mexican gem opals: nano- and micro-structure, Raman spectra, origin of colour, and comparison with other common opals of gemmological significance. 11th Annual Goldschmidt Conf. Abstr. 2001

Johnson, M.L., Kammerling, R.C., DeGhionno, D.G., and Koivula, J.I., 1996. Opal from Sherwa Province, Ethiopia. Notes on new techniques. *Gems & Gemology*, **32**(2), 112-20

Kinnaird, J.A., and Jackson, B., 2000. Somaliland – a potential gem producer in the Mozambique belt. *Journal of Gemmology*, **27**(3), 139-54

O'Donoghue, M., 1988. *Gemstones*. Chapman and Hall, London, 372 pp

Smith, K.L., 1988. Opals from Opal Butte, Oregon. *Gems and Gemology*, **24**(4), 229-36

Spencer R.J., Levinson, A.A., and Koivula, J.I., *1992*. Opal from Querétaro, Mexico: fluid inclusion study. *Gems and Gemology, 28(1), 28-34*

Weldon, R., 1999. Opal nodule. Gemstones and pearls: News. www.professional_jeweler.com/archives

Inclusions in gemstones: their cathodoluminescence (CL) and CL spectra

Johann Ponahlo

*Senior Research Associate at the Dept. for Mineralogy and
Petrography of the Museum for Natural History, Vienna, Burgring 7,
A-1010, Vienna, Austria.*

ABSTRACT: From a study of inclusions in gemstones by means of cold-cathode CL microscopy and microspectrophotometry ten examples containing different inclusions are described. The results of visual microscopic tests of the luminescing inclusions with photomicrographs and spectral curves render valuable information on the type of inclusions present. Strongly luminescing, even small colourless inclusions such as apatite, fluorite or diopside can easily be detected which otherwise may escape notice. Further details on both inclusions and host can be obtained when running CL spectra in the spectral range from 380 to 950 nm. Due to the small penetration depth of electrons into solids, all CL investigations can be carried out only if the inclusions intersect the surface of a facet of the gemstone host. Striking colour differences between the CL colour of the host and the inclusion will assist their differentiation. This method also assists in the distinction between inclusions which otherwise are difficult to separate by optical microscopy. The cold-cathode CL is a non-destructive fast method using commercially available instruments on samples which need no coating or other treatment.

Introduction

Luminescence excited by means of electrons has long been used in research work on minerals and gemstones, primarily on diamonds. Natural and synthetic crystals have been studied within the last forty years, although the beginning of testing gemstones by this method dates back to the beginning of the last century, when Michel (1926) in Vienna carried out many tests on a series of gemstones. About two years ago while studying various rough ornamental gems, traces of ruby and other luminescing substances in the polishing medium could be detected by means of cathodoluminescence (CL). Subsequently, when the idea of using CL to study inclusions reaching the surface of the host crystal was discussed with E. Gübelin and received a favourable response, the author decided to test the applicability of CL for the recognition and differentiation of inclusions in gemstones and ornamental gems.

ISSN: 1355–4565

Cathodoluminescence apparatus

An electron beam of 5 to 15 kV has a penetration depth into solids of not more than 2 µm. Thus, the method of cathodoluminescence (CL) – like the SEM and microprobe – is suitable for the study of surface effects. Inclusions become luminescent only if they reach the surface of the host crystal when they are hit directly by the electron beam. Then textures, growth structures, surface irregularities and crystal defects are made visible which otherwise may not even become noticeable under the microscope. Even very small inclusions enclosed in the surface of the host can be detected and photographed as soon as their CL colours differ from those of the host. CL spectra of inclusions can also reveal the chemical nature of the activator ions that cause the CL effect, give notice of minute differences of the same mineral inclusion in different host gemstones, or can indicate defect centres.

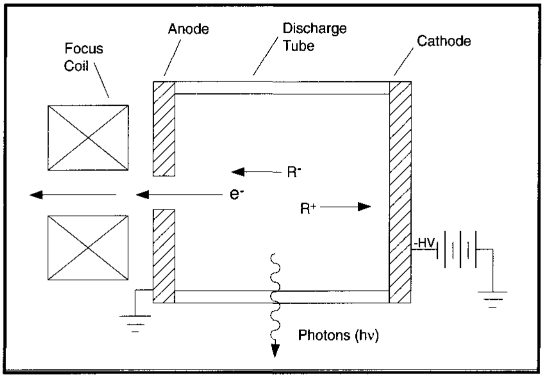

***Figure 1:** Schematic diagram of a cold cathode electron gun. Discharge tube, focus coil and compartment are flanged together and filled with a carrier gas at a low pressure. (Reproduced from Marshall, 1993.)*

Two different ways exist to excite electrons which provoke CL, and these are commonly known as the 'hot cathode' and the 'cold cathode' methods. The first, often called 'scanning CL', operates in a high vacuum of <10^{-6} mbar. The electrons are emitted from a hot filament and although this technique is used world-wide in television tubes, electron microscopes and microprobes, small 'hot cathode' instruments which can be combined with a microscope have not yet been commercially produced (Walker, 1991).

Other devices work by means of the 'cold cathode' method, also called 'microscopic CL'. These instruments are much more easily operated and are commercially manufactured. They operate in a vacuum of less than 100 mbar (Marshall, 1988) and are easily mounted on the table stand of a microscope. The sample rests in an evacuated compartment. The electrons are produced in a small evacuated glass discharge tube which is filled with the carrier gas, either air, nitrogen, or helium (*Figure 1*). During the gas discharge the electrons travel from the cathode through a hole in the anode horizontally into the sample compartment.

On its way through a solenoid (focusing coil) the electron beam can be broadened to about 3 cm diameter or narrowed to 1-2 mm. When entering the sample chamber the electron beam is deflected obliquely onto the surface of the sample (inclusion or host gemstone) by means of two ceramic magnets (not shown in *Figure 1*). The electron beam impinging on the surface of the sample excites luminescence which can be visually observed by the microscopist, or photographed. In contrast to the 'hot cathode method' the sample needs no conductive coating, which increases the brightness of CL images. Today long exposure times for photomicrography are not needed when using 800 ASA colour films. Recently developed digital imagery and processing will also help to improve CL photomicrography.

An electron beam of even less than 5 kV will create secondary X-rays. Therefore, the vacuum compartment is screened against leakage of X-rays by an upper and lower lead glass window. Microscopic inspection of samples is best carried out with long distance objectives (4 to 20 ×) resulting

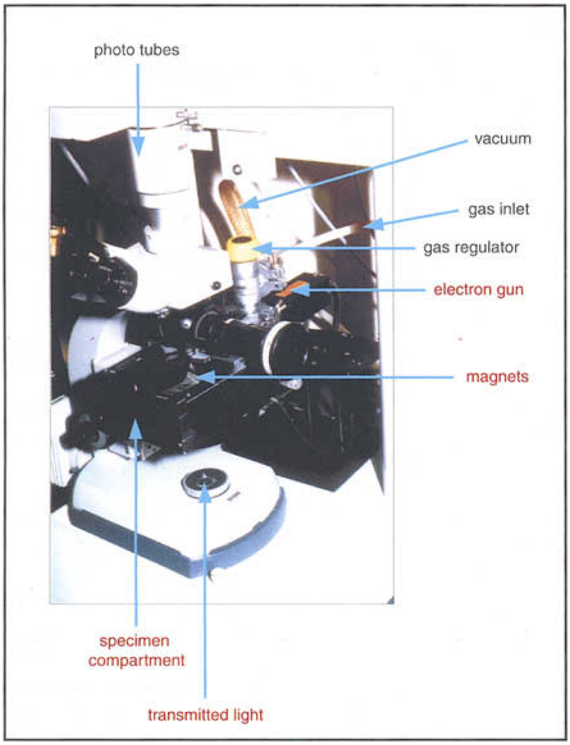

***Figure 2:** The 'cold-cathode' unit with the electron gun flanged to the compartment rests on the table stand of a binocular microscope. For microspectrophotometry the whole assemblage is set in a frame on which the motor-driven monochromator and photomultiplier is mounted. Vacuum pump, amplifier and computer are not shown.*

in magnifications up to 125 ×. Stereomicroscopes may also be used, if there is no need for CL microspectrometry. But the latter method is an excellent complementary means for CL studies as documented in the following paragraph.

Figure 2 shows an unsophisticated version of a CL apparatus for taking CL spectra of a wide range of small and larger samples, crystals and cut stones. The trinocular research microscope is combined with a monochromator and a photomultiplier both of which can be seen on top of the metallic frame of *Figure* 2. The CL signals of the sample pass the microscope and the monochromator, are transformed into electrical signals in the photomultiplier and amplified and processed in a computer (not shown). The whole assemblage is controlled by a software programme. All CL spectra can be taken in less than 25 seconds, and are processed by means of Sigma Plot 5.0. and Origin 5 software programmes (Ponahlo, 2000).

'Hot cathode' CL attachments to SEMs exist which enable the researcher to take CL spectra between 260 and 800 nm, of areas as small as a few μm^2, but only black and white SEM photomicrographs can be taken. Because of their lead glass windows 'cold cathode' instruments do not transmit radiation below 380 nm. To cover the UV range below 380 nm a quartz glass window has to be used with the CL apparatus mounted on the table stand of a quartz microscope. Such rather expensive outfits would enable the microscopist to observe luminescent objects up to 400× magnification and to obtain CL spectra between 240 and 1000 nm. In the present study a binocular research microscope was used which can yield spectra between 380 and 950 nm.

Results

The following descriptions contain both photomicrographs of the visual impressions and CL spectra that the gemmologist obtains when studying an inclusion during the bombardment by electrons. Ten examples are presented to give an idea of the kind of information obtained by this new non-destructive method.

Depending on the activator ions present in the host and in the inclusions a variety of effects may be anticipated. With the far larger area of the host offered to the impinging electron ray, the CL effects of the host gemstone are usually easier to study. But by narrowing the ray to a thin pencil of not more than two millimetres, good CL spectra can be obtained from most luminescing inclusions if the size is not too small. Sometimes it may be necessary to re-adjust the stone so as to offer a horizontal crown or pavilion facet of the host which contains the inclusion to be tested. Some CL spectra of minerals that occur as inclusions are already well known to the gemmologist, which greatly facilitates an assignment of the CL band in question. But different environments of a mineral inclusion often change the spectra of the inclusion obtained rendering a careful chemical analysis obligatory. To study an inclusion by means of CL it is an indispensable prerogative that the inclusion must reach the surface of the facet of the host. The electron ray has to hit a perfectly clean surface to guarantee results free of doubt.

No.	*Host gemstone*	*Inclusion*
1	spinel	apatite
2	spinel	dolomite
3	topaz	quartz and fluorite
4	garnet	apatite
5	kyanite	rutile
6	tourmaline	diopside and zircon
7	kornerupine	apatite
8	plagioclase	ruby
9	calcite	albite
10	dolomite	pargasite

Table I: *List of gemstones and their inclusions.*

(1) Spinel with apatite inclusions

The host is a rose-red round-cut spinel from Mogok, Myanmar (Burma), weighing 4.007 ct that contains numerous globular apatite inclusions, some of which themselves have very small black or red crystal inclusions. A luminescing apatite inclusion reaching the surface of the host is reproduced in *Figure 3*. The host shows a strong whitish-green CL which is caused by divalent manganese ions incorporated in the spinel lattice. After long electron bombardment the CL colour of the host changes to red which is caused by trivalent chromium. The true CL colour of the inclusion is partially masked by two strong CL bands of the host (*Figure 4*). CL spectroscopy at higher magnification reveals the presence of the apatite inclusion by a distinct shoulder in the greenish-yellow spectral range at ~ 600 nm. Other spectral features are Cr^{3+} bands at 676, 688 and 698 nm and a strong Mn^{2+}-based band at 526 nm which all belong to the spinel host.

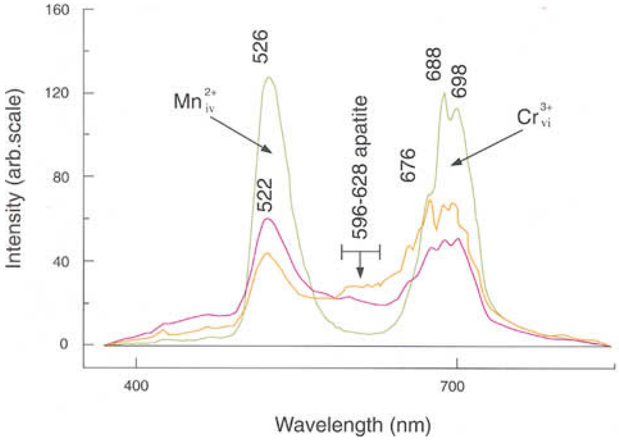

Figure 4: *CL spectra of the host spinel with two distinct bands. The shorter wavelength one is caused by Mn^{2+} ions in tetrahedral configuration, the other by Cr^{3+} ions in octahedral configuration. The shoulder between both bands can be ascribed to Mn^{2+} ions of the apatite inclusion, sevenfold co-ordinated.*

Figure 3: *CL of a globular apatite inclusion showing an orange CL colour. Its true colour is masked by the strong CL of the host crystal. Excitation conditions: 12 kV; 0.85 mA. Enlargement: 40* x.

(2) Spinel with dolomite inclusions

Another spinel (1.367 ct) of orange colour, also from Mogok, Myanmar, hosts a number of colourless dolomite inclusions with tension haloes. One euhedral dolomite crystal reaches the surface of one facet. It can be recognized by both normal microscopic methods and under the impact of electrons (*Figure 5*) when it luminesces red and exhibits the well-known band system (organ-pipe structure) in its spectrum (*Figure 6*). The weak band at 518 nm is ascribed to Mn^{2+} activator ions in the host, whereas the inclusion is indicated by a broad shoulder at 645 nm (*Figure 6*). In contrast to the tetrahedral co-ordination of manganese ions in the spinel lattice, the Mn^{2+} ions in the dolomite are octahedrally configurated which causes a shift of the manganese band from green to orange-red. The noisy bands in the short-wave spectral range are caused by the carrier gas air.

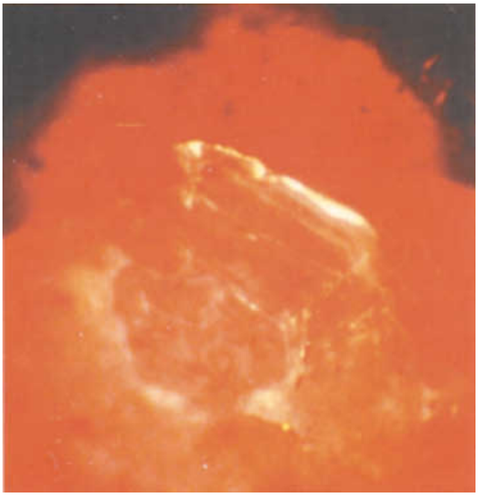

Figure 5: *Yellow CL of a euhedral dolomite crystal inclusion at the surface of the spinel. Part of the inclusion and tension haloes are very near to the surface of the host as yellow luminescing clouds. Excitation conditions: 16 kV; 0.8 mA. Enlargement: 100 x.*

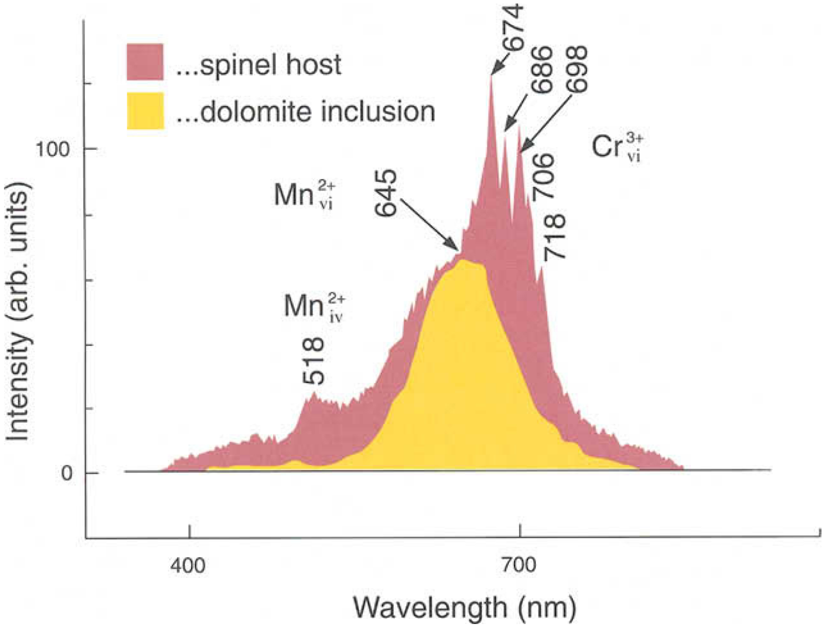

Figure 6: *CL spectra of the spinel host (pink) and curve-fitted dolomite spectrum (orange). Excitation conditions: same as in Figure 5.*

(3) Colourless topaz with quartz and fluorspar inclusions

A plate of polished topaz from Nigeria weighing 6.104 ct, contains numerous small quartz and colourless fluorite inclusions (see *Figure 7*). The host luminesces in a subdued steel blue, while the inclusions show a reddish-brown and a green CL colour for the two quartzes and the euhedral cubes of fluorite respectively. The CL spectra of *Figure 8* are characterized by a multitude of small bands which can be ascribed to the trivalent rare earth ions, dysprosium, terbium and samarium. The first element can be recognized in the CL spectra of both types of inclusion, the latter two are identified in the CL spectra of the fluorites, exclusively. Additionally, the broad short-wave bands of the host topaz indicate the influence of an intrinsic CL feature (defect centres).

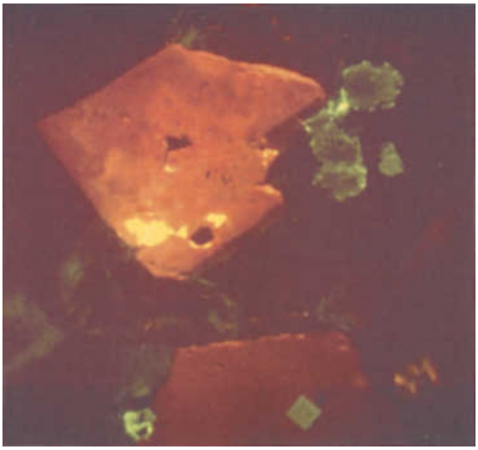

Figure 7: *Reddish-brown CL of quartz and green CL of fluorite inclusions both activated by rare earth elements. Steel-blue CL colour of the host (to the eye) has turned into dark maroon in the photomicrograph. Enlargement: 125 x. Excitation conditions: 12.5 kV; 0.9 mA.*

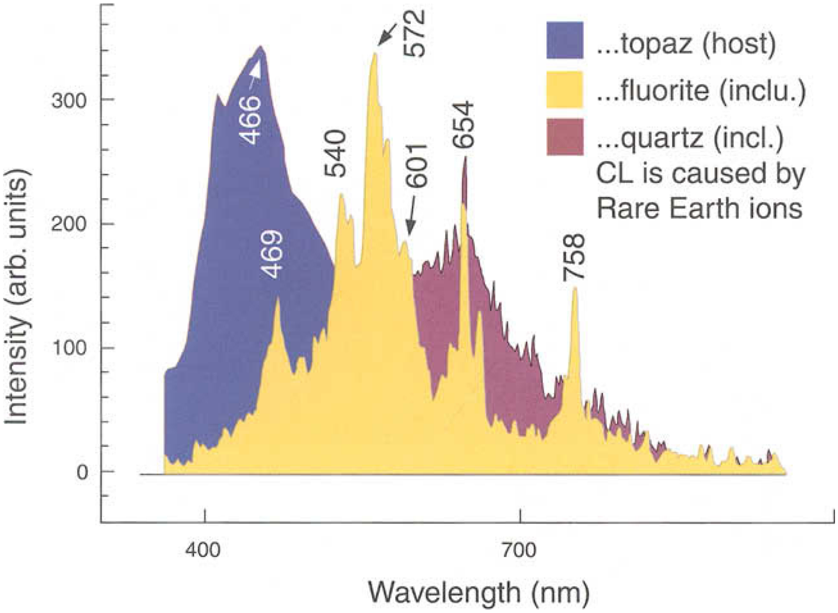

Figure 8: *CL spectra of host and inclusions. Topaz is shaded blue (dark maroon in Figure 7), quartz is shaded violet, and fluorite yellow. Excitation conditions 12.5 kV; 0.9 mA.*

(4) Garnet with apatite and quartz inclusions

Non-luminescing garnets may host a number of luminescing inclusions. An orange umbalite of 3.43 ct containing two apatite and one quartz inclusions which partly penetrate the surface of the rough host, is shown in *Figure 9*. The quartz houses a small zircon daughter crystal. Bombarded by electrons the apatite inclusion shows a bright yellow CL colour (*Figures 9 and 10*) while the quartz displays a greyish-white CL which could not be photographed because of its weak intensity. The CL spectrum of the apatite, as reproduced in *Figure 11*, consists of a broad, medium strong band at 569 nm caused by Mn^{2+} ions superimposed on a range of narrow bands of REE-activator ions of which Dy^{3+}, Sm^{3+} and Sm^{2+} ions are prominent. The broad quartz CL spectrum exhibits additional CL bands which are also caused by REE-activator ions. Such spectra demonstrate the wealth of information that can be obtained by CL microspectrophotometry, provided the inclusion intersects the surface of a stone.

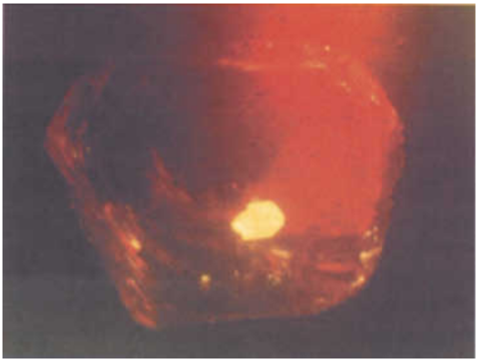

***Figure 9:** An orange umbalite with an apatite inclusion. The luminescing quartz inclusion is not visible. Excitation conditions: 15 kV; 0.95 mA. Enlargement: 40* x.

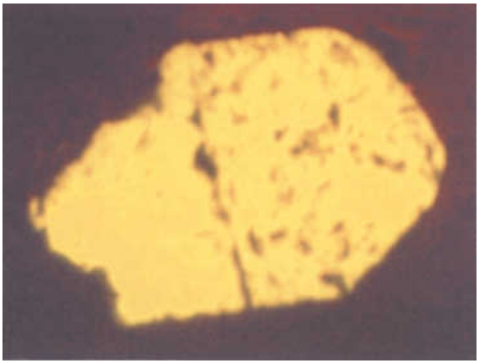

***Figure 10:** The yellow luminescent apatite at higher magnification. The colour is caused by Mn^{2+}, Dy^{3+}, Sm^{3+} and Sm^{2+} ions replacing Ca^{2+} ions in the apatite structure. Excitation conditions: 15 kV; 0.95 mA. Enlargement: 125* x.

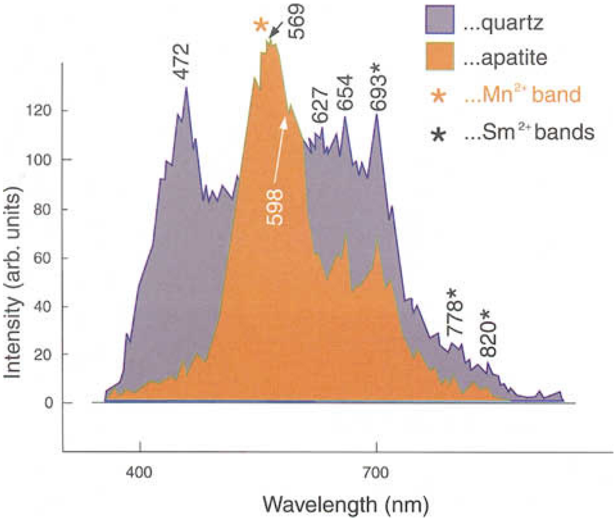

***Figure 11:** The Sm^{3+} band of the apatite at 598 nm (white arrow) is hidden by the prominent Mn^{2+} band at 569 nm. Note that even the quartz spectrum contains Dy^{3+}, Sm^{3+} and Sm^{2+} bands documenting the same growth history as the apatites.*

(5) Kyanite with rutile inclusions luminescing in the NIR

A faceted steel-blue kyanite of 6.925 ct contains a number of irregularly distributed euhedral rutile inclusions (*Figure 12*). The CL colour of the host is a saturated red whereas the rutile inclusions penetrating the surface of a pavilion facet which, although apparently non-luminescent (*Figure 13*), show a pleasing wine-red colour in incandescent light. The red CL colour of the host kyanite manifests itself by two prominent very narrow CL bands in the red at 688 and 704 nm which are a characteristic CL feature of kyanite caused by Cr^{3+} ions in the lattice. An additional spectrum of the non-luminescent rutile inclusion reveals a strong signal in the near infrared (NIR) with a broad band peaking at ~ 800 nm (*Figure 14*). This band cannot be assigned to a special activator ion at present, but there is no doubt that the signal has to be attributed to the rutile inclusion in the kyanite host.

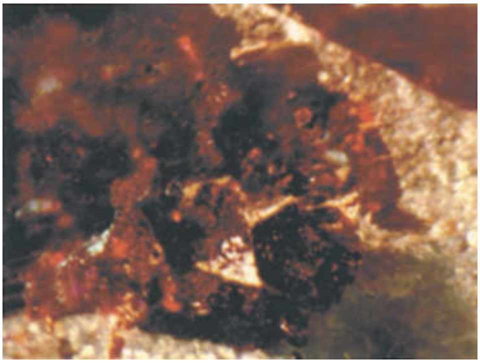

Figure 12: *Rutile inclusions in kyanite at the surface of a pavilion facet. Incandescent light, stereomicroscope ZEISS STEMI 2000C.*

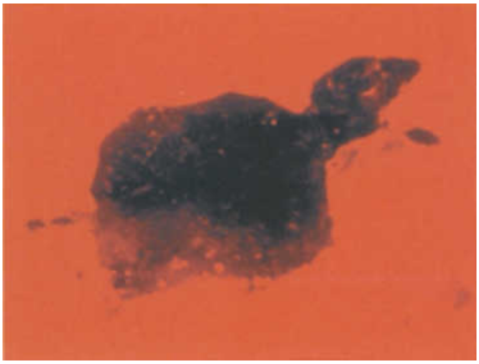

Figure 13: *Red CL of the host crystal with an inert rutile inclusion. It exhibits a strong broad CL band in the NIR. Excitation conditions: 11.0 kV; 0.9 mA. Enlargement: 40 x.*

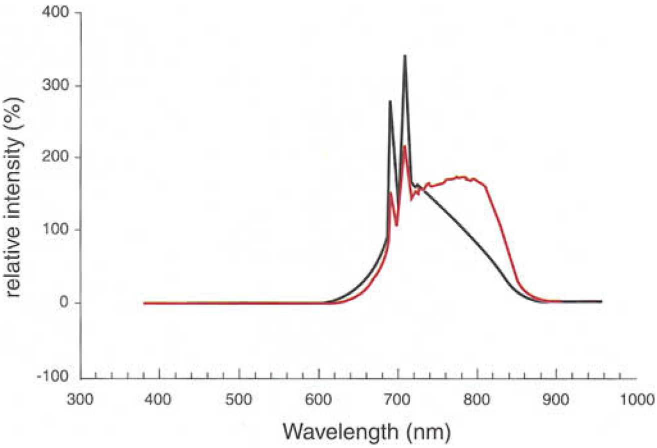

Figure 14: *CL spectra of the kyanite host (black) with its two characteristic narrow R-lines (see text). The rutile inclusion exhibits a broad band in the NIR at ~ 800 nm. Excitation conditions: 9.0 kV, 0.9 mA.*

(6) Tourmaline with a diopside and a zircon inclusion

Among the gemstones investigated, a green polished rough tourmaline of 3.884 ct was of special interest. It contained, besides a number of apatite inclusions, a small diopside crystal luminescing in a yellowish-white CL colour turning pale red after prolonged bombardment (*Figure 15*). The mineral diopside has a very characteristic CL spectrum and, as it has not been reported as an inclusion in tourmaline, SEM analyses were carried out (*Figure 16*). SEM X-ray analysis using an energy-dispersive detector yielded the spectrum shown in *Figure 17* and quantitative analyses of two spots are listed in *Table II*. The diopside inclusion was partly covered by a tiny zircon crystal, but this was too small for CL spectral analysis. The CL spectrum of the diopside (*Figure 18*) consists of three bands: a strong band at 578 nm is always combined with two weaker ones on each side at ~ 470-480 and at 730 nm in the NIR. The 578 nm main band can be ascribed to Mn^{2+} ions (Walker, 1985), the short-wave band is an intrinsic feature, and the band in the NIR is caused by trace amounts of Fe^{3+} ions.

Wt.%	I	II
SiO_2	49.26	48.71
TiO_2	0.62	0.92
Al_2O_3	10.43	11.45
Cr_2O_3	0.15	0.43
FeO	0.00	0.00
MgO	13.04	12.31
CaO	25.41	25.97
Na_2O	0.46	0.00
K_2O	0.40	0.20
Total	99.77	99.99

Table II: *Energy Dispersive XRF analyses of two spots in a colourless diopside inclusion in a green tourmaline host from Tanzania.*

Figure 15: *Pale red CL of a colourless diopside inclusion in a green non-luminescent tourmaline, Langenai, Tanzania. Excitation conditions: 0.8 mA; 11.0 kV. Enlargement: 125* x.

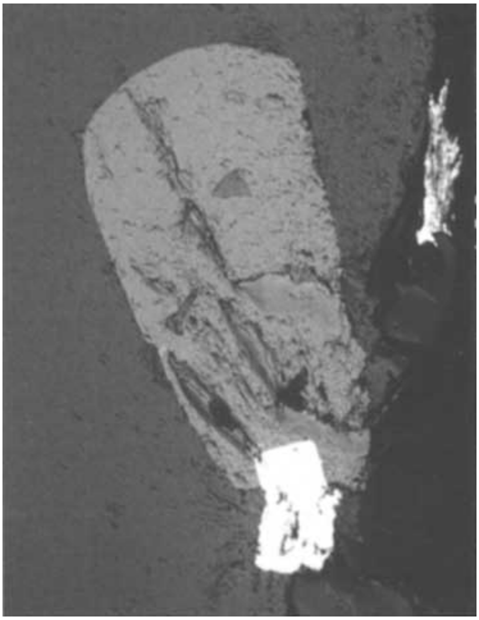

Figure 16: *SEM photo of the diopside inclusion in a green tourmaline (dark grey) with an adhering zircon crystal (white). Compare also the X-ray diagram of Figure 17.*

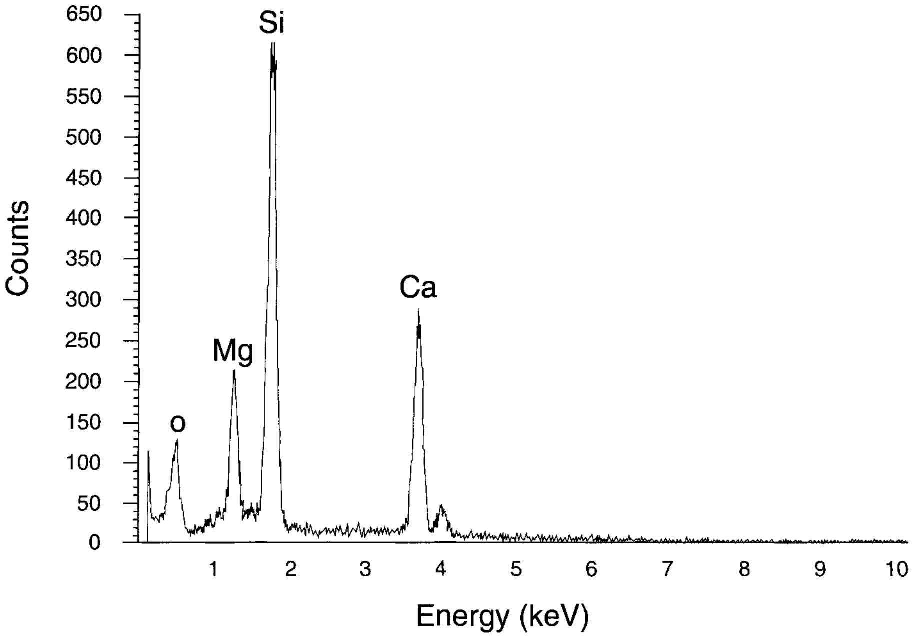

Figure 17: *Energy-dispersive X-ray fluorescence spectrum showing the major elements in the diopside inclusion. See also Table II.*

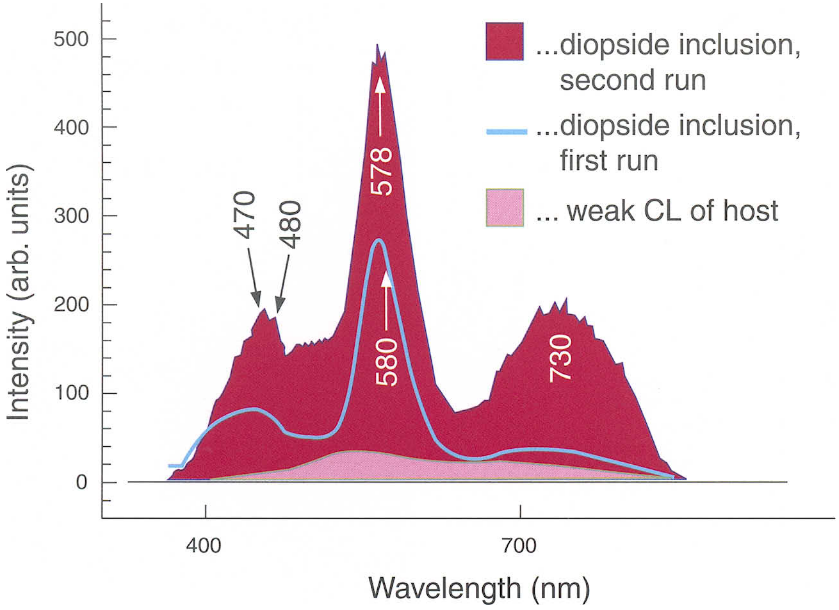

Figure 18: *The CL spectra of the colourless diopside inclusion shows a diagnostic band at 578 nm. The different intensities between the first and the second run reflect the CL colour change of the inclusion from yellowish-white to pale red during longer bombardment. Excitation conditions: 9.0 kV; 0.8 mA.*

(7) Kornerupine with apatite and zircon inclusions

Kornerupine gemstones commonly contain large euhedral apatite crystals and metamict zircons with tension cracks, a good example is the olive green navette of 5.02 ct from Sri Lanka. An apatite inclusion which reaches the table facet luminesces brownish-yellow (*Figure 19*) in contrast to the host which remains inert; this is due to a significant iron content that extinguishes any CL effect. *Figure 19* also shows some brownish-yellow luminescing small zircon crystals which apparently seem to adhere to the apatite inclusion. In reality they are not more than 1-2 µm below the surface of the table facet. The CL spectrum (*Figure 20*) of this apatite inclusion is instructive. While most apatites from pegmatitic, metamorphic or Alpine veins contain enough trace amounts of divalent manganese ions to form a strong band at ~ 570 nm, many apatites originating from other geological environments host a number of di- and trivalent rare earth ions which are responsible for their blue, greenish-yellow to bright yellow or brown CL colours. The CL spectrum reproduced in *Figure 20* reveals the presence of dysprosium, terbium and samarium, whose narrow bands are distributed over the entire visible spectral range and which combine to give the visual impression of brown.

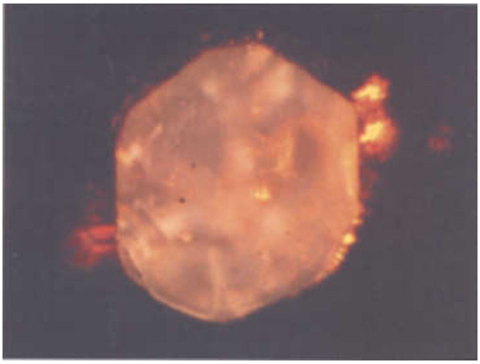

Figure 19: *Brownish-yellow CL of a euhedral apatite in a non-luminescing kornerupine host. Excitation conditions: 9.0 kV; 0.9 mA. Enlargement: 125* x.

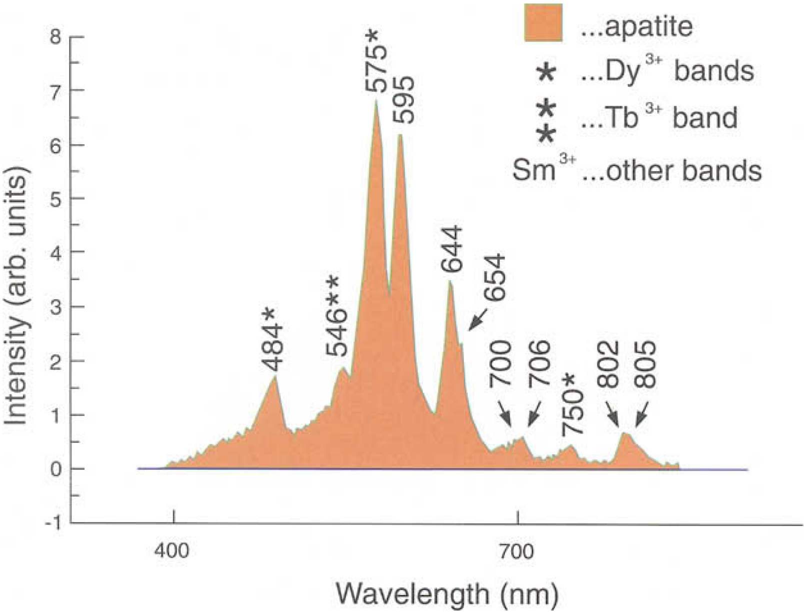

Figure 20: *CL spectrum of a brownish-yellow luminescing apatite inclusion in a green kornerupine from Sri Lanka exhibiting narrow REE^{3+} bands caused by trivalent dysprosium, terbium and samarium. Excitation conditions: 9.0kV, 0.9 mA.*

(8) Plagioclase with ruby and pargasite inclusions

A pleasing white ornamental cabochon from Mogok of 6.39 ct contained large red and small dark brown blotches which turned out to consist of rubies and pargasite respectively. During electron bombardment the host feldspar luminesced green, a vivid contrast to the strong red CL of the ruby inclusions and to the almost inert brown to dark grey CL colour of the pargasite amphibole which is evident in *Figure 21*. The CL spectra in *Figure 22* display a similar contrast between the strong ruby CL spectrum and the less intense broad band of the plagioclase host peaking at 550 and 558 nm. Using cold cathode CL even tiny ruby inclusions of less than 10 µm may become noticeable under the microscope during a bombardment with electrons.

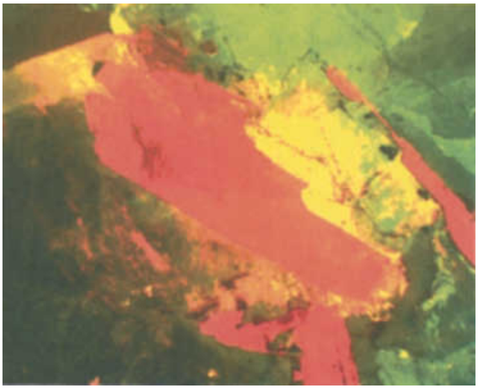

Figure 21: *The bright red luminescence of ruby inclusions provides a perfect contrast to the green CL colour of the plagioclase host. The CL colour of the latter is evoked by* Mn^{2+} *ions. The dark areas on the left are pargasite and the small black blotches are caused by picotite grains. Excitation conditions: 10.5 kV; 0.8 mA. Enlargement: 40* x.

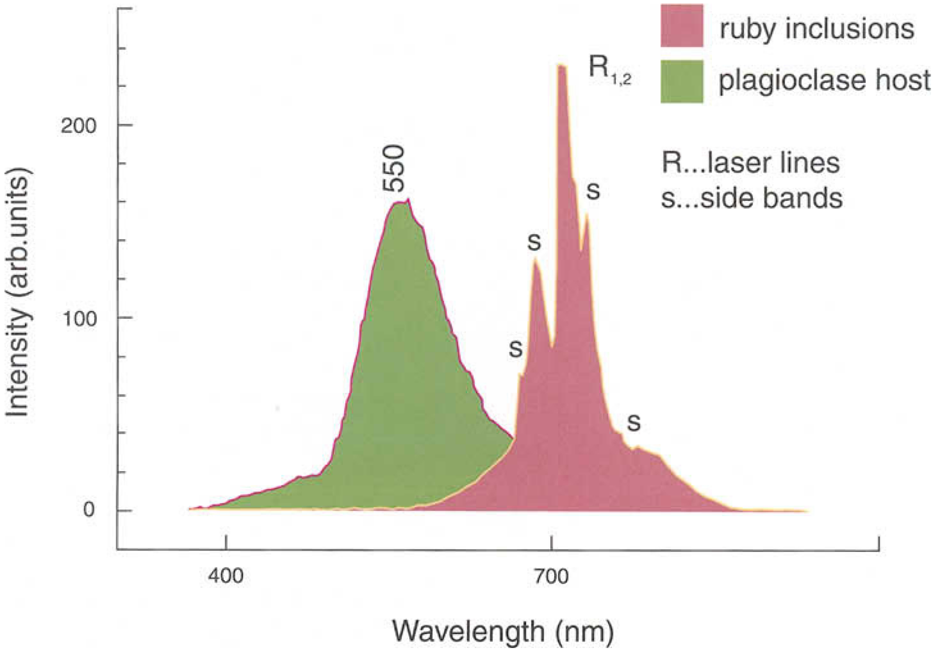

Figure 22: *CL spectra of the plagioclase host and ruby inclusions. Excitation conditions: 5.0 kV; 0.4 mA*

(9) Calcite host with albite inclusions

Grey to blue calcite is mined in Sri Lanka and supplies material for collectors. A sample of 51.8 ct, apparently clean, was inspected using CL and two small bluish luminescing spots (*Figures 23 and 24*) became visible within the overall red CL colour of the rough host. The red CL colour of the calcite stems from divalent manganese ions replacing divalent calcium ions in the carbonate structure. The bluish-white luminescence comes from small albite inclusions which show a typical spectrum (*Figure 25*). During the microscopic investigation the sky-blue luminescing inclusion could not be detected when using incandescent light.

Figure 23: *Red CL of a greyish-blue rough calcite with two whitish luminescing dots of albite. Excitation conditions: 9 kV; 0.9 mA. Enlargement: 10* x.

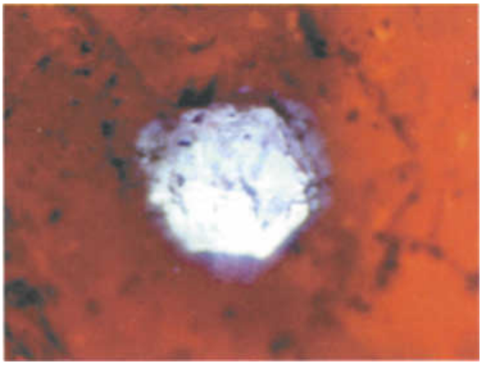

Figure 24: *At higher magnification the CL of the dots appear blue with a CL spectrum characteristic of albite. Excitation conditions: 8 kV; 0.8 mA. Enlargement: 125* x.

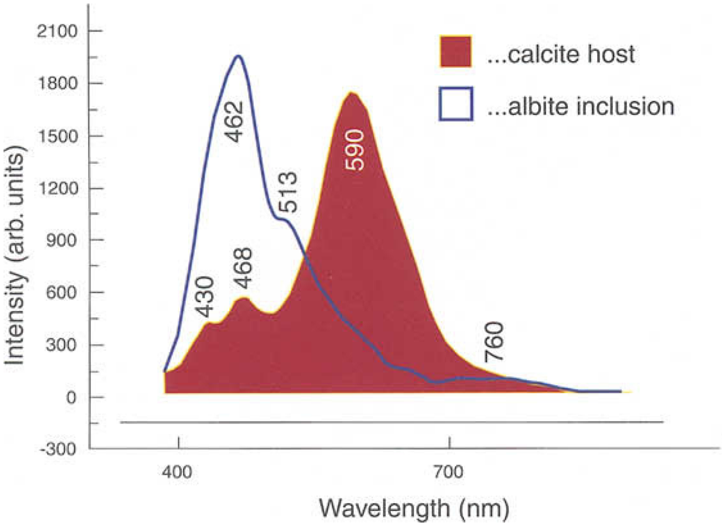

Figure 25: *CL spectra of the rough calcite that hosts two albite inclusions. The host spectrum is dominated by a* Mn^{2+}*-band at 590 nm characteristic for the CL of calcites. The albite inclusion shows a strong band in the violet-blue with its tail reaching into the NIR. This band shape is indicative for defect centres causing the blue CL of the albite inclusion. The intensity of the calcite spectrum is multiplied by a factor of 10.*

(10) Dolomite with a pargasite inclusion simulating mottled white jade

CL microscopy and spectrophotometry are fast and efficient methods to differentiate between natural jadeititic jades and a great number of simulants. One such simulant consisted of a white natural dolomite cabochon of 6.09 ct that contained a bright green blotch of pargasite (*Figure 26*). Bombarded by electrons the cabochon fluoresced an intense violet-tinted red (*Figure 27*) with the non-luminescent amphibole pargasite remaining black. Natural jadeite does not react in this manner. The CL spectrum clearly reveals a broad and intense Mn^{2+} band with divalent manganese ions replacing divalent calcium and magnesium in the dolomite structure. For convenience a Mn^{2+}-based CL spectrum of calcite has been added in *Figure 28* to compare the CL bands of both carbonates.

Figure 26: *Dolomite with a green patch of pargasite simulating green-mottled mutton-fat jade. Total length of the cabochon: 14.8 mm.*

Figure 27: *Dolomite under electron bombardment shows up in a violet-tinted red, the pargasite remains inert. Excitation conditions: 9 kV; 0.8 mA.*

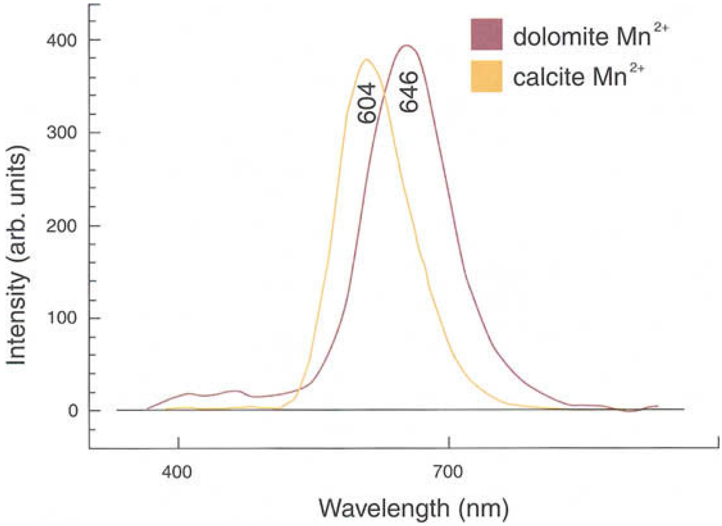

Figure 28: *CL spectra of dolomite and calcite hosts, the first used as a simulant of jade (Figure 26). In both minerals CL is provoked by manganese ions. Calcite shows a more orange to brick-red CL colour, whereas dolomite luminesces violet-tinted red. The main peak of the latter is shifted into the red by more than 40 nm.*

Discussion and outlook

From the above results some basic conclusions about the behaviour of a gemstone host and its inclusion can be drawn:

(a) When host and inclusion exhibit strong CL and show different CL colours, the CL effects of both the host and the inclusions can easily be studied. Representative samples are Nos 3 and 8.

(b) When both host and inclusion are luminescent, but the CL intensity of the host is less intense than that of the inclusion, this also facilitates a close study of the CL properties of the inclusion by both photomicrography and microspectrophotometry. An example is given by No. 9.

(c) When both host and inclusion are known to show strong luminescence, but the high CL intensity of the host masks completely that of the inclusion, CL microspectrophotometry should be used. Examples are given by sample Nos 1 and 2.

(d) When the host luminesces or remains inert when bombarded by electrons, with the inclusion showing no luminescence either, then the CL could have shifted further into the NIR. In this case, the spectral range up to 950 nm should be searched for CL bands. An example is given by No. 5 showing the NIR luminescence of rutile inclusions in blue kyanite.

Considering the many examples of inclusions presented in the *Photoatlas* (Gübelin and Koivula, 1986), it becomes evident that the field of luminescing hosts and inclusions will be enlarged and deepened by future studies which are under way.

The compartments of commercial cold cathode CL instruments are large enough to house more than six 5-10 ct gemstones which can be tested consecutively without opening the evacuated compartment, an advantage that speeds up CL investigations. Occasionally one comes across gemstones that host more than one type of inclusion (see No. 3). It is of advantage, then, to repeat the CL test with all inclusions that reach the surface of facets and run several CL spectra in order to characterize the different types of inclusions. One has to keep in mind that neither by visual CL nor by CL spectrophotometry is it possible to determine the chemical nature of all these inclusions. Use of SEM X-ray analysis may be necessary for conclusive answers. Such an example is documented by No. 7, when a second small inclusion (zircon) was detected by means of SEM.

Sometimes one may discover a strongly luminescing host with an apparently non-luminescent inclusion. This can be puzzling if the latter is known to exhibit a strong CL intensity in the normal spectral range when tested as a rough or cut mineral. Examples are the emeralds from Santa Terezinha in Brazil which frequently contain colourless dolomite inclusions that do not react to an electron bombardment. The mineral dolomite, however, generally luminesces strongly red as documented by sample No. 10. There are also rubies which host non-luminescent calcite inclusions. The mineral calcite, on the contrary, is well known for its strong CL (see Nos 4 and 10).

The reason for the lack of luminescence of some inclusions in gemstones which are well known to be strongly luminescent as minerals, is still obscure. The main obstacle for a reliable answer to this question is the quantitative determination of low concentrations of activator elements which are responsible for the CL effects. Our preliminary tests indicated concentrations of the activator elements chromium and manganese of not more than 13 and 23 ppm respectively (Ponahlo, 1993, tables 5 and 6). These tests were carried out by means of energy dispersive polarized X-ray fluorescence (EDPXRF) using table facets of gemstones and single crystals as large as ~ 6 x 4 mm. However, EDPXRF and similar non-destructive methods cannot be applied to small inclusions covering areas of less than 200 μm^2 and for these, other approaches will be necessary.

Acknowledgements

I am much obliged to Prof. Dr Edward Gübelin for his generous loan of all the gems needed for this investigation and for his continuous and lively interest in this study. Likewise, my thanks to go to Prof. Dr Gero Kurat, Director of the Department for Mineralogy and Petrography at the Museum for Natural History, Vienna, and to Dr Franz Brandstätter who is responsible for the SEM and Microprobe equipment in that department for carrying out the SEM analyses.

References

Gübelin, E.J., and Koivula, J.I., 1986. *Photoatlas of inclusions in gemstones*. ABC Edition, Zurich, 532pp

Marshall, D.J., 1988. *Cathodoluminescence of Geological Materials*. Unwyn Hyman, Boston

Marshall, D.J., 1993. The Present Status of Cathodoluminescence Attachments for optical microscopes. *Scanning Microscopy*, **7**(3), 861-74

Michel, H., 1926. *Die künstlichen Edelsteine*. Verlag Wilhelm Diebener, Leipzig

Ponahlo, J., 2000. Cathodoluminescence as a Tool in Gemstone Identification. In: Pagel, M., Barbin, V., Blanc, P., and Ohnenstetter, D., *Cathodoluminescence in Geosciences*. Springer, Berlin

Ponahlo, J., 1993. Kathodolumineszenz (KL) und KL-Spektren von Edelsteinen (Ausgewählte Beispiele). *Zt. Dt. Gemmol. Ges.*, **42**(4), 149-62

Walker, G., and Burley, St., 1991. Luminescence petrography and spectrographic studies of diagenetic minerals. In: Barker, Ch.E., and Kopp, O.C. (eds), *Luminescence microscopy: quantitative and qualitative aspects*

Walker, G., 1985. Mineralogical Applications of Luminescence Techniques. In: Berry, F.J. and Vaughan, D.J. (eds.), *Chemical bonding and spectroscoy in mineral chemistry*. Chapman and Hall, London

Natural amethyst from the Caxarai Mine, Brazil, with a spectrum containing an absorption peak at 3543 cm^{-1}

Hiroshi Kitawaki

Gemmological Association of All Japan, 5-25-11 Ueno, Taito-ku,
Tokyo 110-0005, Japan

ABSTRACT: Natural amethysts from the Caxarai mine in Rondônia State, Brazil, show markedly different characteristics from those from other well known localities. Their z $\{01\bar{1}1\}$ sectors show deeper colour than their r $\{10\bar{1}1\}$ sectors, and colour zoning in the z sectors is quite sharp with some showing strong purplish-blue pleochroism. An absorption peak in the infrared region at 3543 cm^{-1} is present in about 50% of these Caxarai stones. Due to the presence this 3543 cm^{-1} peak, these amethysts are liable to be misidentified as synthetic amethyst if investigation is not thorough since the peak has been taken as a diagnostic feature for synthetic amethyst.

Keywords: blue-purple pleochroism, Brazil twinning, Caxarai mine, colour zoning, z sectors, 3543 cm^{-1} absorption peak

Introduction

Since amethysts were commercially synthesised in 1970, identification of amethysts has become one of the most difficult tasks for gemmologists. Although the reasons for manufacture of synthetics to imitate rather cheap natural amethysts, or the significance of identifying them are not clear, overproduction of synthetic amethysts and mixing them with natural materials at the place of origin have made their identification an international issue. Following the reorganization of the former USSR, the technique of growing crystals in Russia became focused on jewellery production for export as the market economy grew, and the price for rough synthetic amethysts dropped radically. Furthermore, with growing competition from China the price has fallen as low as that of Verneuil synthetics; thus the importance of amethyst identification is inevitably increasing.

Background

Many identification methods to distinguish between natural and synthetic amethysts have been reported and practised at different laboratories. The chemical composition and crystal structure of natural and synthetic amethysts are the same, so that their physical properties such as RI and SG can not be effective indicators in their identification. At present, the following identification methods are employed as standard.

ISSN: 1355–4565

Figure 1: *The location of the Caxarai mine in Rondônia State, Brazil.*

1. Observation of inclusions

Amethysts with inclusions can be identified using a loupe or a microscope. Goethite is commonly known as a typical solid inclusion in natural amethysts. On the other hand, breadcrumb-like inclusions imply a synthetic origin and if the presence of a seed crystal is detected, this forms decisive proof of synthetic origin. Liquid inclusions are rarely observed in synthetic amethysts, and if internal features or colour zoning in the form of tiger stripes, which are related to Brazil twinning are observed, the stone is most likely to be natural.

2. Observation of colour zoning

Most amethysts on the market are flawless to nearly flawless and do not contain characteristic inclusions useful for identification. Under such circumstances, observation of colour zoning that universally exists in amethysts becomes very important in identifying the stone. Understanding crystal morphology of natural and synthetic amethysts is critical as the colour zoning obviously corresponds to the changes of morphology in the crystal growth process. In natural amethysts, sequences of purple or violet and colourless zones in two or more directions, which correspond to r $\{10\bar{1}1\}$ or z $\{01\bar{1}1\}$ faces, are generally observed, and their boundaries are clear and generally straight. In contrast, mass-produced synthetic amethysts generally show light and dark purple zoning in one direction parallel to z faces. Conical colour zoning that corresponds to the vicinal form on the z faces (i.e. at only a few degrees inclination to the z faces) implies synthetic origin.

3. The presence of twinning

Almost all natural amethysts are twinned on the Brazil law whereas most synthetic amethysts are not twinned. Based on this fact, certain identification methods for amethysts have been suggested and practised, e.g. Schmetzer (1986) and Crowningshield *et al.* (1986). In these methods, the stones are observed along the direction of the optic axis under crossed polarized light using for example, a polariscope. If Brewster fringes are observed in the test, the stone is regarded as a natural stone, and if simple colour rings caused by interference are observed, the stone is most likely synthetic.

4. *Infrared spectrophotometry*

The application of infrared spectrophotometry to amethyst identification has been attempted for a long time, e.g. Lind *et al.* (1983).

Nowadays, with the development of FTIR, infrared spectrophotometry is performed routinely in gemmological laboratories. The absorption at 3543 cm^{-1} in amethyst is commonly regarded as a characteristic feature of synthetics (Balitsky *et al.*, 1993, and other papers), and a clear absorption at 3543 cm^{-1} in over 80% of more than a hundred synthetic amethysts tested in our laboratory has been confirmed.

Samples and methods

The samples of natural amethyst from the Caxarai mine in Rondônia State, Brazil, tested in the present study include two rough stones, six roughly-cut or cut stones and 18 faceted stones. According to Carlos Rohmann, who is developing the Caxarai mine, the mine was only started in September 1999 and amethyst production has not yet reached the market in any quantity. The amethyst mine is located about 130 km north of the capital of Rondônia state, in the north west of Brazil (*Figure 1*). It is on the west bank of the Madeira River, one of the main tributaries of the Amazon River. Mining in the region was very active 50 years ago when columbite/tantalite minerals were discovered 15 km away from the location of the Caxarai mine. According to Rohmann (pers. comm.), there is a possibility that other mineral species in the Caxarai mine will be found as mining progresses. The deposit is most probably of pegmatitic origin.

Figure 2: *A rough crystal of natural amethyst from the Caxarai mine (weighing about 120 g).*

Shown in *Figure 2* is a rough crystal from the Caxarai mine, weighing about 120 g. Its crystal morphology and liquid inclusions clearly indicate its natural origin. Stones to

Figure 3: *Faceted pieces of natural amethyst from the Caxarai mine, ranging in weight from 3.65 to 8.97 ct.*

Figure 4: *The rough stone shown in Figure 2 was cut along the direction of the c-axis. The top end of the piece shows intense purple.*

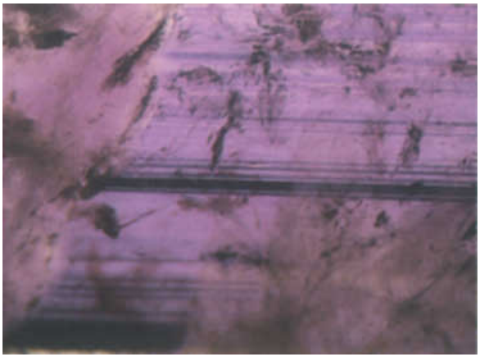

Figure 5: *A piece of Caxarai amethyst sliced perpendicular to the c-axis is observed along the direction of the z* $\{01\bar{1}1\}$ *face. Extremely sharp colour zoning is present.*

be faceted are said to be less included and clearer than our samples.

To inspect colour zoning and the presence of twinning, a sample was sliced both perpendicular and parallel to the *c*-axis of the crystal.

High-quality faceted amethysts (3.65ct – 8.97 ct) from the Caxarai mine are shown in *Figure 3*. In addition to the general gemmological tests, their colour zoning was observed under magnification with diffused light through a white filter while the samples were immersed in water. The presence of twinning in all stones was also detected under crossed polarising sheets which were attached to a binocular gemmological microscope.

The six cut and 18 faceted stones were also analysed by infrared spectrophotometry using a Shimadzu FTIR 8300 spectrophotometer with a resolving power of $4\ cm^{-1}$. Each stone was measured three times or more in random orientations.

Results

Figure 4 shows a rough crystal sliced along the direction of the *c*-axis, with deep colouring at one end. Shown in *Figure 5* is a crystal sliced perpendicular to the c-axis direction and observed along the direction of

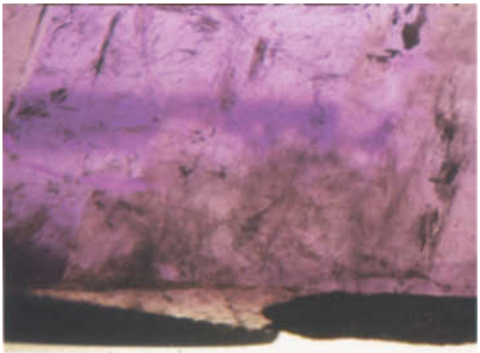

Figure 6a: *A piece of Caxarai amethyst sliced perpendicular to the c-axis is observed along the optic-axis direction. The z sector appears dark purple.*

Figure 6b: *The same piece in Figure 6a is observed under cross polarised light. The z sector displays a uniform interference colour of violet, indicating that the area has no Brazil twinning.*

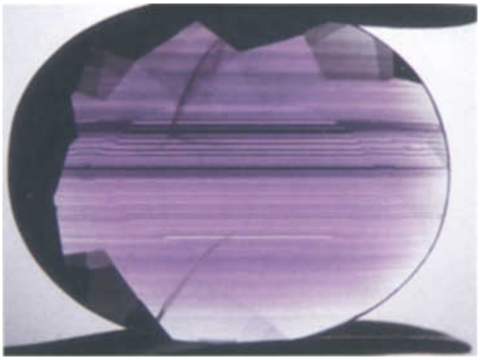

***Figure 7:** The straight and clear colour zoning parallel to the z face.*

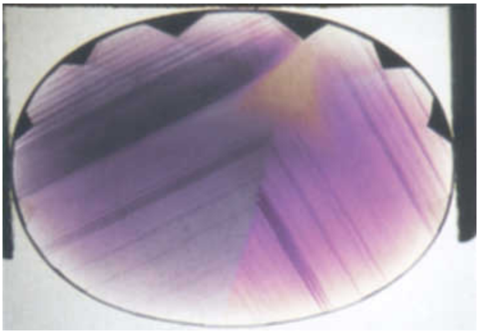

***Figure 8:** The colour zoning in two directions parallel to the z face.*

a rhombohedral face. The amethysts from the Caxarai mine also show a Brewster fringe which originates from Brazil twinning. We interpreted the area that shows the fringe as the r sector, and rhombohedral faces that do not show the fringe as the z sector.

The same piece was observed along the optic axis direction and this is shown in *Figure 6a*, and under crossed nicols in *Figure 6b*. The area showing purple colour zoning in *Figure 6a* shows a uniform violet interference colour in *Figure 6b* (this means than the stone is not Brazil twinned), and it corresponds to the z sector.

Roughly-cut or faceted samples all showed very straight and clear colour zoning. Some samples were cut only from the z sector (*Figure 7*) and did not show Brazil twinning, Many showed colour zoning in two directions parallel to the z face (*Figure 8*), and a few other stones showed a yellow colour in the r sector (*Figure 9a, b*). All samples showed strong pleochroism, some in deep and pale purple, and some in purple to bluish purple (*Figure 10a, b*); according to Rohmann (pers. comm. 2001), the colour of the latter stones is called 'tanzanite colour' at the mine.

Only one sample showed Brazil twinning with conical form combined with Dauphiné twinning which is characteristic of synthetic amethysts (*Figure 11a, b*). In this case, the r sector appeared yellow in colour. The

***Figure 9a:** The r $\{10\bar{1}1\}$ sector appears yellow.*

***Figure 9b:** The piece shown in Figure 9a is observed under cross polarised light. The yellow area clearly shows Brazil twinning.*

***Figure 10a:** Some z sectors show strong bluish-purple to purple pleochroism (the picture was taken by using a polariser).*

***Figure 10b:** The polariser used in Figure 10a was rotated to observe the pleochroic change of colour.*

differences in Brazil twinning in natural and synthetic amethysts have been discussed by Lu Taijing *et al.*, 1990, and I. Sunagawa, 1999.

Infrared spectra

Infrared spectra of 12 of the 24 cut stones showed absorption at 3543 cm^{-1}. Most of the samples that showed this absorption were dominated mainly by the z sector and did not show Brazil twinning, and indeed the absorption at 3543 cm^{-1} was only recognized in the deeply coloured z sector (*see Figure 12*). Before the Caxarai samples arrived we had tested several hundred natural amethysts and none of them showed clear absorption at 3543 cm^{-1}. So the natural amethysts from the Caxarai mine are quite extraordinary. The cause of the absorption at 3543 cm^{-1} has not yet been clarified, but it may well be related to the z sector, as the mass-produced synthetic amethysts are z sector-dominant.

Conclusions

The unusual features of natural amethysts from the Caxarai mine in Rondônia State, Brazil may be summarized thus:

1. Unlike the amethysts from most localities the z sectors show deeper colour than the r sectors, and their beautiful colours are suitable for gem use.
2. The boundaries of light and dark purple zoning observed in the z sector are straight and very sharp.

***Figure 11a:** The r sector (pale yellow) that may be induced by the Dauphiné twinning is seen in the z sector (purple).*

***Figure 11b:** The same piece in Figure 11a is seen under cross polarised light. The Brazil twinning is present in the r sector.*

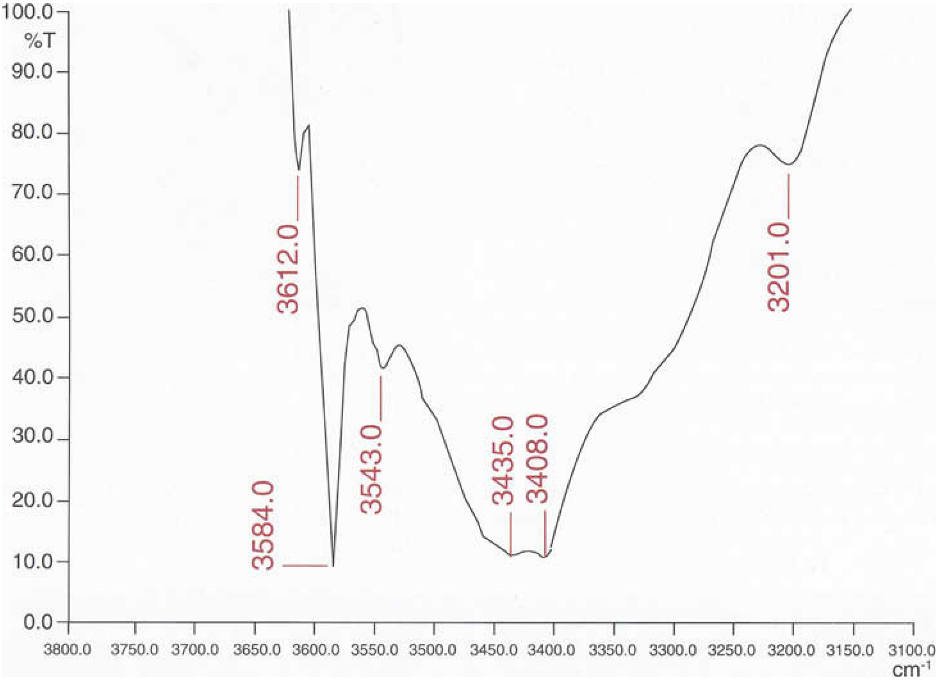

Figure 12: *The infrared absorption spectrum of a natural amethyst from the Caxarai mine. Absorption at 3543 cm^{-1} is clearly seen.*

3. Strong bluish-purple to purple pleochroism is present in parts of certain stones.
4. The Brazil twinning with conical form combined with Dauphiné twinning is present and has been considered as characteristic of Brazil twinning in synthetic amethysts.
5. Infrared spectra mainly of z sector stones contain an absorption at 3543 cm^{-1}, which is generally regarded as a characteristic identifying feature of synthetic amethysts.

It follows from these results that, if only the beautifully coloured z sector is used to cut gemstones from the natural amethyst from the Caxarai mine, they may possibly be misidentified as a synthetic amethyst

(a) because of the peculiar colour zoning;

(b) because of the lack of Brazil twinning; and

(c) the presence of infrared peak at 3543 cm^{-1}.

If a gemmologist has little knowledge of crystal morphology and twinning in quartz and relies too much upon infrared spectrophotometry, the risk of misidentification is increased.

Acknowledgements

I express my deepest thanks to Mr Akira Ito of the ITO Co., Ltd for supplying the samples, to Mr Rikiya Kameyama of the Miyuki Co., Ltd for cutting rough samples, and to our technical staff at GAAJ for assistance with the analysis, discussion of the problems and for providing constructive advice. I am also grateful to Dr Ichiro Sunagawa for revising the first draft of this manuscript.

References

Balitsky, V.S., Taijin, L., Rossman, G.R., Makhina, I.B., Mar'in, A.A., Shigley, J.E., Elen, S., and Dorogovin, B.A., 1999. Russian synthetic ametrine. *Gems & Gemology*, **35**(2), 122-34

Crowningshield, R., Hurlbut, C., and Fryer, C.W., 1986. A simple procedure to separate natural from synthetic amethyst on the basis of twinning. *Gems & Gemology*, **22** (3), 130-9

Lind, T., and Schmetzer, K., 1983. A method for measuring the infrared spectra of faceted gems such as natural and synthetic amethysts. *Journal of Gemmology*, **18**(5), 411-20

Schmetzer, K., 1986. An improved sample holder and its use in the distinction of natural and synthetic ruby as well as natural and synthetic amethyst.. *J. Gemm.*, **20**(1), 20-33

Sunagawa, I., 1999. Quartz crystals twinned after Brazil and Japan Laws – Origin of their morphological and textural characteristics. *Journal of Gemmological Society of Japan*, **20**, 23-36

Taijin, L., Sunagawa, I., and Balitsky, V.S., 1990. Brazil twinning in natural and synthetic amethyst crystals. *Journal of Crystal Growth*, **99**, 1232-7

Letter to the Editor

Production of fake asterism

Introduction

A 'new' method for imitating asterism in natural cabochon-cut gem materials was recently described by McClure and Koivula (2001). The optical phenomenon is caused by a series of man-made parallel scratches on the curved surfaces of the gemstones. Although no details of the production process of this 'new' type of artificially produced asterism were given, it was suggested that 'the use of a polishing wheel with a coarse grit' and 'some type of spinning wheel' is involved. Sinhalite, cassiterite, chrysoberyl, garnet, rutile and samarskite(?) cabochons with this type of fake asterism were described by McClure and Koivula (2001). Garnet and tourmaline were recently mentioned by Schmetzer and Steinbach (2002) as further examples of manipulated gem materials with artificially induced asterism.

Searching for patents dealing with special gem cuts and light effects in gemstones, the author accidentally discovered an old United States patent document by Mukai (1950), in which a process for the production of man-made asterism in cabochon-cut gem materials is described. The procedure mentioned in this document or a variation of this process has possibly been applied in the recent production of fake asterism in natural gem materials. The technical part of the description given by Mukai (1950) is cited in the following section. This description is self-explanatory:

"Referring now to Fig. 1 (left) the cabochon-cut stone 10 has a plane base 11. The stone and base may be finely ground and polished; that is, there is usually no need for further grinding or polishing after the asterism-producing step. The stone 10 may be set in cement 12 on a dop stick 14 for support (Fig. 2). Then, using means such as the cylindrical iron bar 15 suitably held in a rotating chuck 16 and fine gem-polishing dust, the base 11 is given a great multiplicity of minute, sharp, shallow cuts or grooves over the three intersecting areas 17. Three areas of engraving intersection as shown in Fig. 1 (left) will produce a six-rayed star. This is the desired treatment because it simulates the asterism of a natural gem. The individual cuts or engravings are short and may be considered to be substantially

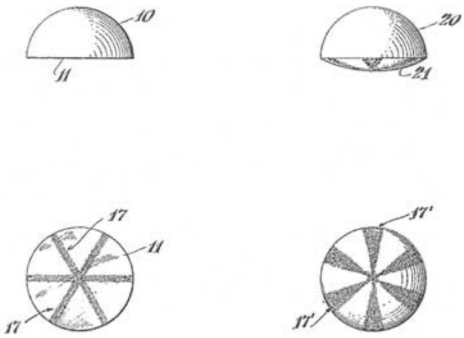

Figure 1: By scratching the flat (left) or curved (right) surface of a cabochon-cut gemstone in different regions, asterism is produced which can be seen as a moving star from various directions relative to a light source; 10, 20 cabochon-cut gemstones, 11 flat base of the gemstone, 21 curved surface of the gemstone, 17, 17' engraved areas with artificially produced scratches or grooves (from Mukai, 1950).

ISSN: 1355–4565

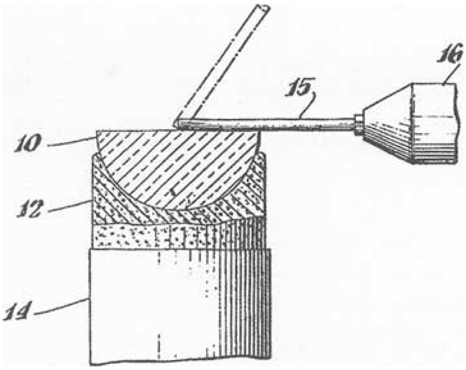

Figure 2: *Production of scratches on the flat base of a cabochon-cut gemstone by use of a rotating or vibrating iron rod; for the artificial production of scratches or grooves on curved surfaces, the rod is held at an angle to the surface (dot and dash lines); 10 cabochon-cut gemstone, 12 cement, 14 support, 15 iron rod, 16 rotating chuck (from Mukai, 1950).*

parallel one with the other. The individual cuts should extend at an angle, preferably a right angle, with respect to the radii of the back of the stone.

"In the Fig. 1 (right) embodiment the stone 20 has a double cabochon-cut in that the base 21 is also convex. A somewhat different pattern of engraving has been employed, as will be noted: the respective engraved areas 17' are wider at the girdle than at the center of the base. Preferably said areas are not truly triangular in that there is no clearly defined apex. The asterism thus produced is also characterized by a bright center and well-defined luminous rays.

"The engravings or markings of the forms of Fig. 1 (right) are perhaps best accomplished by holding the rod 15 at an angle as shown in dot-dash lines of Fig. 2. A vibrating tool, rather than a rotating tool, may be employed, and other mechanical expedients will suggest themselves to the skilled lapidary.

"It should be understood that the respective figures exaggerate the prominence of the engraved areas. In fact, the individual lines of engraving are exceedingly fine and when the stone is viewed under indirect light are hardly discernible.

"The asterism is produced by the reflection of rays of direct light from the multitudinous facets or side walls of the engraved lines. A feature of asteriae produced by my method is that the stars thereof seem to move within the stone as the stone and the light source are moved relative to each other."

It is evident that the technique described in US patent 2,511,510 by Mukai (1950) or a slightly varied embodiment may be used for the recent production of fake asterism. The irregularities of the artificially produced stars as described recently (e.g. 'satellite lines', asymmetrical or curved rays) indicate an individual, non-automatic production procedure.

Dr Karl Schmetzer

Taubenweg 16, D-85238 Petershausen, Germany

References

McClure, S.F., and Koivula, J.I., 2001. A new method for imitating asterism. *Gems & Gemology*, **37**(2), 124-8

Mukai, R.S., 1950. Artificial asteria. United States Patent 2,511,510, issued June 13, 1950

Schmetzer, K., and Steinbach, M.P., 2002. Fake asterism – two examples. *Journal of Gemmology*, **28**(1), 41-2

Abstracts

Diamonds

Gems and Minerals

Instruments and Techniques

Synthetics and Simulants

Diamonds

Study of diamonds from chromitites in the Luobusa ophiolite, Tibet. (Chinese with English abstract)

W. Bai, J. Yang, P. Robinson, Q. Fang, Z. Zhang, B. Yan and X. Hu. *Acta Geologica Sinica*, **75**(3), 2001, 404-9.

A newly discovered occurrence of diamonds in chromitites of the Luobusa ophiolite, Tibet, is described, together with details of the diamonds and of their numerous metallic inclusions. Examination of 25 grains of diamond recovered from the chromite ores revealed about 70 varieties of native elements (Cr, Cu, Ni, Fe, C, Si, Au, Pb, W, Ir, Os, Ru), alloys (Fe-Ni, Fe-Co, Fe-Mn, Fe-Si, Fe-Ni-Cr, Fe-Ni-Co, Si-C, Cr-C, Ir-Os, Os-Ir, Os-Ir-Ru, Fe-Pt), silicates and sulphides. Photomicrographs of the diamonds are accompanied by IR and Raman spectra and a plot of their B-defects vs H (x 10^{-6}). R.A.H.

A non-cognate origin for the Gibeon kimberlite megacryst suite, Namibia: implications for the origin of Namibian kimberlites.

G.R. Davies, A.J. Spriggs and P.H. Nixon. *Journal of Petrology*, **42**(1), 2001, 159-72.

Unaltered kimberlites, clinopyroxene and garnet megacrysts have Sr and Pb isotopic disequilibrium between the kimberlites and the megacrysts showing that the latter are not cognate. The megacryst *REE* (data given) indicates equilibrium with an alkali basaltic magma. Rb-Sr phlogopite ages, ~72 m.y., show that kimberlite volcanism occurred between 5 and 10 m.y. after the inferred passage of the Discovery plume beneath the Gibeon region of Namibia, but the Sr-Nd-Pb isotopes of the kimberlite and clinopyroxene and garnet megacrysts (data listed) are distinct from those of the plume and so it presumably contributed little to the volcanism. The megacrysts have a strong DUPAL Pb isotope signature, believed to be derived from the sub-continental lithospheric mantle due to Discovery plume-provoked 'basaltic' asthenospheric-derived melts that ponded at the base of and interacted with the sub-continental lithosphere with polybaric fractionation. Less likely is a lower mantle source for the DUPAL Pb isotope signature. B.E.L.

Identification of GE POL™ diamonds.

E. Fritsch, J-P. Chalain and H.A. Hänni. *Australian Gemmologist*, **21**(4), 2001, 172-7.

GE POL diamonds, also marketed as Pegasus and Bellataire diamonds, are brownish type IIa stones that have been colour enhanced by the General Electric Company of the USA using a high-pressure high-temperature (HPHT) process. The Bellataire diamonds currently marketed by Lazare Kaplan are being laser-inscribed on the girdle with the inscription GE POL™, which as a possible identifying feature, can be removed by repolishing. Other identifying features include transparency to SW UV, cross-hatched tatami graining of weak to moderate intensity, generalized haziness, etched surface-reaching cleavages and rare mineral inclusions surrounded by disc-like stress fractures. A more sophisticated confirmation of identity can be obtained by the use of luminescence excited by the 514nm laser beam of a Raman spectrometer. This, with the diamond cooled to the temperature of liquid nitrogen, reveals the treated stone's N-V (nitrogen vacancy) centre either as an absorption of light at 637 nm or an emission at 575 nm. Also using a Raman spectrometer with liquid nitrogen cooling, the research scientists at De Beers have proposed use of the ratio of the intensity of luminescence at 637 nm and 575 nm. The 637:575 nm ratio is always less than 1.6 for untreated type IIa diamonds, while that of GE POL diamonds is higher than 2.5. P.G.R.

Composition chimique et isotopique des mégacristaux et des diamants des kimberlites du Kundulugu (Zaïre).

D.M. Kampata, J. Demaiffe, J. Hertogen, J. Moreau and P.H. Nixon. *Annales de la Société géologique de Belgique*, **119**(1), 1996, 55-70.

EPMA results are given for megacrysts of olivine, pyroxene, garnet and ilmenite occurring in a matrix of

Abstractors

R.R. Harding	R.R.H.	G. Raade	G.R.	I. Sunagawa	I.S.
R.A. Howie	R.A.H.	P.G. Read	P.G.R.	R.Van Tassel	R.V.T.
B.E. Leake	B.E.L.	E. Stern	E.S.	P.M. Whelan	P.M.W.
M. O'Donoghue	M.O'D.				

ISSN: 1355–4565

olivine, spinel, perovskite, monticellite, serpentine and carbonate. The kimberlites contain some diamonds, ultramafic and crustal inclusions. Parental liquid in equilibrium with diopside has been similar to that of alkali basalts. The liquid in equilibrium with garnet was much more enriched in LREE. The low $^{87}Sr/^{86}Sr$ ratios of the diopsides indicate a source more depleted in Rb, but the Sm/Nd ratio is comparable to the source of the 'host' kimberlite. Garnet is probably contaminated by Sr, and orthopyroxene by Sr and Nd. Diamond shows a large range of $\delta^{13}C$ from -24.5 to -4.5‰ corresponding with a peridotitic or eclogitic type. R.V.T.

Oxidation during metasomatism in ultramafic xenoliths from the Wesselton kimberlite, South Africa: implications for the survival of diamond.

C. A. McCammon, W. L. Griffin, S. R. Shee and H. S. C. O'Neill. *Contributions to Mineralogy and Petrology*, **141**(3), 2001, 287-96.

Garnets in xenoliths in the Wesselton kimberlite show significant zoning in major and trace elements. Their study by Mössbauer spectroscopy showed an increase in $Fe^{3+}/\Sigma Fe$ from core to secondary rim. Determination of T and P using garnet-olivine, garnet- orthopyroxene and Ni in garnet formulae indicate conditions near 1000°C and 37 kbar for most of these garnets. Calculations of fo_2 show an increase of ~1 log-bar unit from garnet core to secondary rim, relative to the Q-F-M buffer curve. Combined with re-analysis of literature data from unaltered material, from the same locality, there was an increase in relative fo_2 of ~2 log-bar units during the course of the metasomatism. Existing data for other South African garnet peridotites when similarly recalculated indicate relative fo_2 that lie at least 2 log-bar units below the diamond-carbonate equilibrium in peridotitic systems, which define the maximum limit of diamond stability in peridotite. Hence diamond would be preserved during the final stages of metasomatism, but in later stages, fluid would react with the diamonds leading to their re-absorbtion and eventual destruction. R.A.H.

Modelling the appearance of the round brilliant-cut diamond: an analysis of fire, and more about brilliance.

I.M. Reinitz, M.L. Johnson, T.S. Hemphill, A.M. Gilbertson, R.H. Geurts, B.D. Green and J.E. Shigley. *Gems & Gemology*, **37**(3), 2001, 174-97.

The latest results are presented of research into the interaction of light with fully faceted colourless symmetrical round brilliant-cut diamonds of various proportions. 'Fire' is the visible extent of light dispersed into spectral colours. As fire is best seen with directed (spot) lighting, the measure of fire (dispersed coloured light return or DCLR) uses this lighting condition. DCLR values were computed for more than 26,000 combinations of round brilliant proportions. In general, different sets of proportions maximize DCLR and WLR (weighted light return), but there are some proportion combinations that produce above-average values. Analysis of these values with variations of five proportion parameters showed that every facet contributes to the appearance of a round brilliant diamond. In particular, star and lower girdle facet lengths could have a noticeable effect on WLR and DCLR. R.A.H.

Are Majhgawan-Hinota pipe rocks truly group-I kimberlite?

R. Shanker, S. Nag, A. Ganguly, A. Absar, B.P. Rawat and G.S. Singh. *Proceedings of the Indian Academy of Sciences – Earth and Planetary Sciences*, **110**(1), 2001, 63-76.

Although the four or more diamond-bearing, Proterozoic (1170 ± 20 – 974 ± 30 m.y.) pipe rocks in Majhgawan-Hinota occur as intrusives in sandstones in the SE margin of the Aravalli craton and have been called 'micaceous kimberlite', it is considered that this name is not justified. The absence of primary monticellite, the abundance of cognate phlogopite, and the presence of baryte and primary carbonate, coupled with their ultrapotassic and volatile-rich nature and high contents of incompatible elements, indicate a close similarity to the orangeites of South Africa. R.A.H.

Gems and Minerals

Bunte Calcite aus Spanien.

R. Augsten. *Lapis*, **26**(10), 2001, 27-31.

Fine red gem-quality sphaerocobaltite is reported, with other carbonates, from three Spanish locations. M.O'D.

Zebra Rock: an ornamental stone from the East Kimberley, Western Australia.

A.W.R. Bevan. *Australian Gemmologist*, **21**(4), 2001, 165-8, 5. Illus. in colour.

Zebra rock, also known as zebra stone and ribbon stone, is a distinctive reddish-brown and white banded sedimentary rock first discovered in 1924 near the present day diamond source at Argyle, south of Kununurra in the East Kimberley. The rock consists of small particles of quartz with fine-grained white mica, the clay mineral kaolinite, dickite and alunite. Because of its softness and high clay content it does not take polish, and items of hollow ware made from this ornamental rock have to be varnished to give them a high gloss and to protect the surfaces. P.G.R.

La collezione di gemme del Vicentino al Museo Civico 'G. Zannato' in Montecchio Maggiore (Vicenza).

M. Boscardin. *Mineralogia Scientifica.*, **16**(1), 2000, 51-60.

A collection of some 500 samples, including faceted and cabochon gemstones, and polished or engraved ornamental stones, has been assembled in this museum in Vicenza, NE Italy. Prominence is given to the 'enhydros' (a variety of chalcedony also termed 'Vicenza drop'), and to specimens of xonotlite and johannsenite (gems peculiar to the Vicenza district). R.A.H.

Fibrous nanoinclusions in massive rose quartz: the origin of rose coloration.

J. S. Goreva, C. Ma, and G. R. Rossman, *American Mineralogist*, **86**(4), 2001, 466-472.

Pink nanofibres with widths of 0.1-0.5 µm were extracted from rose quartz from 29 different pegmatitic and massive vein localities throughout the world. Optical absorption spectra of the fibres and the initial rose quartz imply that these nanofibrous inclusions are the cause of coloration of massive rose quartz worldwide. These fibres do not occur in the rare, euhedral variety of pink quartz. Redox and heating experiments showed that the pink colour of the fibres is due to Fe-Ti intervalence charge transfer that produces an optical absorption band at 500 nm. Based on the XRD patterns and characteristics of pleochroism, the best match for these inclusions is dumortierite. However, FTIR and Raman spectra consistently did not exactly match the standard dumortierite patterns, suggesting that this fibrous nano-phase may not be dumortierite itself, but rather a closely related material. P.M.W.

Pyrope from the Dora Maira massif, Italy.

A. Guastoni, F. Pezzotta, M. Superchi and F. Demartin. *Gems & Gemology*, **37**(3), 2001, 198-204.

Large crystals of pyrope containing gem-quality portions occur in Dora Maira massif in the Western Alps. These crystals have yielded pale purple to purplish-pink gemstones ≤1 ct. Electron microprobe results show 87-97 mol. % of the pyrope component. They have n 1.717–1.730, with SG 3.58–3.67 and contain several types of microcrystalline inclusions (including ellenbergerite) and show undulatory extinction with cross-polarized light due to strain caused by tectonic deformation. The IR spectrum has four sharp bands in the 3660–3600 cm^{-1} region. R.A.H.

Beobachtungen an hitzebehandeltem Rubin mit künstlicher Rissheilung.

H.A. Hänni. *Gemmologie. Z. Dt. Gemmol. Ges.*, **50**(3), 2001, 123-36, 12 photographs, 1 table, 1 graph, 1 diagram, bibl.

This paper deals with heat-treated rubies with glass fillings in fractures and subsequently healed fissures examined over the last twenty years. Flux assisted heat treatment with borax, lithium tetraborates and additives of glass, quartz or melted natural inclusions may form a melt that spreads over the surface and is drawn into cavities and fractures during subsequent heat-treatment. The flux character of such melts produced during the treatment helps recrystallization of some fissures. During cooling a small portion of synthetic ruby is formed that heals the former fissures. The flux may stay amorphous and glassy, but often precipitation of devitrification products are seen. This results in healing characteristics similar to natural 'fingerprints', and also residual portions of flux (commonly called 'glass') in fine droplets, channels, or thin films, up to the surface-reaching larger cavities. The different amounts of foreign substances in ruby led to a request for a quality scale, which has now been widely accepted. The amounts are divided into minor, moderate and significant/prominent. E.S.

Staurolite from the Lai Hka and Mong Keng areas, Myanmar.

U.T. Hlaing. *Australian Gemmologist*, **21**(4), 2001, 169-70, **4** illus. in colour, 1 map.

Crystals of reddish-brown to brownish-black cabochon grade staurolite crystals were discovered in schists to the west of the townships of Lai Hka and Mong Keng in Myanmar's Shan State. The crystals have a prismatic untwinned habit and are pseudomorphic, belonging to the monoclinic crystal system. P.G.R.

Sapphires and their imitations on medieval art objects.

J. Hyrsl. *Gemmologie. Z. Dt. Gemmol. Ges.*, **50**(3), 2001, 153-62, 17 photographs, 1 table, bibl.

Most sapphires used in medieval objects come from Sri Lanka; they have been common in Europe since Roman times. The stones are usually blue, sometimes yellow, pink, purple or colour-changing. Some show asterism. Almost all old sapphires are pierced pebbles; faceted stones did not appear before the 9th to 14th centuries. Dark blue translucent sapphires of basaltic origin are much rarer; they probably came from the LePuy region in central France. Sometimes iolites and aquamarines were confused with sapphires. Common sapphire imitations included blue glass, colourless foiled glass and doublets. The Ardennes cross in Nuremberg which was probably made in France in the 9th century contains 15 stones assumed to be sapphires. They turned out to be quartz pebbles which had been thrown into molten blue glass; they were then polished leaving remnants of blue glass on the surface. E.S.

Micro organisms associated with gemstones.

M.R. Khan, M.L. Saha and H. Afroz. *Bangladesh J. Bot.*, **30**(2), 2001, 93-6.

A total of 21 gems, including varieties of beryl, chrysoberyl, corundum, feldspar, opal and turquoise were tested for microbial growth. Thirteen species of the genus Bacillus were identified but all were in an inactive-moribund state. Under normal conditions there was no appreciable microbial growth but after incubation, bacterial colonies grew from the gems and demonstrated their chemoautotrophic nature. R.R.H.

Gem news international.

B.M. Laurs (Ed.). *Gems & Gemology*, **37**(3), 2001, 222-45.

Items of interest include reports on the progress of the Ekati and Diavik diamond mines in the Northwest Territories of Canada, Maxixe-type green-blue beryls with eye-visible pleochroism (with UV-VIS and EDXRF spectra), a vanadium-coloured green beryl from China, an account of recent gem discoveries (morganite, tourmaline and kunzite) at mines in Pala (California), cultured pearls from Tahiti and Australia, faceted translucent green powellite from Chile, and blue-to-green and also purplish-red faceted tourmaline from Nigeria. R.A.H.

Gemmologie Aktuell. Kupferhaltige Turmaline aus Nigeria.

C.C. Milisenda. *Gemmologie. Z. Dt. Gemmol. Ges.*, **50**(3), 2001, 121-2, 4 photographs.

The gem-quality tourmalines which owe their colour to the trace elements manganese and/or copper come from the Edoukou mine in the Nigerian State of Oyo near the Benin border. The stones weighed between 2 and 25 carats and were of blue-violet to amethyst colour. Heating produces an aquamarine colour. The stones are marketed in Idar-Oberstein under the name of 'Indogo Tourmaline'. E.S.

Edelsteine aus Sambia - Teil 3: Amethyst.

C.C. Milisenda, V. Malango and K.C. Taupitz. *Gemmologie. Z. Dt. Gemmol. Ges.*, **50**(3), 2001, 137-52, 11 photographs, 3 maps, 2 tables, 2 graphs, 1 diagram, bibl.

Amethyst was the first gemstone to be mined in Zambia in 1959 at the Kundalilla Mine (now the Kariba Minerals Mines) in the Kalomo Mapatizya field. Since then many hundreds of occurrences have been found over an area of 750 sq. km, being perhaps the largest deposit of high grade amethyst in the world. The occurrences can be divided into two types, long veins which are only 10–60 cm wide, but contain a good percentage of quality gems and the so-called 'stockworks' or giant breccia which are large rocks with many small veins but not high quality stones. The resources overall are very substantial, but there is a need to introduce underground mining; where this has been tried, it has yielded good results. E.S.

Gem trade lab notes.

T.M. Moses, I. Reinitz, S.F. McClure and M.L. Johnson. *Gems & Gemology*, **37**(3), 2001, 212-19.

Notes are given on a faceted 0.54 ct brown baddeleyite, a 13 ct yellowish-green datolite, blue and pink high-*P*/high-*T* processed diamonds, carved beads of maw-sit-sit, and a star sapphire with stars of two different colours (silvery white on one side and golden on the other side). R.A.H.

[Chromium-bearing garnets from rodingites of Dlinnogorsky mafic-ultramafic massif, Valizhgen Peninsula, Russia.]

A.B. Osipenko, E.G. Siderov, L.G. Osipenko and E.N. Grib. *Proceedings of the Russian Mineralogical Society*, **130**(1), 2001, 72-80.

New data are reported for Cr-rich garnets in peripheral zones of the Dlinnogorsky massif, Valizhgen Peninsula, SW Koryakia, NE Russia, in which bright emerald-green Cr-Ti uvarovite is found in association with light green Cr-bearing and colourless Cr-poor grossular. EPMA results are given for 10 garnets ($Uv_{33-62}Gr_{7-64}And_{2-25}$) and for Cr-spinels, diopside, titanite and Cr-chlorite (kammererite). The uvarovite is relatively rich in Ti (TiO_2 1.3-1.69 wt.%) and is related to the process of primary accessory Cr-spinel decomposition during rodingitization of gabbro inclusions in serpentine. High alkalinity of the metasomatic fluids led to an increase in Cr and Ti mobility (both are usually immobile) with their release, redistribution and accumulation in newly formed garnet and chlorite. R.A.H.

Jeremejevite: a gemological update.

K. Scarratt, D. Beaton and G. Du Toit. *Gems & Gemology*, **37**(3), 2001, 206-11.

A large cut (4.54 ct) yellow jeremejevite from Namibia is described, together with details of two blue stones from Namibia and two yellow examples from E Tajikistan. They have ε 1.640–1.642, ω 1.649–1.651, with SG 3.27–3.31. UV, IR and Raman spectra are presented. R.A.H.

The origin of colour of chrysoprase from Szklary (Poland) and Sarykul Boldy (Kazakhstan).

M. Sachanbinski, J. Janeczk, A. Platonov and F.J.M. Rietmeijer. *Neues Jahrbuch für Mineralogie, Abhandlungen*, **177**(1), 2001, 61-76.

A study is reported of chrysoprase from the Szklary type locality, using analytical transmission electron microscopy and both optical and infrared spectroscopy. The allochromatic 'apple green' colour of the chrysoprase results from nanometre-size inclusions of aggregates of Ni-bearing sheet silicates, mainly Ni-kerolite and minor pimelite, that occur on sub-grains of silica. There is no evidence for the presence of bunsenite (NiO). Mineral inclusions containing Fe^{3+} ions modify the green colour of the chrysoprase by adding a yellowish hue. The bluish hues result from light scattering on microdefects in the chalcedony matrix, e.g. silica globules, nano- and micrometre mineral inclusions and gas-liquid inclusions. R.A.H.

The chemical composition of Burma jadeite ore and its significance. (Chinese with English abstract)

J. Yang. *Kuangwu Yanshi (Journal of Mineralogy and Petrology)*, **21**(4), 2001, 28-30.

The results of EPMA, trace element and *REE* analyses for jadeite from Burma [Myanmar] are reported, and the colour-producing mechanisms are discussed. The characteristic assemblage of trace elements and *REE* are considered to indicate that the jadeite was derived from serpentinized peridotite. This conclusion should be of help in prospecting for jadeite. R.A.H.

Instruments and Techniques

Raman microspectrometry of fluid inclusions.

E.A.J. Burke. *Lithos*, **55**(1-4), 2001, 139-58.

For many kinds of fluid inclusions, the coupling of microthermometry and Raman microspectrometry is still the only viable option to obtain compositions of single fluid inclusions. A review is given on the basis of 16 years' experience and helped with about 120 references of the instrumentation, analytical conditions and methodology of the application of Raman microspectrometry to gaseous, aqueous and hydrocarbon inclusions, and their daughter minerals. [Author's abstract] G.R.

Dispersion measurement with the gemmologist's refractometer – Part 2.

D.B. Hoover and T. Linton. *Australian Gemmologist*, **21**(4), 2001, 150-60, 5 graphs, 2 tables.

Continuing on from Part 1 of their paper, the authors explain the problems in calculating a gem's RI at wavelengths other than that of sodium. This is because the relationship between RI and wavelength is a non-linear curved function rather than a linear one, and large errors occur if a constant function (such as the ratio of the wavelength differences) is used in the calculation. If dispersion is to become a useful determinative property, and the literature values of dispersion converted accurately from C-F (or any other wavelength interval) to B-G values, then the dispersion curves must first be linearized. This the authors have done by using the Sellmeier linearizing equation in their calculations. The paper gives details of the procedures used by the authors to obtain an empirical calibration of two commercial gemmological refractometers. This procedure involves the selection of light sources, linearization of dispersion curves by the Sellmeier equation, and the measurement process. Empirical calibration is necessary because the manufacturers of refractometers do not provide users with dispersion calibration curves of their refractometer glass. Unfortunately, empirical calibration compounds any errors, and this limits the potential use of refractometer dispersion measurements for determinative use. The situation could be resolved if manufacturers provided users with the RI and dispersion properties of their refractometer glass. P.G.R.

Brandt proportion loupe.

T. Linton, A. Cumming, N. Masson and B. Sweeney. *Australian Gemmologist*, **21**(4), 2001, 161-4, 4illus. in colour.

Light directed to a red ring surrounding the objective lens of the Brandt loupe generates red reflections of table and crown facets from the pavilion facets of a diamond. The size and geometry of this characteristic image can be directly related to the size of the table, the pavilion angle, and the thickness of the crown and the girdle, all of which can be related to the diameter of the girdle as percentages. This Instrument Evaluation Report found the rapid sight method of assessing the cut of a faceted diamond to be very accurate for estimating the pavilion angles that produce maximum brightness. Reference is made to earlier papers on the assessment of cut, advice is given on the use of the Brandt loupe, and illustrations show the pattern of red reflections produced by a shallow cut, a well cut and a deep cut diamond. P.G.R.

Synthetics and Simulants

Gemmologische Kurzinformationen. Synthetischer Moissanit – ein kurzer historische Rückblick.

H. Bank, U. Henn. *Gemmologie. Z. Dt. Gemmol. Ges.*, **50**(3), 2001, 163-6, 3 photographs, bibl.

Since 1997 synthetic moissanite (SiC) in gem quality has been marketed as a new product and diamond imitation. However, artificially produced silicon carbide has been known since 1948 and some transparent green specimens were cut in 1956. The natural product was found by Henri Moissan as tiny, green hexagonal crystals in Arizona in 1904. Synthetic SiC has been and is being used as industrial grit under the name of Carborundum. E.S.

[Quartz crystals: their device industry status and numerical simulation of convection in autoclave.] (In Japanese with English abstract)

K. Hirano and K. Nagai. *Journal of The Japanese Association for Crystal Growth*, **27**(2), 2000, 69-75, 11 figs.

Due to increasing industrial demand for larger single crystals of synthetic quartz with higher perfection, the present-day requirements for an autoclave are a size over 600 mm diameter and up to 2500 kg capacity. It is necessary to know and control convection in such a large scale autoclave. Numerical simulation of natural convection in an autoclave with a baffle has been performed with the finite element method. When the length of the heated part on the autoclave wall becomes greater than 2% of the height of the autoclave with 60% baffle closure, circulating flows in the upper and lower sections of the autoclave oscillate periodically. As the Rayleigh number is increased, the frequency and the amplitude of the flow oscillation increases. I.S.

An experimental demonstration of diamond formation in the dolomite–carbon and dolomite–fluid–carbon systems.

A.G. Sokol, Y.M. Borzdov, Y.N. Pal'yanov, A.F. Khokhryakov and N.V. Sobolev. *European Journal of Mineralogy*, **13**(5), 2001, 893-900.

A study of diamond crystallization in dry and fluid-rich dolomite–carbon systems is reported. For the dry system, an induction period before spontaneous diamond nucleation was found to be ~ 4 h at 7 GPa, 1700°C. No diamonds were observed after 42 h of reaction at 5.7 GPa, 1420°C. The addition of H_2O and H_2O-CO_2 fluids to the dolomite–carbon system resulted in spontaneous diamond nucleation at 1420°C, and growth of diamond on seed crystals at 1300–1420°C. In the presence of H_2O or H_2O-CO_2 fluids, dolomite decomposes to dolomite solid solution + brucite + aragonite. Experimental results indicate that dolomitic melts in the mantle, enriched in H_2O and CO_2, promote the formation of natural diamond. R.A.H.

BOOK REVIEWS

Tropical gemstones.

C. Clark, 1998. Periplus Editions (HK) Ltd., Hong Kong. pp 64. Illus. in colour. Hardcover, ISBN 962 593184 8. £6.50.

Very small but quite pleasantly illustrated book describing a number of gem species of Asian origin. Apart from the same photograph appearing (or seeming to appear) up to three times in different guises, it easily fits into a pocket or handbag and is good to look at when you want to see attractive gemstones. M.O'D.

A history of White Cliffs opal 1889-1999.

L. Cram, 2002. The Author, Lightning Ridge (PO Box 2, Lightning Ridge, NSW 2834, Australia). pp 368. Illus. in colour. Hardcover, ISBN 0 9585414 5 0. [*A journey with colour*. Vol. 2 Part A.] A$168.

A journey with colour began with a magnificently illustrated study of Queensland opal and the project has the aim of covering all the opal fields of Australia in three volumes. Part B of Volume 2 will cover Lightning Ridge and Volume 3 the three mines of South Australia. This reviewer is impatient for the next two volumes! Readers should note that the print run of 1500 is small and copies will quickly be hard to come by.

As before, Cram gives us not only a set of beautiful photographs of specimens but also has found and reproduced pictures of mining and social activity which would otherwise almost certainly have been lost. The first mention of White Cliffs (New South Wales) was in 1852 and the fields still produce a small amount of opal. Cram makes the point that the community has shrunk but developed very successfully after the output from the fields had diminished and is well worth a visit.

The opal is beautiful and specimens include pseudomorphs after fossils, especially the torpedo-shaped belemnites. As always, the standard of reproduction is excellent and the many mining scenes, from original pictures which were not always in very good condition, have come out very well. There is a glossary and a useful bibliography in which a number of government publications are included. M.O'D.

Beautiful Coober Pedy, home of the desert opal.

L. Cram, 2001. The Author, Lightning Ridge (PO Box 2, Lightning Ridge, NSW 2834, Australia). pp 32. Illus. in colour. Softcover, ISBN 0 9585414 42. Price on application.

Len Cram continues to perform good service to the Australian opal industry through his most beautifully illustrated books covering the major opal-producing areas. This one describes the settlement of Coober Pedy in South Australia and some of the opal specimens found there, the photographs accompanying a text giving some of the history and details of the celebrated underground houses used by the miners. M.O'D.

Queensland minerals: A summary of major mineral resources, mines and projects. (1st edn)

P.G. Garrad *et al*., 2000. Queensland Department of Mines and Energy, Brisbane. pp 356, includes maps and diagrams, softcover. ISBN 0 7242 7245 3 ISSN 1443 8747. Includes CD-ROM containing digital data. A$55.

While gemmologists will look first for the sections dealing with opal, corundum and chrysoprase, it does no harm for them to consult material in which geology, mineral occurrences and mining organization also find a place. While the greater part of this first directory of the mining industry of Queensland gives an alphabetical listing of mining companies with, in some cases, their results. Preliminary material covers geology and mineralogy with maps and a good deal of other useful information. Since many of Queensland's mines produce gold, details of that material are also welcome. In recent years Queensland opal has progressed from boulder opal only, to production of some of the finest specimens to be found in Australia and the world's finest chrysoprase still comes from the Marlborough mine, about 90 km north-west of the town of Rockhampton. M.O'D.

Ultraviolet spectroscopy and UV lasers.

P. Misrsa and M.A. Dubinskii (eds), 2002. Dekker, New York. pp XV, 569. Hardcover ISBN 0 8247 0668 4. [Practical spectroscopy series, Vol. 30] Price on application.

While having no direct bearing on gemmology or mineralogy this review volume covers the application of UV techniques to a variety of problems and in particular to lasers. The use of doped crystals is featured in a number of chapters which also cover chemical physics, photolithography and laser spectroscopy. Each chapter has its own, often extensive, list of references. M.O'D.

Lovozero massif: history, pegmatites, minerals.

I. V. Pekov, 2000. Ocean Pictures Ltd, Moscow. pp 497. Illus. in colour, hardcover. ISBN 5 900395 27 8. DM 169.

Though I was unable to find any mention in the text the book is a companion to *Dalnegorsk* and other works in the monographic series succeeding *Mineralogical almanac*. As there is no other survey of this important area (part of the geologically celebrated Kola Peninsula), at least in English, it will immediately achieve the status of a standard work – the extensive 13-page bibliography covers the many Russian papers on the area. The book is well presented and the colour photographs reasonably good, considerable support for the project was provided by Lomonosov State University and the Russian Geological Society.

While the area provides no regular ornamental species, those gemmologists and species collectors who are concerned with minerals and their occurrence will find this in-depth study of a major pegmatite body of considerable interest, and some attractive, possibly gemmy specimens do occur: on the pre-title page is a fine transparent red villiaumite crystal! The main sections of the book cover history of exploration (including some graphic accounts of how the miners lived in a most inhospitable area), the pegmatites and the mineral species – a list of names, full descriptions, chemical classification, a list of species found as new in other locations but also found at Lovozero at the same time or earlier, crystal structures, fluorescent minerals, giant crystals and a section on geographic names in which Saami words used for local geological features and place names are translated and explained.

I strongly recommend early ordering of any book in this series as I know from experience how soon the small print-run is exhausted. The publishers are at Box 368, Moscow 103009, fax/phone (from the UK) 00 7 095 203 3574. M.O'D.

Las otras piedras preciosas.

M.A. Pellicer, 2001. Zaragoza. pp 350. Illus. in colour. Softcover, ISBN 84 607 1826 3. Euro 36.

A comprehensive survey of the mechanisms of crystallization and of the details of the methods used to grow gem-quality crystals. The text is well illustrated with diagrams showing how the growth methods work and the occasional colour plate shows examples of crystals and some characteristic inclusions. Although the book could not seriously be used as an everyday adjunct to testing in the laboratory as this would not seem to have been the main aim of the author (perhaps more testing details would be necessary). Nevertheless the text gives a good picture of crystal growth (notoriously difficult to explain to non-growers) and it would certainly be very useful to Spanish-speaking gemmology students. The colour pictures are quite good without achieving excellence; each major section includes a list of references and the production as a whole is very good value for its comparatively low price. M.O'D.

The amber forest: a reconstruction of a vanished world.

G. Poinar Jr and R. Poinar, 1999. Princeton University Press, Princeton, NJ. pp xviii, 239. Illus. in colour. Softcover, ISBN 0 691 05728 1. £13.95.

A survey of the amber fossils from the ancient forests of the Dominican Republic constructed as a natural history of the area's ecosystem at the time of the amber's formation. This is a beautiful and well-illustrated book with a central section containing 171 colour photographs of insects included in amber specimens and continuous comment on their life and behaviour. Each chapter has its own list of references to biological literature, providing students of amber with an insight into aspects of the material which deserves more scholarly treatment than it has hitherto received. M.O'D

Cristal de roche.

S. Raulet, 1999. Editions Assouline, Paris [26-28 rue Danielle-Casanova, 75002]. pp 239. Illus. in colour. Hardcover, ISBN 2 84323 26 137 X. FF560.

Beautifully produced survey of rock crystal used in and as ornament from Classical times to the present. After introducing rock crystal with notes on its geology and occurrence the book takes quite large historical periods at a time to describe how it was worked and, in the case of the Egyptian civilizations, how it acquired magical and medicinal significance.

The mostly large illustrations are attractive and there is a useful bibliography; disregard some quaint and inaccurate gemmology! M.O'D.

Les types d'espèces minérales et les collections de synthèses anciennes du Muséum National d'Histoire Naturelle.

H-J. Schubnel, 1999. Galerie de Minéralogie et de Géologie [36 Rue Geoffroy Saint-Hilaire, 75005 Paris]. pp 28. Illus. in colour. Softcover ISBN 2 85653 259 4 (*Dossiers de la Galerie*, numéro spécial) FF 50.

A completely admirable short and beautifully illustrated introduction to the classification of mineral species on the basis of their composition and crystallography, using material, often of great historical interest, from the collections of the Museum, including specimens once in the collections of Haüy, De Bournon and others. This would be quite enough in itself to make an excellent guide but the author even more admirably goes on to describe some of the early syntheses of minerals, including and illustrating beryl and spinel crystals grown by Ebelmen, Hautefeuille and Perrey's synthetic emeralds and De Berthier's synthetic diopside among others. M.O'D

Trésor du Muséum: cristaux précieux, gemmes et objets d'art.

H-J. Schubnel, 1998. Muséum National d'Histoire Naturelle, Paris. pp 119. Illus. in colour. Hardcover, ISSN 1168-4798 [as numéro spécial of *Dossiers de la Galerie*] FF 50.

A fairly brief but far more than adequate account describing some of the specimens and artefacts to be found in the Mineral Gallery of the Muséum National d'Histoire Naturelle, Paris. All photographs are in colour, examples illustrated carry their Museum accession number and their size where relevant and references to the appropriate literature are plentiful. Details of the history of the collections are given: many of the specimens were collected by celebrated French scientists of the past and many of the photographs display gem crystals and in some cases fashioned stones. There is a short bibliography and the whole book is a model at whose standard I wish other national museums could aim. M.O'D

Strunz mineralogical tables. (9th edn)

H. Strunz and E.H. Nickel, 2001. E. Schweizerbart'sche

Verlagsbuchhandlung, Stuttgart, Germany. pp ix, 870. Illus. in black-and-white. Hardcover, ISBN 3 510 65188 X. US$142.00.

This welcome reappearance of an old friend reminds the reviewer that the first edition was published in 1941 and the previous (eighth) edition in 1978. Such large gaps are easily explained: despite the title, *Strunz* is much more than a table of mineral names and compositions – there are several good versions extant – as it includes its own classification based upon a chemical-structural system. In this system all species are assigned to one of ten classes according to its principal anionic constituents: each class is subdivided into divisions, subdivisions and groups, still based on composition and structure and within the groups each species carries its own unique alphanumeric identification (gaps make the system capable of expansion as new species are validated).

Entries where possible include references to the literature as well as structure diagrams for the more important species and groups, and the presentation is in tabular form. Group membership is given where applicable. Taking at random an example of a gem mineral, the beryl group unique number is 9.CJ.05 and the diagram shows the structure projected on (0001). The group is dealt with on a single page.

The index carries the names of validated species in bold, making it easy to read and the presentation and typeface of the main text are well chosen. The binding seems satisfactory on first examination though, as with all such reference books, heavy use may strain it eventually. This is a most valuable addition to mineralogical references literature. M.O'D.

Gem care. (Revised edn)

F. Ward, 2002. Gem Book Publishers, Bethesda, MD. pp 33. Illus. in colour. Softcover, ISBN 1 887651 07 10. [*Fred Ward Gem Series*] £8.95.

Excellently produced and attractive guide to some of the ways in which gemstones may suffer accidental and unexpected damage. Metals (gold and silver) are included and there are many sensible remarks which wearers and collectors could well take to heart. It is surprising how much information can be accommodated in so small a compass, especially when the text has to share space with the fine colour photographs. M.O'D.

Proceedings of the Gemmological Association and Gem Testing Laboratory of Great Britain and Notices

MEMBERS' MEETINGS

London

On 9 January at the Gem Tutorial Centre, 27 Greville Street, London EC1N 8TN, E. Alan Jobbins gave an illustrated lecture entitled 'An orgy of organic gem materials'.

On 5 and 6 March visits to the Diamond Information Office at the DTC were held.

On 9 April there was a private viewing and tour of the Tiaras exhibition at the Victoria and Albert Museum, South Kensington, with exhibition curator Geoffrey Munn.

Midlands Branch

On 25 January at the Earth Sciences Building, University of Birmingham, Edgbaston, a Gemmology Quiz and Bring and Buy were held.

On 22 February at the Earth Sciences Building, E. Alan Jobbins gave a talk entitled 'An orgy of organics'.

On 24 February a one-day conference to celebrate the 50th anniversary of the Midlands' Branch was held at Barnt Green. Speakers included Professor Dr Henry Hänni, E. Alan Jobbins and Ian Mercer. A report of the event will be published in the June issue of Gem & Jewellery News.

On 29 March at the Earth Sciences Building, Martyn Pugh gave a talk entitled 'The art of the goldsmith and silversmith'.

North West Branch

On 20 February at Church House, Hanover Street, Liverpool 1, Irene Knight gave a talk on her time as Branch Chairman entitled 'The Chairman's mantra – don't forget the speaker's name'.

On 20 March members of the Branch visited the Archaeology, Egyptian and Mineral Department of the Liverpool Museum.

Scottish Branch

A Quiz Night was held on 16 January at the College Club of Glasgow University.

On 25 February at the British Geological Survey, Murchison House, West Mains Road, Edinburgh, Professor Dr Henry Hänni gave a lecture on 'Pearls in close up'.

On 6 March at the Hunterian Museum, Glasgow University, Alan Hodgkinson gave a talk entitled 'Poking in gemmological corners'.

GEM DIAMOND EXAMINATION

In the Gem Diamond Examination held in January 2002, 80 candidates sat of whom 50 qualified including five with Distinction and nine with Merit. The names of the successful candidates are listed below:

Qualified with Distinction

Leeks, David R., Java, Indonesia
Morrish, Rachel, Sutton Coldfield, West Midlands
Read, Julian, Goole, East Yorkshire
Wen Chun, Wuhan, Hubei, P.R. China
Xing Yuan, Beijing, P.R. China

Qualified with Merit

Cui Xiwen, Beijing, P.R. China
Deng Xin, Beijing, P.R. China
Ding Yifei, Beijing, P.R. China
Falnes, Lene, Birmingham, West Midlands

ISSN: 1355–4565

GIFTS TO THE ASSOCIATION

The Association is most grateful to the following for their gifts for research and teaching purposes:

Terry Davidson, London, for a laptop computer to be used for presentation purposes.

The Diamond Trading Company, London, for the permanent loan of a DiamondView™1. This will complement the DiamondSure™1 loaned by the DTC in 2001.

John A. Kessler, London, for faceted blue topaz and irradiated brown topaz

Michael Parsons, the Gold and Silver Studio, Bath, for a selection of study gemstones.

Mariana-Maria Photiou, San Francisco, California, U.S.A., for rough and cut specimens of Oregon sunstones from a variety of mines.

Gerald H. Stonely, Haddenham, Aylesbury, Buckinghamshire, for a box of cut gemstones for student use.

Bear Williams, Bear Essentials Co., Jefferson City, Missouri, U.S.A., for a large quantity of emerald crystals and cut amethysts.

An anonymous donation of £5000.

He Zixi, Wuhan, Hubei, P.R. China
Liu Wei, Beijing, P.R. China
Squires, Caroline A., Tring, Hertfordshire
Yin Wei, Beijing, P.R. China
Yu Lijun, Beijing, P.R. China

Qualified

Amliwala, Panna, Solihull, West Midlands
Bolter, Rachel L., Chiseldon, Swindon, Wiltshire
Borahan, Fatma O., Kalamis, Istanbul, Turkey
Cheung Li, Alex, Kowloon, Hong Kong
Child, Catherine J., Lewes, East Sussex
Cristol, Agata, Marseille, France
Dyre, Pablo, Nairobi, Kenya
Gu Jing, Beijing, P.R. China
Hei Kwok, Tsing Yi, New Territories, Hong Kong
Ho Sau Lan, Tsuen Wan, Hong Kong
Humphrey, Brian, Fulham, London
Kamani, Priscilla, Arkley, Barnet, Hertfordshire
Kaushal, Opinder J.S., Reading, Berkshire
Lai Mei Oi, Emily, Tuen Mun, Hong Kong
Lau Chun Kit, New Territories, Hong Kong
Mafara, Ezekiel M., Harare, Zimbabwe
Mei Chuan Ma, Kowloon, Hong Kong
Monney, Christelle V., Geneva, Switzerland
Petrozello, Ryan J., Randolph, New Jersey, U.S.A.
Qingren Ji, Wuhan, Hubei, P.R. China
Stinglhamber, Renata, Brussels, Belgium
Sutton, Collette S., Hampton in Arden, Solihull, West Midlands
Tsuor Wai Hing, Shatin, Hong Kong
Verdi, Nasib, Edgbaston, Birmingham, West Midlands
Wang Pei, Wuhan, Hubei, P.R. China
Wang Weina, Wuhan, Hubei, P.R. China
Wong Sau Han, Branda, Kowloon, Hong Kong
Wong Sheung Ling, Shirley, Kowloon, Hong Kong
Wu Derong, Wuhan, Hubei, P.R. China
Wu Jiatao, Wuhan, Hubei, P.R. China
Yanagihara, Satomi, Ehime, Japan
Yeung Yee Wai, Margery, Kwun Tong, Hong Kong
Zhang Hong, Beijing, P.R. China
Zhang Shuling, Beijing, P.R. China
Zhang Xiao Ling, Kowloon, Hong Kong
Zhou Yi, Wuhan, Hubei, P.R. China

EXAMINATIONS IN GEMMOLOGY

In the Examinations in Gemmology held worldwide in January 2002, 120 candidates sat the Diploma Examination of whom 63 qualified, including one with Distinction and five with Merit. In the Preliminary Examination, 107 candidates sat of whom 88 qualified. The names of the successful candidates are listed below:

Diploma

Qualified with Distinction

Hudson, Sally, Battersea, London

Qualified with Merit

Gordon, Carole, Kew, Richmond, Surrey
Holt, Jason B.A., London
Hudson, Lawrence M., London

Roy, Maryse, Montreal, Quebec, Canada
Steward, Sarah, Hove, East Sussex

Qualified

Abimbola, Adedapo, London
Allsopp, Christopher J., St Saviour's, Guernsey, Channel Islands
Bai Yunlong, Guilin, Guangxi, P.R. China
Basile, Appadoure, London
Chan See Lan, Shirley, Kowloon, Hong Kong
Choi Jung-Hae, Daejon, Korea
de Vries, Yvonne, Den Haag, The Netherlands
Fang Lan, Guilin, Guangxi, P.R. China
Francis, Melanie, Toronto, Ontario, Canada
Furze, Cindy, Cheshunt, Hertfordshire
Gu Siyuan, Shanghai, P.R. China
Ho Pui Cheung, Kowloon, Hong Kong
Hsieh Ming Tsung, Taichung, Taiwan, R.O. China
Htay Yin, Bago, Myanmar
Htun Su Su, Yangon, Myanmar
Jiang Linhui, Guilin, Guangxi, P.R. China
Jinnam-olarn, Wichuda, Udonthani, Thailand
Kalischer, Janice, Finchley, London
Kwok Hei, Tsing Yi, New Territories, Hong Kong
Lee Soo-Jin, Seoul, South Korea
Li Yikuang, Guilin, Guangxi, P.R. China
Lowe, Mimi J., San Francisco, California, U.S.A.
Lwyn Mon Mon Myat, Yangon, Myanmar
Mate, Nikhil Shripad, Mumbai, India
Meng Xiangdong, Shanghai, P.R. China
Mitch, Alexandra, Atlanta, Georgia, U.S.A.
Morton, Aude Alexandra, London
Myint Kyaw, Yangon, Myanmar
Pan Jingchen, Shanghai, P.R. China
Pavaro, Thitintharee, Bangkok, Thailand
Pi Zhengfan, Wuhan, Hubei, P.R. China
Rademaker, Gerriedina J., Weekt, The Netherlands
Roberts, Justin J., Wembley, Middlesex
Sakkaravej, Somruedee, Nonthatburi, Thailand
Schraa, Catharina N., Goes, The Netherlands
Smeets-van den Berg, Wopje R., Wassenaar, The Netherlands
Soe Moe Tun, Yangon, Myanmar
Sun Jiexian, Shanghai, P.R. China
Suraseth, Peerapol, Bangkok, Thailand
Susser, Jennifer L., London
Symes, Evelyn R., Bath, Avon
Takala, Ville P., Lannavaara, Sweden
Tang, Elaine Wai Ling Ng, Chesham, Buckinghamshire
Tangsubkul, Hiranya, Bangkok, Thailand
Tantisiriphaiboon, Yenrudee, Bangkok, Thailand
Toullic, Nathalie, Brentford, Middlesex
Tsang, Judy, Kwai Chung, Hong Kong
van der Made, B.C., Ermelo, The Netherlands
Vyvere, Vinciane Vande, London
Wang Kai, Wuhan, Hubei, P.R. China
Wu Lai Ngor, Kowloon, Hong Kong
Xia Zhen, Shanghai, P.R. China
Yanagihara, Satomi, Ehime, Japan
Yang Chau Yuan, Taipei, Taiwan, R.O. China
Yuanyuan Li, Shanghai, P.R. China
Yun Jing Wen, London
Zhou Yujie, Shanghai, P.R. China

Preliminary

Agarwal, Vibha, New Delhi, India
Ayer, Elizabeth, Cambridge
Barnett, Catherine, Balham, London
Berry, Susan E., London
Bertrand, Sylvia, London
Carmichael, Jeanie A., London
Chan Kok Nang, Eric, Bahru, Malaysia
Chen Shanxi, Guangzhou, P.R. China
Cheung Li, Alex, Kowloon, Hong Kong
Cheung See Ming, Myra, Kowloon, Hong Kong
Chiu Yung-Tung, Taipei, Taiwan, R.O. China
Choudhary, Gagan, Rajasthan, India
Dash, Sandra Y., London
De Lasteyrie Du Saillant, Valentine, London
Deuling, Elsbeth M., De Haag, The Netherlands
Eleen, Lynn, Halewood, Knowsley, Merseyside
Fitzgerald, John, Flanagan, Illinois, U.S.A.
Gao Boqian, Guilin, Guangxi, P.R. China
Giancola, Maria L.C., Milan, Italy
Govindara Julu, Suresh, Ilford, Essex
Gregory, Nualchan, London
Gurevich, Lina, Finchley, London
Hedenskog, Elin M.S., London
Houghton, Agnes, London
Htin Lynn Aung, Yangon, Myanmar
Hu Zhikun, Shanghai, P.R. China
Jinnam-olarn, Wichuda, Udonthani, Thailand
Jose, Kadavi F., Ilford, Essex
Juan Chun Wei, Taichung, Taiwan, R.O. China
Karimjee, Farida N., Chingford, London
Kontopoulou, Theoni, London
Kuo Chi-Cheng, Taipei, Taiwan, R.O. China

2001 Gemmology Awards

Patricia Wong travelled to London from Hong Kong to receive the Anderson Medal at the Presentation of Awards held at Goldsmiths' Hall on 5 November 2001. This medal is awarded to the best Preliminary candidate of the year.

Patricia Wong Bick San, Hong Kong, receiving the Anderson Medal from Raymond Sancroft-Baker. © Peter Dyer Photographs Ltd.

Dong Lan of Wuhan, P.R. China, receiving the Anderson-Bank Prize from Ian Mercer.

Dong Lan received the Anderson-Bank prize during Ian Mercer's visit to China in November 2001. The prize is awarded to the best non-trade Gemmology Diploma candidate of the year.

We apologize for confusing the caption and photograph of these award winners in the January issue of The Journal.

Kwan, Susana, Kowloon, Hong Kong
Lam Koon-Wah, Francis, Kowloon, Hong Kong
Lee Chun Ming, New Territories, Hong Kong
Lee Hing Fan, Kowloon, Hong Kong
Lee Kuang Chung, Taichung, Taiwan, R.O. China
Lee Kwok Wai, Joe, Kowloon, Hong Kong
Lee Ting-Ju, Cristina, Yangon, Myanmar
Lee Ting-Ju, Michelle, Yangon, Myanmar
Lei Jiali, Guilin, Guangxi, P.R. China
Li Wenjian, Guangzhou, P.R. China
Li Wing Chiu, Kowloon, Hong Kong
Lian Poh Chu, Yvonne, Johor, Malaysia
Liao Yueh-Hua, Taipei, Taiwan, R.O. China
Liao Zhonghua, Guilin, Guangxi, P.R. China
Liem, Deborah A., Singapore
Liu Chun, I., Taichung, Taiwan, R.O. China
Liu Lili, Guilin, Guangxi, P.R. China
Liyana Arachchige, Nilmini S., Kandy, Sri Lanka
Lui Sze-Wai, Alice, Quarry Bay, Hong Kong
Luk Sau Nam, Kowloon, Hong Kong
Luo Xuan, Matthew, Camberwell, London
Luther, Jane, Shepton Mallet, Somerset
Maier, Mona, Valencia, California, U.S.A.
Mukhopadhyay, Nita, Kolkata, West Bengal, India
Ngan Hin Wah, Michael, Kowloon, Hong Kong
Okazaki, Maki, London
Phyu Thin Khine, Yangon, Myanmar
Robinson, David, Shankill, Co. Dublin, Ireland
Rogers, Emily I., Putney, London
Ruckel, Daphne, London
Rupani, Nalina, Nairobi, Kenya
Sabah, Yaffa, Kraainem, Belgium
Sayed, Shakir, Harrow, Middlesex
Scott-Dawkins, Jacqueline, West Malling, Kent
Selvamani, Parvathi, Poplar, London
Stephens, Pippa H., Groby, Leicester
Stephenson, Michelle D., London
Stevenson, Polly V., London
Tanapad, Kiattikun, Patumtanee, Thailand
Thin Thin Hlaing, Yangon, Myanmar
Tsang, Jasmine, Kennedy Town, Hong Kong
Tsoi Pui Pui, Karen, Kowloon, Hong Kong

Tulsi Valia, London
Wang Donglei, Guilin, Guangxi, P.R. China
Wei Xiaoling, Guilin, Guangxi, P.R. China
Wenham, Diana L., North Harrow, Middlesex
Whalley, Joanna, Walthamstow, London
Wong Nga Sze, Kowloon, Hong Kong
Wong Ka Yee, Kowloon, Hong Kong
Wong Man Kuen Purdey, Kowloon, Hong Kong
Xiongfeng Xin, Shanghai, P.R. China
Xing Zengmin, Guilin, Guangxi, P.R. China
Xu Banghui, Guilin, Guangxi, P.R. China
Yaddanapudi, Pratima, Hounslow, Middlesex
Yin Yu, Guilin, Guangxi, P.R. China
Zhu Xulei, Guilin, Guangxi, P.R. China

MEMBERSHIP

Between 1 January and 31 March 2002 the Council of Management approved the election to membership of the following:

Fellowship and Diamond Membership (FGA DGA)

Russell, Lionel H., Hampstead, London, 1969/ 1971

Fellowship (FGA)

Chan, Albert Hiu Sang, Hong Kong, 1988
Cheng Chan Fan, Henry, Kowloon, Hong Kong, 1987
de Wit, Lambertus, Westervoort, The Netherlands, 1992
Heasman, David J., Tonbridge, Kent, 1961
Lai Sau Ha Melody, Kowloon, Hong Kong, 1990
Maxwell, John A., London, 1956
Ou Yang, Chiu Mei, Central, Hong Kong, 1979

Ordinary Membership

Anderson, Ian, Shipley, West Yorkshire
Aki, Miou, Osaka City, Osaka, Japan
Arjan, Anand, East Ham, London
Ashida, Eisuke, Koyoto City, Kyoto, Japan
Balls, Serra, London
Banno, Norihisa, Nagoya City, Aichi Pref., Japan
Bogomolova, Yana, London
Borahan, Fatma Oya, Istanbul, Turkey
Cheshire, Anna E., Littledean, Gloucestershire
Cowley, Vivien, Ballaghaderreen, Co. Roscommon, Ireland
Daouk, Ziad, Beirut, Lebanon
Deares, Haydon M., Southend-on-Sea
Droujinina, Valentina, Highgate, London
Dryburgh, William, Kirkcaldy, Fife, Scotland
Fiala, Adele, London
Firth, Richard Antony, Kennington, London
Forbes-McCaig, Charlotte, Belfast, Northern Ireland
Fukuoka, Yoshimi, Kisarazu City, Chiba Pref., Japan
Guldman, Melanie, Maritou Springs, Colorado, U.S.A.
Hamaoka, Minako, Takasuki City, Osaka, Japan
Hardwick, Christine J.E., Crail, Fife, Scotland
Ingridsson, Anna-Lis, Lannavaara, Sweden
Inoue, Koichi, Suita City, Osaka, Japan
Ito, Ayako, Nishikyo-ku, Kyoto City, Kyoto, Japan
Kaffo, Bassiti Moulero, Hounslow, Middlesex
Kamara, Malcolm M., London
Kendirci, Ibrahim, Stone, Staffordshire
Loaker, Alistair, Stevenage, Hertfordshire'
Lucic, Radoslav, London
Maruyama, Sawako, Shibuya-ku, Tokyo, Japan
Matoba, Ayumi, Minoo City, Osaka, Japan
Mayumi, Kaneyama, Higashi-Osaka City, Japan
Mitani, Toshiyasu, Tokushima City, Japan
Muhammad, Taimur Ali, Islamabad, Pakistan
Nakamura, Aki, Chuo-ku, Osaka City, Japan
Nakazawa, Kenichi, Mitaka City, Tokyo, Japan
Nishitani, Yumi, Nishi-ku, Osaka City, Japan
Odfjell, Abraham, London
Ohara, Yasuko, Koshien, Nishinomiya City, Japan
Partridge, Caroline, London
Ritchie, Sara, Glen Ridge, New Jersey, U.S.A.
Rohm, Peter, Linz, Austria
Rose, Charles L., Germantown, Tennesee, U.S.A.
St John Lewis, Delyth, Winchmore Hill, London
Satake, Rika, Chou-ku, Osaka City, Osaka, Japan
Scoles, Eric, Newbury, Berkshire
Shelementiev, Yuri, Moscow, Russia
Tanaka, Yumi, Toyonaka City, Osaka, Japan
Tonomoto, Noriko, Wakayama City, Japan
Tsutani, Miho, Osaka City, Osaka, Japan
Wakefield, Dominic, Horesham, West Sussex
Washi, Shogo, Matsudo City, Chiba Pref., Japan
Yasutake, Megumi, Shizuoka City, Japan
Zheng, Lisa, South Kensington, London

TRANSFERS

Fellowship to Fellowship and Diamond Members (FGA DGA)

Amliwala, Panna, Shirley, West Midlands
Bolter, Rachel L., Chiseldon, Swindon, Wiltshire

Dyre, Pablo, Nairobi, Kenya
Ho Sau Lan, Tsuen Wan, Hong Kong
Mafara, Ezekiel M., Harare, Zimbabwe
Morrish, Rachel, Sutton Coldfield, West Midlands
Read, Julian, Goole, East Yorkshire
Squires, Caroline A., Tring, Hertfordshire
Sutton, Collette S., Hampton-in-Arden, West Midlands

Diamond Membership to Fellowship and Diamond Membership (FGA DGA)

Furze, Cindy, Cheshunt, Hertfordshire
Gordon, Carole, Kew, Richmond, Surrey
Susser, Jennifer L., London
Yun Jing-Wen, London

Ordinary Membership to Fellowship (FGA)

Allsopp, Christopher J., St Saviour's, Guernsey, Channel Islands
Hudson, Sally, Battersea, London
Hudson, Lawrence M., London
Kalischer, Janice, Finchley, London
Smeets van den Berg, Wopje R., Wassenaar, The Netherlands
Symes, Evelyn R., Bath, Avon
Tang Wai Ling Ng, Elaine, Chesham, Buckinghamshire
Vyvere, Vinciane Vande, London
Wu Lai Ngor, Kowloon, Hong Kong

Ordinary Membership to Fellowship and Diamond Membership (FGA DGA)

Yanagihara, Satomi, Ehime, Japan

Ordinary Membership to Diamond Membership (DGA)

Borahan, Fatma O., Istanbul, Turkey
Child, Catherine J., Lewes, East Sussex
Cristol, Agata, Marseille, France
Kamani, Priscilla, Arkley, Barnet, Hertfordshire
Kaushal, Opinder J.S., Reading, Berkshire
Stinglhamber, Renata, Brussels, Belgium

Pearls Coral Amber Bead Necklaces Carvings Cameos Mineral Specimens

Opal Precious Topaz Ruby Star Ruby Sapphire Star Sapphire Tourmaline

The World of Gemstones

Ruppenthal (U.K.) Limited

Gemstones of every kind, cultured pearls, coral, amber,
bead necklaces, hardstone carvings, objets d'art and
18ct gold gemstone jewellery.

We offer a first-class lapidary service.

By appointment only
1a Wickham Court Road, West Wickham, Kent BR4 9LN
Tel: 020-8777 4443, Fax: 020-8777 2321, Mobile: 07831 843287
e-mail: roger@ruppenthal.co.uk, Website: www.ruppenthal.co.uk

Gemstones Aquamarine Alexandrite Amethyst Emerald Jade Lapis-Lazuli

Modern 18ct Gem-set Jewellery

FELLOWS & SONS

Auctioneers & Valuers of Jewels, Silver & Fine Art

Established in 1876 Fellows & Sons are one of the UK's leading provincial auction houses, specialising in the sale and valuation of jewellery & watches, silver, furniture and collectables.

We hold over 30 auctions per annum of fine diamond and gem set jewellery; loose gemstones; memorial jewellery; novelties; and wrist and pocket watches, including Rolex, Piaget & Patek Phillipe.

Fully illustrated catalogues are available on our website
www.fellows.co.uk
and our Antique & Modern Jewellery & Watches auctions are available live on the internet to bidders around the world on
www.ebayliveauctions.com

Contact us now for further information on our services.

Augusta House, 19 Augusta Street, Hockley, Birmingham B18 6JA
Tel: 0121 212 2131 Fax: 0121 212 1249


F.M. JEWELLERY

Secured Minerals

is able to offer the following:-

A collection of facetted fluorites from Greencleugh vein, Rookhope, County Durham which in natural light are a good deep green colour and intensely fluorescent under longwave u.v. light. Also available are yellows from Hilton Mine, near Appleby, Cumbria, various shades of brown and purple from Boltsburn Mine, Rookhope, and deep greens from Heights and Rogerley Mines in Weardale.

Stone sizes from 5 ct. to 63 ct.

Matrix fluorite specimens from the above locations are also available.

"Birchfield", 16 Sedbergh Road, Kendal, LA9 6AD U.K.
e-mail: securedminerals @aol.com
fax: UK 1539 734761

Pearls
Gemstones

Lapidary Equipment

GENOT L
Since 1953

CH. De Wavre, 850
B-1040 Bxl – Belgium

Tel : 32-2-647.38.16
Fax : 32-2-648.20.26
E-mail : gama@skynet.be

www.gemline.org
www.geofana.net

ROCK 'n' GEM SHOWS

Exhibitors Displaying & Selling
Treasures of the Earth

NEWARK SHOWGROUND
Winthorpe, Newark, Notts (Off A46)
27-28 APRIL

KEMPTON PARK RACECOURSE
Sunbury on Thames, Middx (On A308)
8-9 JUNE *

CHELTENHAM RACECOURSE
Prestbury Park, Cheltenham, Glos
20-21 JULY

KEMPTON PARK RACECOURSE
Sunbury on Thames, Middx (On A308)
10-11 AUGUST *

All shows are indoors and open to trade & public from 10am - 5pm
Refreshments ~ Free Parking
Wheelchair Access

Adults £2.50/*£3.00
Seniors £2.00/*£2.50
Children (8-16 yrs) £1.00
THE EXHIBITION TEAM LTD 01628 621697
Email: Rockngems@aol.com

FORTHCOMING EVENTS

3 May	**London.** *New aspects of cut in round brilliant-cut diamonds.* *Joseph Tenhagen of Miami, Florida*
15 May	**North West Branch.** *Diamonds. Rosamond Clayton.*
19 May	**South West Branch.** The colour of money. *Michael Norman.* Followed by 'Do you know right from wrong?' – a practical gemmology session.
19 May	**Midlands Branch. Gem Club.** *Photomicroscopy* with *Doug Morgan and David Larcher.*
21 May	**London.** Private viewing and curatorial tour by *Geoffrey Munn* of the Tiaras exhibition at the V&A.
19 June	**North West Branch.** Bring and Buy Social Evening.
22 June	**Midlands Branch.** Summer Supper Party.
18 September	**North West Branch.** *Chasing rainbows. John Harris.*
26 September	**Annual General Meeting and Lecture**
16 October	**North West Branch.** *Jewels for a Royal occasion. Rosemary I. McIver.*
4 November	**Presentation of Awards and Reunion of Members.** Goldsmiths' Hall, Foster Lane, London EC2

Gem-A Conference 2002

To be held on

Sunday 3 November

at Kempton Park Racecourse, Sunbury on Thames, Middx.

In conjunction with the Rock 'n' Gem Show

Speakers will include:

Prof. Dr Edward J. Gübelin
Professor Andrew Rankin
Dr Robert Symes OBE

Full details will be published in the June issue of *Gem & Jewellery News*

Contact details

(when using e-mail, please give Gem-A as the subject):

London: Mary Burland on 020 7404 3334; e-mail gagtl@btinternet.com
Midlands Branch: Gwyn Green on 0121 445 5359; e-mail gwyn.green@usa.net
North West Branch: Deanna Brady 0151 648 4266
Scottish Branch: Catriona McInnes on 0131 667 2199; e-mail scotgem@blueyonder.co.uk
South West Branch: Bronwen Harman on 01225 482188; e-mail bharman@harmanb.freeserve.uk

Gem-A Website

For up-to-the-minute information on Gem-A events visit our website on www.gagtl.ac.uk

Guide to the preparation of typescripts for publication in *The Journal of Gemmology*

The Editor is glad to consider original articles shedding new light on subjects of gemmological interest for publication in *The Journal*. Articles are not normally accepted which have already been published elsewhere in English, and an article is accepted only on the understanding that (1) full information as to any previous publication (whether in English or another language) has been given, (2) it is not under consideration for publication elsewhere and (3) it will not be published elsewhere without the consent of the Editor.

Typescripts Two copies of all papers should be submitted on A4 paper (or USA equivalent) to the Editor. Typescripts should be double spaced with margins of at least 25 mm. They should be set out in the manner of recent issues of *The Journal* and in conformity with the information set out below. Papers may be of any length, but long papers of more than 10 000 words (unless capable of division into parts or of exceptional importance) are unlikely to be acceptable, whereas a short paper of 400–500 words may achieve early publication.

The abstract, references, notes, captions and tables should be typed double spaced on separate sheets.

Title page The title should be as brief as is consistent with clear indication of the content of the paper. It should be followed by the names (with initials) of the authors and by their addresses.

Abstract A short abstract of 50-100 words is required.

Key Words Up to six key words indicating the subject matter of the article should be supplied.

Headings In all headings only the first letter and proper names are capitalized.

A **This is a first level heading**

First level headings are in bold and are centred on a separate line.

B *This is a second level heading*

Second level headings are in italics and are flush left on a separate line.

Illustrations Either transparencies or photographs of good quality can be submitted for both coloured and black-and-white illustrations. It is recommended that authors retain copies of all illustrations because of the risk of loss or damage either during the printing process or in transit.

Diagrams must be of a professional quality and prepared in dense black ink on a good quality surface. Original illustrations will not be returned unless specifically requested.

All illustrations (maps, diagrams and pictures) are numbered consecutively with Arabic numerals and labelled Figure 1, Figure 2, etc. All illustrations are referred to as 'Figures'.

Tables Must be typed double spaced, using few horizontal rules and no vertical rules. They are numbered consecutively with Roman numerals (Table IV, etc.). Titles should be concise, but as independently informative as possible. The approximate position of the Table in the text should be marked in the margin of the typescript.

Notes and References Authors may choose one of two systems:

(1) The Harvard system in which authors' names (no initials) and dates (and specific pages, only in the case of quotations) are given in the main body of the text, (e.g. Collins, 2001, 341). References are listed alphabetically at the end of the paper under the heading References.

(2) The system in which superscript numbers are inserted in the text (e.g. ... to which Collins refers.^{3}) and referred to in numerical order at the end of the paper under the heading Notes. Informational notes must be restricted to the minimum; usually the material can be incorporated in the text. If absolutely necessary both systems may be used.

References in both systems should be set out as follows, with *double spacing* for all lines.

Papers Collins, A.T., 2001. The colour of diamond and how it may be changed. *J.Gemm.*, **27**(6), 341-59

Books Balfour, I., 2000. *Famous diamonds*. 4th edn. Christie's, London. p. 200

Abbreviations for titles of periodicals are those sanctioned by the *World List of scientific periodicals* 4th edn. The place of publication should always be given when books are referred to.

Volume 28 No. 2 April 2002

The Journal of Gemmology

Contents

Registered Office: Palladium House, 1–4 Argyll Street, London W1V 2LD

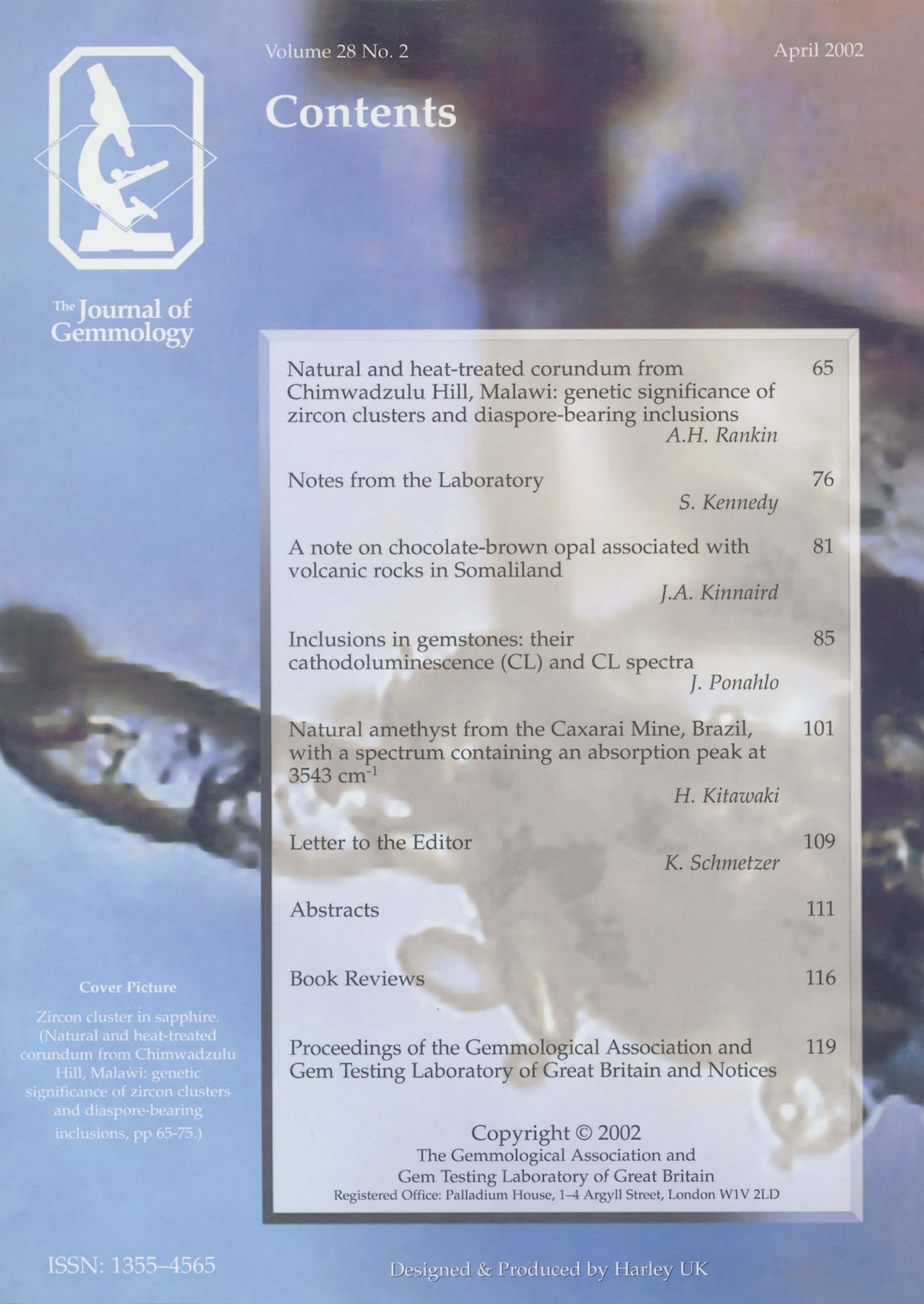

Cover Picture

Zircon cluster in sapphire. (Natural and heat-treated corundum from Chimwadzulu Hill, Malawi: genetic significance of zircon clusters and diaspore-bearing inclusions, pp 65-75.)

ISSN: 1355–4565

Designed & Produced by Harley UK